AD-A119 065 NATIONAL CENTER FOR RESOURCE RECOVERY INC WASHINGTON DC F/G 13/3
INVESTIGATION OF ENGINEERING AND DESIGN CONSIDERATIONS IN SELEC--ETC(U)
AUG 81 Z KAHN, M L RENARD, J CAMPBELL MIPR-N-80-33
UNCLASSIFIED AFESC/ESL-TR-81-58 NL

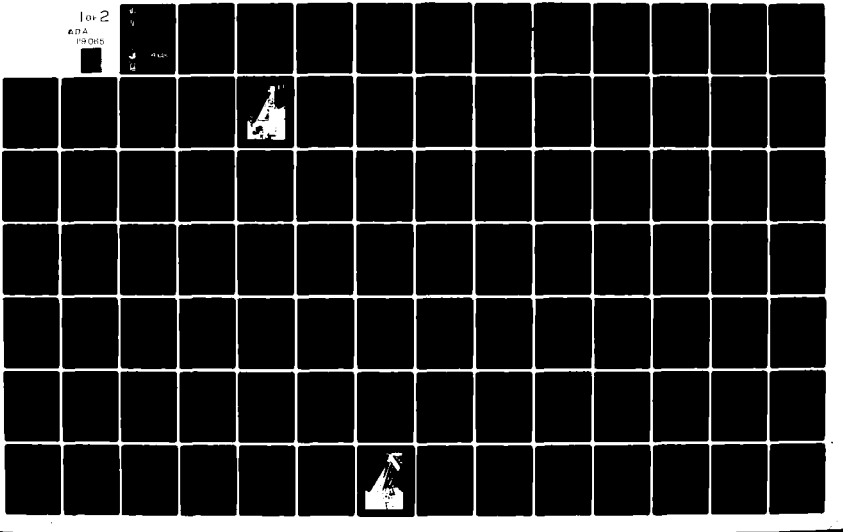

ESL-TR-81-58

(12)

INVESTIGATION OF ENGINEERING AND DESIGN CONSIDERATIONS IN SELECTING CONVEYORS FOR DENSIFIED REFUSE-DERIVED FUEL (dRDF) AND dRDF: COAL MIXTURES

ZAHID KHAN, MARC L. RENARD, JAY CAMPBELL

NATIONAL CENTER FOR RESOURCE RECOVERY, INC.
1211 CONNECTICUT AVENUE, N.W.
WASHINGTON, D.C. 20036

AUG 1981

FINAL REPORT
JUNE 1980 - SEPTEMBER 1981

AFESC

ENGINEERING & SERVICES LABORATORY
AIR FORCE ENGINEERING & SERVICES CENTER
TYNDALL AIR FORCE BASE, FLORIDA 32403

NOTICE

PLEASE DO NOT REQUEST COPIES OF THIS REPORT FROM HQ AFESC/RD (ENGINEERING AND SERVICES LABORATORY). ADDITONAL COPIES MAY BE PURCHASED FROM:

NATIONAL TECHNICAL INFORMATION SERVICE
5285 PORT ROYAL ROAD
SPRINGFIELD, VIRGINIA 22161

FEDERAL GOVERNMENT AGENCIES AND THEIR CONTRACTORS REGISTERED WITH DEFENSE TECHNICAL INFORMATION CENTER SHOULD DIRECT REQUESTS FOR COPIES OF THIS REPORT TO:

DEFENSE TECHNICAL INFORMATION CENTER
CAMERON STATION
ALEXANDRIA, VIRGINIA 22314

UNCLASSIFIED

SECURITY CLASSIFICATION OF THIS PAGE (When Data Entered)

REPORT DOCUMENTATION PAGE		READ INSTRUCTIONS BEFORE COMPLETING FORM
1. REPORT NUMBER ESL-TR-81-58	2. GOVT ACCESSION NO. A119 065	3. RECIPIENT'S CATALOG NUMBER
4. TITLE (and Subtitle) Investigation of Engineering and Design Considerations in Selecting Conveyors for Densified Refuse-Derived Fuel (dRDF) and dRDF: Coal Mixtures		5. TYPE OF REPORT & PERIOD COVERED Final Report JUN 1980 - SEP 1981 6. PERFORMING ORG. REPORT NUMBER
7. AUTHOR(s) Zahid Khan, Marc L. Renard, Jay Campbell		8. CONTRACT OR GRANT NUMBER(s) USAF MIPR N-80-33
9. PERFORMING ORGANIZATION NAME AND ADDRESS National Center for Resource Recovery, Inc. 1211 Connecticut Avenue, N.W. Washington, D.C. 20036		10. PROGRAM ELEMENT, PROJECT, TASK AREA & WORK UNIT NUMBERS Program Element 64708F JON 20545017
11. CONTROLLING OFFICE NAME AND ADDRESS Air Force Engineering and Services Center HQ AFESC/RDVA Tyndall AFB FL 32403		12. REPORT DATE AUG 1981 13. NUMBER OF PAGES 130
14. MONITORING AGENCY NAME & ADDRESS(if different from Controlling Office)		15. SECURITY CLASS. (of this report) UNCLASSIFIED 15a. DECLASSIFICATION/DOWNGRADING SCHEDULE

16. DISTRIBUTION STATEMENT (of this Report)

Approved for public release; distribution unlimited.

17. DISTRIBUTION STATEMENT (of the abstract entered in Block 20, if different from Report)

18. SUPPLEMENTARY NOTES

Availability of this report is specified on verso of front cover.

19. KEY WORDS (Continue on reverse side if necessary and identify by block number)

conveyors	refuse-derived fuel conveyors
fuel conveyors	solid fuel
boiler fuel conveyors	solid fuel conveyors

20. ABSTRACT (Continue on reverse side if necessary and identify by block number)

An engineering evaluation and experimental program involving several types of conveyors applied to blends of densified refuse-derived fuel (dRDF) and blends of dRDF and coal, was conducted by the National Center for Resource Recovery. The final project report discusses the properties of waste affecting conveyability and presents experimentally determined values or observed characteristics. A procedure was selected for the assessment, selection, and operation of belt conveyors based on spillage rate. Corroborating experimental results from

DD FORM 1 JAN 73 1473 EDITION OF 1 NOV 65 IS OBSOLETE

UNCLASSIFIED

SECURITY CLASSIFICATION OF THIS PAGE (When Data Entered)

a recirculating test rig operated with samples of dRDF and a blend of dRDF and coal over a range of belt configurations, velocities and flow rates were also presented. Experiments conducted on a vibrating pan conveyor over a range of frequencies and stroke length, and on a small apron conveyor, were described and the test results analyzed.

SUMMARY

An engineering evaluation and experimental program involving several types of conveyors applied to blends of densified refuse-derived fuel (dRDF) and blends of dRDF and coal, was conducted by the National Center for Resource Recovery. This final project report discusses the properties and characteristics of waste affecting conveyability and presents experimentally determined values or observed characteristics. A procedure is developed for the selection, assessment and operation of belt conveyors based on spillage rate. Corroborating experimental results from a recirculating test rig operated with samples of densified refuse derived fuel and a blend of dRDF and coal over a range of belt configurations, velocities and flow rates are presented. Experiments conducted on a vibrating pan conveyor over a range of frequencies and stroke length, and on a small apron conveyor, are described and the test results analyzed.

The investigation of the dRDF and dRDF/coal blend was supported by the Air Force and was part of a large investigation of conveying systems for a variety of processed waste feed stocks conducted by the National Center for Resource Recovery from the U.S. Environmental Protection Agency. Some results from this broader investigation are included in this report for comparison.

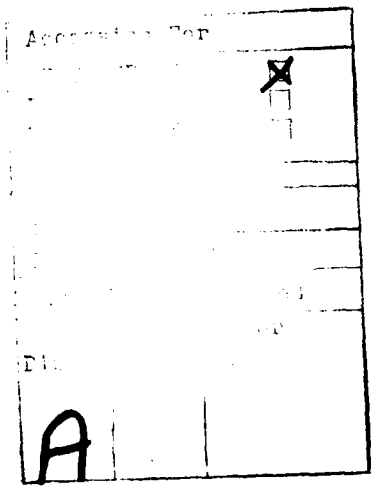

(The reverse of this page is blank)

PREFACE

This report was prepared by the National Center for Resource Recovery, Inc., 1211 Connecticut Avenue, N.W., Washington, D.C. 20036. It was prepared under contract No. USAF MIPR N-80-33 with the Air Force Engineering and Services Center, HQ AFESC/RDVA, Tyndall AFB, Fl 32403.

This work was performed under an Interagency Agreement between the U.S. Air Force Engineering and Services Laboratory and the U.S. Environmental Protection Agency through EPA Grant No. R806709.

This report covers the period beginning June 1980 and ending September 1981.

The contribution of NCRR colleagues Harvey Alter in establishing the program approach and scope and Bill Schlag, Dave Mark and Sushant Kapur in the equipment operation and testing are acknowledged. Thanks to William Horton of Carman Industries for his cooperation in providing the test vibrating conveyor, to the Maryland Environmental Service and Teledyne National, Inc., and to Tom Shoup, Wright-Patterson AFB, for providing dRDF and dRDF/coal blend samples.

The project officer was Stephen A. Hathaway, Chief, Energy Research.

This report has been reviewed by the Public Affairs Office and is releasable to the National Technical Information Service (NTIS). At NTIS it will be available to the general public, including foreign nationals.

This technical report has been reviewed and is approved for publication.

Paul C. Vitucci
PAUL C. VITUCCI, 1LT, USAF
Alternate Project Officer

Jimmy N. Fulford
JIMMY N. FULFORD, MAJ, USAF
Chief, Assessment Technology and Energy Branch

Michael J. Ryan
MICHAEL J. RYAN, LTCOL, USAF
Chief, Environics Division

Robert E. Brandon
ROBERT E. BRANDON
Deputy Director, Engineering And Services Laboratory

(The reverse of this page is blank)

TABLE OF CONTENTS

TABLE OF CONTENTS CONTINUED

LIST OF FIGURES

LIST OF FIGURES CONTINUED

LIST OF TABLES

(The reverse of this page is blank.)

SECTION I

INTRODUCTION

There exist in established literature guidelines for the selection, design and operation of various types of conveyors for most bulk solids. From these sources there also are data or relevant physical and other descriptive properties for a large number of materials that are essential for proper application of conveyor design guidelines.

The Belt Conveyor Design Handbook, published by the Conveyor Equipment Manufacturer's Association (Reference 1), is an excellent example of such a handbook with properties on over 400 materials and detailed guidelines on belt conveyor design. Yet, with the exception of glass cullet, no information is available in this or any other single publication on properties or conveyability of processed MSW fractions (such as dRDF or dRDF/coal blends).

Lacking such information on materials properties, the design engineer or equipment vendor has been hampered in efforts to apply well-founded engineering data and principles to the selection and construction of conveyors for solid wastes or to conduct proper evaluation and assessment at existing plants. As a result, problems with conveyors have been common to nearly all existing waste processing facilities, both on a large and small scale.

---

[1]Conveyor Equipment Manufacturers Association, Belt Conveyors for Conveyors for Bulk Materials, 2nd Edition (Boston, Massachusetts: CBI Publishing Company. 1979).

For example, attempts to handle and convey dRDF and dRDF coal mixtures in systems designed for coal typically result in poor equipment performance. Implementation of nonoptimal systems often results in low availability, low reliability and high costs for maintenance and repair.

In response to these expressed needs, the Municipal Environmental Research Laboratory of the U.S. Environmental Protection Agency (EPA) implemented a program to investigate engineering design considerations in selecting conveyors for resource recovery facilities. The final report is available as Reference 2.

The study included construction and operation of a laboratory-scale, closed-loop test rig to examine and quantify the performance of a variety of conveyors working on: raw mixed solid waste (MSW), shredded MSW, air classified light fraction MSW, air classified heavy fraction MSW and separated ferrous metals.

Midway through the study, discussions between NCRR, EPA and the Headquarters Air Force Engineering and Services Command led to an Interagency Agreement and participating Air Force funding for a broadened study to include densified refuse derived fuel (dRDF) and dRDF/coal mixtures. The Air Force had made a multi-year Research, Development, Test and Evaluation (RDT&E) commitment in conjunction with an experimental dRDF cofiring program at a large coal-designed heating/power plant at Wright-Patterson Air

---

[2] Z. Khan, M. Renard, and J. Campbell, Considerations in Selecting Conveyors for Solid Waste Applications, draft for Final Report (Washington, D.C., July 1981).

Force Base, Ohio. These investigations of dRDF and dRDF/coal handling and conveying are to be integrated with this larger, long term RDT&E program at Wright-Patterson.

OBJECTIVES

The objectives of the project were to:

- Determine through engineering analysis and experimentation which properties and characteristics of dRDF and dRDF:coal mixtures have significance in conveyor design, selection, operation and assessment.
- Measure these significant properties.
- Provide reliable engineering data to be used in new and modified conveyor systems for dRDF and dRDF:coal mixtures.

SCOPE

This full conveyor study investigated properties and characteristics of six processed waste fractions and evaluated performance on three conveyor types. The scope of the Air Force supported investigation included analysis of samples of dRDF and a 1:1 dRDF: coal mixture and then evaluation on belt (horizontal and inclined), vibrating pan and apron conveyors. The laboratory and test work was conducted in the period of June through October 1980.

The samples of dRDF and dRDF/coal mixtures were obtained from the Baltimore County Resource Recovery Facility in Cockeysville, MD, and from WPAFB. In spite of the recognition that the dRDF properties were likely to vary from sample to sample, and thus

have some impact on conveyor performance, the scope of the program did not allow test rig evaluations on multiple dRDF or blend samples. Rather, through careful sampling and monitoring of sample properties, the goal was to obtain and test material samples representative of the individual processed fractions and reasonably consistent from test to test.

FACILITY AND TEST RIG DESCRIPTION

The experimental activities in this program were conducted at the National Center's Resource Recovery Laboratory, a 3000 ft^2 process test facility located in Upper Marlboro, MD, southeast of Washington. Concurrent engineering and analytical activities were supported from the main NCRR offices in Washington.

The design of the test rig was based on several considerations:

- Ability to fix mass flow rates.
- Accessibility for dynamic measurements and sampling.
- Flexibility to interchange, incline, or vary the speeds of the test conveyors.

A continuous loop, recirculating flow configuration as shown in schematic in Figure 1 and pictured in Figure 2 was selected for the tests. A surge hopper with a variable speed pan conveyor to control feedrate was tried initially, but found to result in surging and thus poor feedrate control. The second and successful approach was to fix conveyor speeds and charge a measured quantity of the test material into the system and thus obtain a constant mass flow rate throughout the loop. It was experimentally established that the mass flow rate could be held within a range of

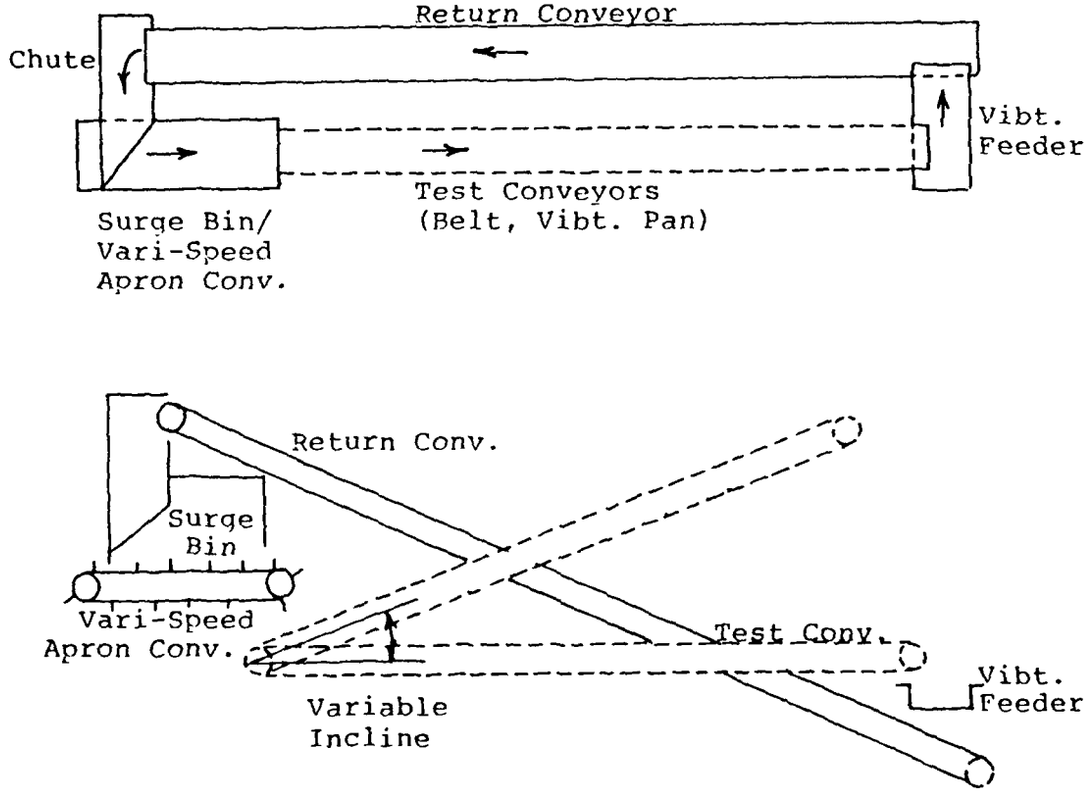

Figure 1. Schematic of Conveyor Test Rig

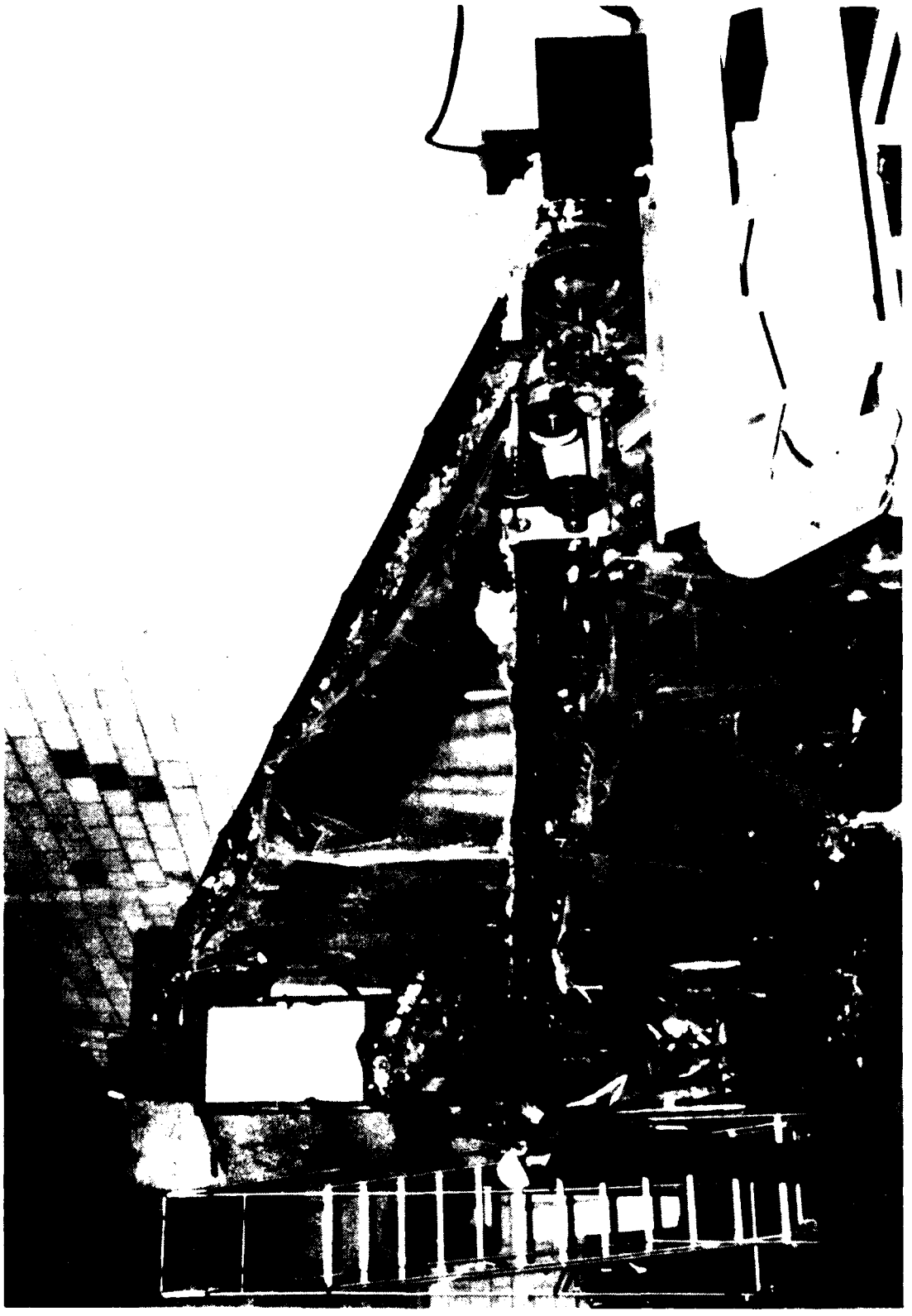

Figure 2. Conveyor Test Rig

plus or minus 5% of the measured average.

Table 1 provides specifications for each of the conveyors in the test rig. Both the test belt conveyor and test vibrating conveyor required modifications to provide the ranges of operating conditions that are shown.

ORGANIZATION OF THE REPORT

Section II of the report provides data and discussion on the key properties and characteristics of solid waste fractions affecting conveyability. Property and characteristic data are provided in this section on all the six processed waste samples included in the investigation (Reference 2). This is done to permit comparison of the results and in view of a potentially growing interest of the Air Force in waste-fuel utilization. Section III develops the rationale and approach for design of the test program and judging belt conveyor performance and includes results of belt conveyor test in the horizontal and inclined modes. Sections IV and V present the results of testing the dRDF and dRDG/coal blend on vibrating pan conveyors and apron conveyors respectively. Selected experimental results are again provided on other material fractions for purposes of comparison (Reference 2).

---

[2] Z. Khan, et al., Considerations in Selecting Conveyors for Solid Waste Applications.

TABLE 1. TEST RIG CONVEYOR SPECIFICATION

Conveyor	Width m (in.)	Length m (ft)	Drive	Idlers angle	Stroke/ freq.	Incline	Speed	Manufacturer
Feed Apron	0.749 (29.5)	2.06 (6.75)	variable	N/A	N/A	0°	0.14 m/s (27 fpm)	Bonded Equipment
Test belt conveyor	0.457 (18)	7.63 (25)	variable	20°/ 35°	N/A	0°-32° max.	0.20-2.44 m/s (40-480 fpm)	Bonded Equipment
Vibrating conveyor	0.603 (23.75)	4.58 (15)	variable	N/A	12.7 mm (1/2 in.)/ 400-560 cpm 22.2 mm (7/8 in.)/ 470-545 cpm	0°	N/A	Carman Industries
Transfer vibrating conveyor	0.508 (20)	1.83 (6)	constant	N/A	4.8 mm (3/16 in.)/ 1300 cpm	0°	N/A	Meyer Machine Co.
Return conveyor	0.508 (20)	9.67 (31.7)	constant	35°	N/A	17°	1.04 m/s (205 fpm)	Bonded Equipment

SECTION II

PROPERTIES AND CHARACTERISTICS OF SOLID WASTE FRACTIONS AFFECTING CONVEYABILITY

As discussed earlier, in conveyor design it is essential to have engineering data on material properties and material handling interactions. This information is available for most bulk solids but not for MSW or processed fractions or blends.

The properties and characteristics of bulk materials affecting conveyability and their test methods have been researched and published by the Conveyor Equipment Manufacturers Association (CEMA) (Reference 3). Table 2 shows a complete list of properties and characteristics that affect conveyability. The asterisks in Table 2 indicate those which were considered unrelated to the conveyability of solid waste fractions. The daggers rate properties for which test methods have yet to be developed.

MEASURED PROPERTIES AND RESULTS

The following are the results from reviews or measurements of the properties listed in Table 2. Test methods, as available or applied, are given in Appendix A.

Angle of Maximum Inclination

The angle of maximum inclination is defined for a belt conveyor to be that angle, in degrees to the horizontal, at which an empty conveyor belt will successfully transport the material fed to it. The results were observed to be dependent on belt config-

---

[3] Conveyor Equipment Manufacturers Association, Classification and Definitions of Bulk Materials, No. 550 (Washington, D.C., 1970).

TABLE 2. PROPERTIES AND CHARACTERISTICS OF BULK MATERIALS AFFECTING CONVEYABILITY (Reference 3)

Properties (measured)

1. Abrasiveness†
2. Angle of External Friction†
3. Angle of Internal Friction†
4. Angle of Maximum Inclination (of a belt)
5. Angle of repose
6. Angle of slide
7. Angle of surcharge
8. Bulk Density - loose
9. Bulk Density - vibrated
10. Cohesiveness†
11. Elevated Temperature*
12. Flowability - flow function†
13. Lumps - size - weight
14. Specific gravity*
15. Moisture Content
16. Particle Hardness†
17. Screen Analysis and particle size consist
18. Sized and unsized material

Characteristics (assessed)

1. Aeration - Fluidity*
2. Becomes plastic or tends to soften*
3. Builds up and hardens
4. Corrosive
5. Generates static electricity*
6. Degradable - size breakdown
7. Deteriorates in storage - decomposition
8. Dusty
9. Explosiveness
10. Flammability
11. Harmful dust, toxic gas or fumes
12. Hygroscopic*
13. Interlocks, mats and aggleomerates
14. Oils or fats present*
15. Packs under pressure
16. Particle shape
17. Stickiness - adhesion
18. Contaminable
19. Very light & fluffy - may be windswept

* Considered unrelated to conveyability of solid waste.
† Test methods for processed solid waste fractions yet to be developed.

TABLE 3. ANGLES OF MAXIMUM INCLINATION

SOLID WASTE FRACTION	Belt width mm (in.)	Belt idlers (°)	Belt speed m/s (ft/min)	Flow rate Mg/h (TPH)	Angle of maximum inclination (°)
MSW	457 (18)	35	0.51 (100)	0.9 (1.0)	19
RDF	457 (18)	35	0.51 (100)	0.9 (1.0)	21
d-RDF	457 (18)	35	0.51 (100)	4.5 (5.0)	30
HEAVY FRACTION	457 (18)	35	0.51 (100)	4.5 (5.0)	28
FERROUS FRACTION	457 (18)	35	0.51 (100)	4.5 (5.0)	28
d-RDF/COAL (1:1 volumetric basis)	457 (18)	35	0.51 (100)	9.1 (10.0)	27

Test Conditions: (1) Belt width = 457 mm (18 in.)

(2) Belt idlers = 35°

(3) Belt velocity = 0.51 m/s (100 fpm)

uration, belt speed and mass flow rate. Table 3 presents maximum angle of inclination for mid-range mass flow rates for each material and at a fixed belt velocity of 0.51 m/s (100 fpm). Angles are seen to be greater with feedstock of higher densities such as the coal/dRDF mixture. The test procedure is given in Appendix A.

Angle of Repose

The angle of repose for bulk material in a stockpile is the angle between the horizontal and a sloping line from the top of the pile to the base. The measurement procedure is provided in Appendix A. The results as a range for each material are shown in Table 4.

Angles of repose will vary due to irregularities in particle size, shape and concentrations. Also, the piles of waste materials were never observed to be uniformly conical, and thus several angles of repose were measured around the pile. The angle of repose for the dRDF was observed to vary with the level of unpelletized material. For loosely bound pellets with significant unpelletized material, higher angles were noted. For hard, stable pellets, angles of repose toward the lower end of the range were observed.

Angle of Slide

The angle of slide is that angle to the horizontal of an inclined flat surface on which an amount of material will begin to slide downward due to its own weight. Such a measurement is of particular use in design of chutes or diverters.

TABLE 4. ANGLE OF REPOSE

SOLID WASTE FRACTION	ANGLE OF REPOSE	
	RANGE	AVERAGE
MSW	25° - 52°	39
RDF	29° - 49°	40
d-RDF	27° - 46°	38
HF	30° - 59°	40
Ferrous Fraction	N/A*	N/A*
dRDF/coal	40° - 45°	42

* No measurement made as small sample size led to slumping to a monolayer.

TABLE 5. ANGLE OF SLIDE

SOLID WASTE FRACTION	ANGLE OF SLIDE	
	STEEL PLATE	CONVEYOR BELTING
MSW	29.3°	30.0
RDF	31.0°	35.0
dRDF	32.8°	34.5
Heavy Fraction	27.5°	28.5
Ferrous Fraction	17.5°	32.0
dRDF/coal	22.0°	24.0

Experimental determination of the angle of slide will be affected by the:

- type and condition of the underlying surface.
- state of compaction of the material.
- rate of change in slope (controlled by the operator).

Tests were conducted both on a steel plate and rubber conveyor belting. For each test, approximately 14.2 dm^3 (0.5 ft^3) was utilized. The results in Table 5 indicate that all of the waste fractions will slide, under static conditions, at a lower angle on steel than conveyor belting. The low angle of slide for the dRDF/coal mixture (22^o) compared to the dRDF alone (33^o) suggests that chute or hopper systems designed for coal only may in practice be suboptimal for dRDF. The test procedure is given in Appendix A.

Angle of Surcharge and Maximum Angle of Surcharge

The angle of surcharge is the angle to the horizontal which the surface of the material assumes while at rest on a moving conveyor belt. Figure 3 shows the angle of surcharge, α, for three types of conveyors. For bulk solids listed in the CEMA Handbook on belt conveyors and when tested on a moving belt, this angle is said to be observed to be 5^o to 15^o lower than the angle of repose (Figure 3).

The angle of surcharge as defined (on a moving belt) could not be experimentally determined, because the available equipment and quantity of material were too small for the prescribed procedure.

In this program, a maximum angle of surcharge on a belt (α_{max})

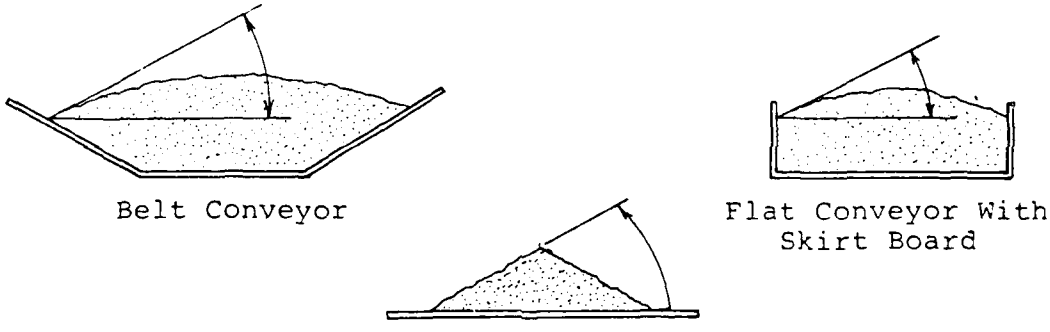

Figure 3. Angle of Surcharge for Three Types of Conveyors

has been defined as the experimentally determined angle at which the conveyor can be loaded to a maximum capacity (i.e., filling a maximum belt cross section) under static conditions (i.e., with the belt at rest). These figures are shown for the six materials and two idler configurations in Table 6. Take note of the low value for the dRDF/coal mixtures. This result is lower than the angle of repose, contrary to the increases for the other materials and suggests an unrepresentative sample or a measurement error. The procedure for this measurement of angle of surcharge is given in Appendix A.

Loose Bulk Density

While there are several published standards for determining bulk density, such as the American Society for Testing and Materials (ASTM) methods for aggregates and coal, they are not generally applicable to solid waste. The two methods to measure bulk density that were applied in this study, loose and vibrated, are described in Appendix A.

The loose bulk density appears to be more representative of the two methods in representing the density of a material on a conveyor belt. Loose bulk density is the weight per unit volume of a sample discharged from a container into a pile or cone without any other compaction. The results are provided in Table 7. Note the narrower ranges in loose bulk density for the dRDF/coal blend compared to the more heterogeneous MSW and heavy fraction samples, due mainly to the presence of discrete heavy or larger-sized material. Such uniformity in bulk density will

TABLE 6. MAXIMUM ANGLE OF SURCHARGE

SOLID WASTE FRACTION	MAXIMUM ANGLE OF SURCHARGE	
	20° Idler	35° Idler
MSW	55°	54°
RDF	51°	65°
dRDF	not measured	49°
HEAVY FRACTION	48°	59°
FERROUS FRACTION	not measured	52°
dRDF/COAL	not measured	40°

TABLE 7. BULK DENSITY (LOOSE)

SOLID WASTE FRACTION	BULK DENSITY (LOOSE) (kg/m³) (lbs/ft³)	
	RANGE	AVG.
MSW	61-152 (3.8 - 9.5)	106 (6.6)
RDF	34-50 (2.1 - 3.1)	43 (2.7)
dRDF	361-387 (22.6 - 24.2)	374 (23.4)
FERROUS	N/A*	N/A*
HEAVY FRACTION	366-598 (22.9 - 37.4)	482 (30.1)
dRDF/COAL	712 (44.5)	712 (44.5)

* No measurement made as sample size too small and material slumped to monolayer.

be seen to result in reduced tendency for conveyor spillage and is one advantage with a densified form of waste fuel.

Vibrated Bulk Density

The vibrated bulk density is the weight per unit volume of a sample which is in a compacted condition as a result of vibrating or tapping of the test container as it is being filled.

This method (Appendix A) is comparable to a standard recently developed by The American Society for Testing Materials Committee on Resource Recovery (E-38) but substitutes the CEMA vibration method which is more applicable for coal and aggregates. The results are given in Table 8.

The reason for the lower vibrated bulk density for the dRDF/coal mixture contrary to trends of increased density with the other materials is not known. It is possible the ratio of coal to dRDF varied slightly between the samples used for the two tests. This anomaly and the probable explanation serves to emphasize the impact of a minor change in the blend ratio on bulk density and thus conveyor capacity.

Comparing the results in Tables 7 and 8, it can be seen that the vibrated bulk densities are higher by about 20% than the loose density. Whereas the vibrated bulk densities are generally utilized for determining volumetric flow rates, it is proposed that the loose bulk density value should be measured and used in conveyor design for MSW or its processed fraction as it is more representative of the actual as-handled material conditions.

TABLE 8. BULK DENSITY (MAXIMUM)

Solid waste fraction	Range	Bulk density kg/m^3 (lb/ft^3)	Average
MSW	66 - 200	(4.1 - 12.5)	134 (8.4)
RDF	37 - 72	(2.3 - 4.5)	54 (3.4)
d-RDF	402 - 486	(25.1 - 30.4)	445 (27.8)
Heavy fraction	334 - 451	(20.9 - 28.2)	435 (27.2)
Ferrous fraction	194	(12.1)	194 (12.1)
d-RDF/coal	590	(36.9)	590 (36.9)

Angle of External Friction, Angle of Internal Friction, Coheisveness, Flowability

Brief definitions of these properties are as follows:

The Angles of External and Internal Friction are properties of a material related to shearing resistance between the material and a surface of another material (external) and resistance to sliding or rolling of particles in relation to themselves (internal). They are experimentally determined by a direct shear-controlled stress tester (Reference 4). Cohesiveness in bulk material is characterized by the degree to which individual particles tend to cling together and is also measured in direct shear-controlled stress tests. Flowability (flow function) characterizes the freedom of constituent particles or groups of particles to move when the bulk material is put in motion and is determined in

[4] J.R. Johanson, Know Your Material - How to Predict and Use the Properties of Bulk Solids, Chemical Engineering Handbook, October, 1978), pp. 9 - 17.

direct shear-controlled strain testing.

These properties have their primary application in the design and assessment of storage and discharge systems and are not currently used to any significant degree in conveyor design, selection or evaluation.

In any case, the scope of the test program did not present evaluation of the dRDF and blend sample flow properties with the shear-controlled stress tester. Reference is made to flow property test results on a dRDF product of similar size and composition from a project initiated by the U.S. Army, Construction Engineering Laboratory (Reference 5). Two samples of 1/2 inch diameter dRDF were analyzed as part of a design effort on a bin and feeder for reliable dRDF flow. The results involve substantial tabular and graphical presentations so are not reported here.

Particle Hardness

Particle hardness, by the CEMA definition, is of interest in relation to possible abrasiveness, potential for cracking or crumbling to smaller particles in handling and the ease with which it may be intentionally cracked or broken in crushing or grinding. For dRDF and blends, the second factor, referred to here as pellet integrity, is of the greatest concern related to effects of reducing density and increasing fines content of the dRDF. These changes can in turn increase volumetric loading and wind-swept spillage of the dRDF during transport on the conveyors.

There have been a number of efforts made toward establishing

a procedure to quantify pellet integrity. In two densification projects at NCRR (References 6,7), separate tumbler and drop/ shatter coal test procedures were adapted and applied to samples of dRDF from various points in the production, handling and storage processes. The requirements for a larger number and size of samples, the rigor in measuring changes in length and fines content, the frequent absence of statistically significant changes and inability to relate the test results to loss of integrity in actual handling were drawbacks to the tests. For these reasons, these procedures were not applied to the dRDF or blends in the conveyor test program.

Some comments on the factors effecting pellet integrity may be of value. Observations during the production, transport and storage indicate resistance to abuse to be a function of pellet density, moisture content and pellet temperature. Low density pellets tend to have partly separated shear planes and ragged edges that make them more susceptible to breakage. Pellets with higher moisture contents, as a result of moisture in the feedstock of moisture absorbed in storage, tend to swell and delaminate and are more easily broken. Pellets that are not cooled after production or are subjected to higher temperatures in storage were observed to be less cohesive and, thus, more easily broken.

Abrasiveness

In the case of abrasiveness, a test to assess relative

abrasiveness of the various waste fractions was developed, but proved unsuccessful. A sheet of material (rubber belting and aluminum) was placed in the material trajectory at one of the right angle turns on the test rig. Measurements were made of the weight loss of the impact sheet related to mass flow and time for each waste fraction. Unfortunately, the results obtained during the test program were inconclusive. Much longer periods of time than were available and repetitive tests would appear to be required to provide meaningful results. For dRDF and blends, the abrasiveness would not be expected to exceed that experienced with coal alone.

Size and Weight of Lumps

According to the CEMA definitions, lump size is the maximum linear dimension of a large particle, or stable agglomeration thereof, in a bulk material. The lump weight is the weight of the maximum size lump. The measurements of the largest lump size were made in conjunction with the particle size distribution test outlined in Appendix A. For sized material like dRDF and stoker coal, this material property is not relevant.

Moisture Content

The moisture content of a material reflects the absorbed and adsorbed water and is measured by evaporation through drying. The procedure used in this program is provided in Appendix A. Because of the wide variations in moisture content of MSW and its processed fractions, and the potential

for changes between sampling and measurements, the results in Table 9 should be viewed only as general indicators.

Waste materials with higher moisture content, although beneficial in limiting dust, may contribute to either operational or maintenance problems. Moisture will increase material stickiness and adhesion onto belts or chutes and can lead to corrosion.

Screen Analysis and Particle Size Distribution

A screen analysis using a conventional shaker screen technique (see Appendix A) was conducted to obtain a particle size distribution (PSD) for four of the six solid waste fractions. No conventional PSD analysis was performed for the dRDF or coal/dRDF blends, because the fixed pellet diameter (13 mm) makes a screen size analysis meaningless.

Pellet length and fines content (defined for dRDF as -10 mm (-3/8 inch) material) are alternate methods for assessing dRDF size, and as mentioned in the discussion of particle hardness, have application to pellet integrity tests for empirically assessing the effects of actual handling in the field. Although not considered a relevant parameter in the recirculating test program, dRDF and coal/dRDF fines content was measured at various points in the tests to assure the test sample had not degraded significantly and thus would not substantially effect the results.

TABLE 9. MOISTURE CONTENTS.

Solid Waste Fraction	Moisture Content (% as received)	
	Range	Avg.
MSW	18.0% - 30.0%	21.8%
RDF	9.1% - 19.0%	14.2%
dRDF	20.5% - 22.7%	20.6%
Heavy Fraction	9.2% - 20.8%	15.9%
Ferrous Fraction	2.6%	2.6%
dRDF/coal	-	9.3%

The results for the other materials are presented for reference in Figure 4. Such information is of value in specifying conveyor parameters such as belt width, idler angles, conveyor skirting and in the design of conveyor loading and discharge configuration.

Sized and Unsized Materials

A sized material consists of particles which have been passed through some defined mesh screen and retained on some smaller mesh screen; a partially sized material is made of sized and unsized material.

Under those definitions, the solid waste fractions evaluated in this program are unsized, with the exception of the dRDF, which is produced by an extrusion process and thus effectively sized and uniform in physical dimensions. Processed

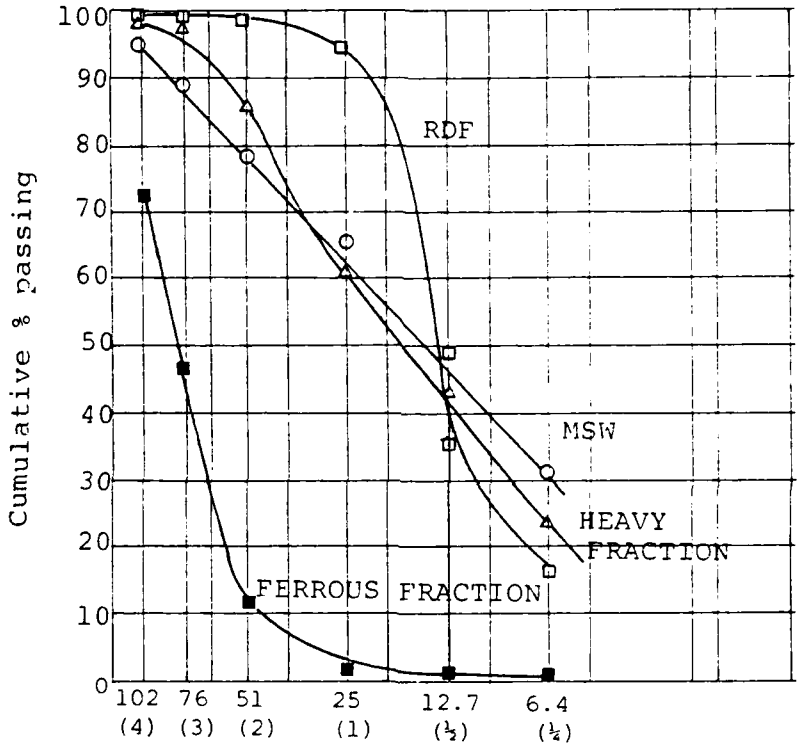

Figure 4. Particle Size Distribution of Test Samples

waste fractions encountered in other waste processing plants may have undergone a screening process and thus be considered sized.

CHARACTERISTICS ASSESSED

Certain material characteristics do not have defined measurement techniques, but still must be addressed in designing a conveyor system. Several of the key characteristics and selected physical properties have been combined and coded in a material class description form shown in Table 10. Further discussion on these characteristics and their assessment are given by CEMA (References 1,3).

Using this CEMA classification approach, Table 11 provides coding for the six material evaluated in this program. It is recommended that they be used with the awareness of their limitations, due to the heterogeneity and variability of these types of material.

For reference, the CEMA Material Code for sized bituminous coal (the closest coal listed to the stoker coal utilized in the tests) is 50 $D_3$35QV (Reference 3). Comparing the code to that established for the dRDF/coal mixture (45 $D_3$45HJQL) reveals the changes in material characteristics resulting from blending the dRDF, and suggests the potential for problems in handling a dRDF product or blend in a material handling system designed for coal.

---

[1]Conveyor Equipment Manufacturers Association, Belt Conveyors for Bulk Materials.

[3]Conveyor Equipment Manufacturers Association, Classification and Definitions of Bulk Materials.

TABLE 10. MATERIAL CLASS DESCRIPTION.

	Material Characteristics	Code
Size	Very fine - less than 100 mesh	A_{100}
	Fine -1/8 in. or less	B_6
	Granular -3 in. or less	D_3
	Lumpy - containing lumps 16 in. or less	D_{16}
	Irregular - stringy, interlocking	E
Flow-Ability	Very free flowing - angle of repose less than 19°	1
	Free flowing - angle of repose 20° to 29°	2
	Average flowing - angle of repose 30° to 39°	3
	Sluggish - angle of repose 40° and over	4
Abrasiveness	Non-abrasive	5
	Abrasive	6
	Very abrasive	7
	Very sharp - cuts or gouges belt conveyors	8
Characteristics (Assessed)	Builds up and hardens	F
	Deteriorates in storage	H
	Corrosive	T
	Degradable - Size Breakdown	Q
	Dusty	L
	Explosiveness	N
	Flammability	J
	Harmful dust, toxic gas or fumes	R
Characteristics	Interlocks, matts or agglomerates	V
	Packs under pressure	X
	Stickiness - Adhesion	O
	Very light fluffy	Y

TABLE 11. MATERIAL CHARACTERISTICS

Fraction	Average loose bulk density kg/m^3 (lbs/ft^3)	Angle of repose (degrees)	Angle of maximum inclination (degrees)	CEMA material code
MSW	106 (6.6)	25 - 52	19	E36HJVO
RDF	43 (2.7)	29 - 49	21	E35HJLXY
dRDF	374 (23.4)	27 - 46	30	$D_3$35HJQL
Heavy Fraction	481 (30.1)	30 - 59	28	E47HQVO
Ferrous Fraction	192 (12.0) (maximum B.D.)	N/A	28	D_{16}6
d-RDF/coal	712 (44.5)	40 - 45	27	$D_3$45HJQL

These changes and impacts on conveyor systems include: reduced density and therefore increased volumetric flowrates; reduced angle of repose with potential for increased flow problems; added potential for deterioration in storage with resultant impacts on density, size and other properties affecting conveyability; and increased dusts with potential effects on spillage and dust control requirements. The CEMA designation of the coal as having interlocking and matting characteristics is not understood; the CEMA definition does not seem to apply to the coal/dRDF mixture.

SECTION III

BELT CONVEYORS

INTRODUCTION

Belt conveyors have wide applications in mining, construction and processing industries. Compared to other types of conveyors, they have advantages of being relatively simple and economical and suitable for conveying material of varying composition, size and moisture. They can be operated in the horizontal, inclined or declined mode. Belt conveyors are commonly present in resource recovery plants for transportation of MSW or the variety of its processed fractions.

Resource recovery plant operating experience has indicated that, in spite of simplicity in design and operation, numerous problems still beset belt conveyors such as spillage, jams, roll-back, dusting and wear. Some of these problems are attributable to the properties and characteristics of the materials being conveyed, as have been discussed in the previous section. But, other problems are related to operating variables over which a designer or operator has control such as belt size, speed and inclination; idler type and angles; and loading and discharge configuration. However, to understand or optimize design and operation, the influence of the conveyor configuration movement, shape and speed on these problems must first be understood.

The approach in this investigation was to explore the impact and interrelationship of these equipment and operating variables

on conveyor performance through a systematic series of tests on a horizontal and inclined belt.

However, prior to the conduct of the tests, an analysis of the rationale and criteria for evaluating and judging conveyor performance had to be developed, and was published earlier in 1981 (Reference 8). The analysis and development of a test plan are described next and will be followed by the results and discussion of the tests.

ANALYSIS AND DEVELOPMENT OF A TEST PLAN

Rationale: Designing for a Rate of Spillage

In designing a series of tests to define the range of "good" or "best" operation of a belt conveyor carrying a given material, some thought should be given to the criteria by which such labels as "good" or "best" might be awarded.

As noted above, experience of observations gathered at a number of operating plants with systems to convey solid waste fractions strongly suggests that, by far, the most undesirable feature in such systems is a high rate of spillage. Spillages on the sides of conveyor belts, or at transfer points, will fall on the floor, jam up rotating pieces of equipment and be a cause of constant problems in maintenance, odor, sanitation and clean-up. As an illustration, assume a rate of spillage of 1% of the mass flow rate on a conveyor belt 30.5 m (100 ft) long. The belt carries 1.8 Mg/h (2 ton/h) of light fraction (fluff RDF) having a bulk density of 54 kg/m^3 (3.4 lb/ft^3). After an 8-hour shift,

0.14 Mg (0.16 ton) will have accumulated along the belt, representing a total volume of 2.1 m^3 (94 ft^3). On each side of the belt, this would be the equivalent of a layer 30.5 cm (1 ft) wide and 15 cm (0.5 ft) high. Needless to say, such rate of spillage would be intolerable in steady operation.

Other desirable (but possibly less crucial) features of a belt conveyor system of known geometry, carrying a given material, are:

(a) High throughput for a given size (as measured by the width of the belt).

(b) Low power consumption.

(c) High reliability and trouble-free operation.

(d) Low levels of dust emissions.

(e) Ease of transfer of material to and from the belt.

In view of the extreme importance of limiting spillage to a low, admissible level, it was decided at the outset to design the conveyability on the basis of a criterion of acceptable spillage. Then, consideration was given to high throughputs (feature (a) above) by studying the dependence of throughput on belt speed.

Item (b) above, the power consumption, was measured at the various operating points, with no attempt being made to modify the design of the belt being tested for lower power consumption. (It should be kept in mind, however, that high power consumption might be one of the essential deciding factors when choosing between an open, skirted or covered conveyor belt system (Reference 1)).

High reliability and trouble-free operation, item (c), can only be ascertained after much longer periods of time than would be possible in this test program. Still, whenever possible and justified, incidents of operation, jamming of equipment or other conditions were noted and documented.

As will be detailed below, dust levels were recorded and evaluated in a relative, and to some extent, absolute manner. These levels were obtained at various typical locations (near transfer points, in the middle of a straight run, etc.), thus allowing comparison of the dependence of dust levels on location as well as on the operating parameters and the kind of solid waste fraction being conveyed.

Finally, the ease of transfer of the material studied onto and from the belt will be highlighted in two principal ways: first, by observing and recording trajectories of the material at the discharge point from the conveyor belt and comparing them to those predicted by methods conventionally used in applications for materials other than solid waste; second, by making experimental observations, largely qualitative, and ad hoc improvements during the course of the tests to serve as a guide for assessing the proper mode of feeding the belt with a variety of feedstocks. This is particularly true in the case of a steeply inclined belt, for which transfer and acceleration on the belt in the zone located directly under the chute or feeding stream are the mechanisms critically limiting throughput and/or producing surges.

Horizontal Belt: Choice of Test Variables and Parameters

As a help in the discussion, a schematic representation of the conveyor belt system is shown in Figure 5. The belt has length L_B, and can be either horizontal ($\alpha = 0$) or inclined at angle α on the horizontal. At the inlet point A, the input mass flow rate (having dimension mass/unit time, or (MT^{-1})) is noted m_{in}; the mass flow rate exiting the belt at Point B is noted m_{out}.

Spillage Rate

The spillage rate ($\dot{s}$) is a relative measure of the mass of conveyed material being spilled, per unit of mass flow rate conveyed and unit length of belt.

This would appear as a logical definition, but it implicitly contains some assumptions or simplifications. First, the input mass flow rate, m_{in} defined above and in Figure 5, is assumed to be known and constant. In actuality, the mass flow rate (m_{in}) is steadily decreasing with time, due to spillage and the fact that the mass spilled is not replaced on the belt. For small spillage rates (1% or less over the length considered), this effect is of second order, provided the duration of the test is not too long. This is quantified in Appendix B. Second, the rate of spillage is construed to be proportional to belt length, and for long, straight runs, this might be the case only after the "discrete" spillage at transfer points A and B in Figure 5 has been subtracted from the total spillage. More will be said about these limitations further in the text, when discussing the experimental procedure and test results.

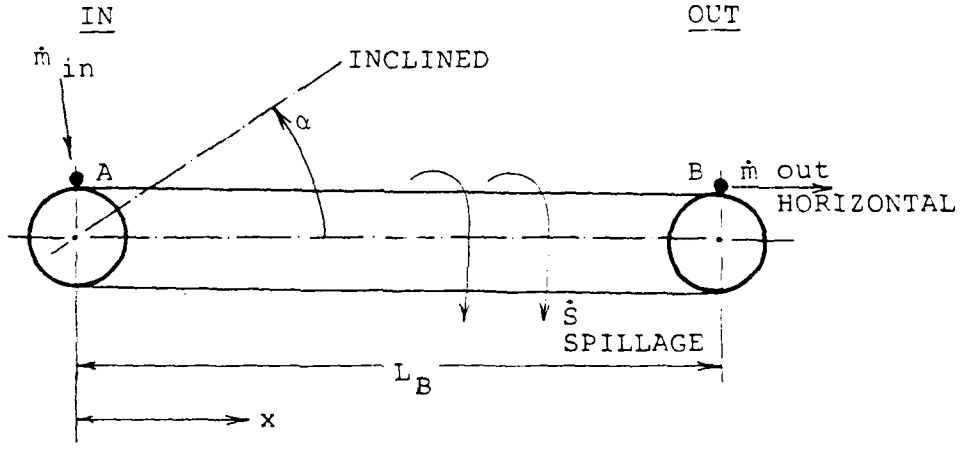

Figure 5. Schematic of Belt Conveyor System

Let $\dot{m}_s$ be the mass flow rate of material spilled per unit length of belt. The formal definition of the spillage rate, as a fraction (p.u.), or percentage, will be (with the above qualifications):

$$\dot{s} = \frac{d\dot{m}_s/dx}{\dot{m}_{in}} = \frac{\dot{m}_{in} - \dot{m}_{out}}{\dot{m}_{in} \times L_B} \qquad \text{(per unit)}$$

or

$$\dot{s}_{\%} = 100\ \dot{s} \qquad \text{(percent)}.$$

Note that $\dot{s}$ and $\dot{s}_{\%}$ have dimensions mass/unit time and length ($ML^{-1}T^{-1}$).

For example, spillage rate of 10^{-5} or 0.001% per 0.30 m (1 ft) of belt on a belt 30.5 m (100 ft) long fed at the rate of 1.8 Mg/h (2 ton/h) would amount to a total amount of mass spilled, over 1 hour, equal to

$$10^{-5} \times 10^{2} \times 1.8 \text{ Mg} = 1.8 \text{ kg (4 lb)}$$

This would represent 28 dm^3 (1 ft^3) of a material having a bulk density of 64 kg/m^3 (4 lb/ft^3).

The concept of admissible (or maximum) spillage rate, $\dot{s}_{max}$, can now be introduced at that upper bound on the spillage rate which, over the time periods and lengths of belt considered, is deemed to be tolerable under the conditions of use. As sketched in Figure 6, the designer might be able to choose, for a given material and system geometry, an operating point "P" leading to lower spillage, $\dot{s}$, than the maximum tolerable one, $\dot{s}_{max}$.

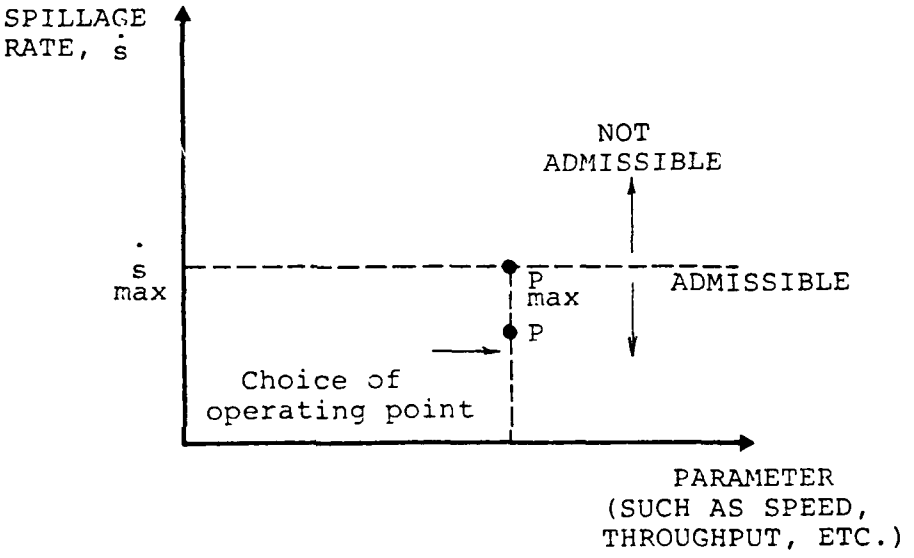

Figure 6. Choosing an Operating Point for Lower Spillage Than Maximum Admissible

Obviously, the absolute level of such spillage rate is partly a matter of judgment and partly specific to the material conveyed and the operating conditions at the site. In designing a test procedure for the present investigation, the admissible (or maximum) spillage rate was selected on the basis of engineering judgment. The selected rate was not so small that it could not be measured with a good degree of accuracy, yet not so large that it would make the volumes physically intractable and the flow rates unsteady. Thus, to some extent the choice of threshhold "$\dot{s}_{max}$" is also influenced by the material conveyed, the characteristics of the experimental set-up and the attainable ranges of test parameters, such as capacity, belt speed, etc.

Materials Conveyed

In the present discussion, the material being conveyed is assumed to be given from among the fractions listed and described in Section II. Its properties and characteristics, in the sense explained previously, have been measured and recorded.

System Geometry

The size and geometric characteristics of the conveyor belt are assumed to be known. In the present case, this amounts to giving (Figure 7):

- The belt width, w. This width can be divided in the part of the belt resting on the horizontal rollers, w_1, and the part resting on the idlers w_2; $W = w_1 + w_2$.

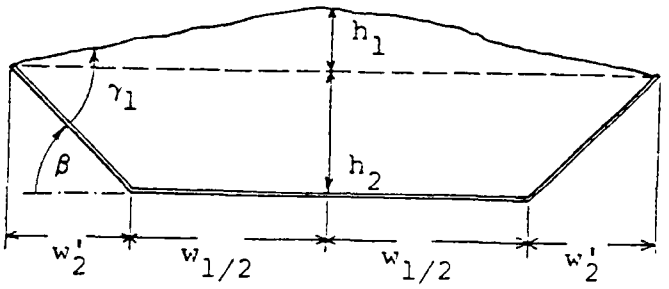

Figure 7. Cross-section of loaded belt (at rest)

- The idler angle, β.
- The spacing between idlers, ℓ, along the direction of the motion (not represented in Figure 7).

Static Capacity

Assume that on a length of belt sufficiently long to ignore end effects, the material under study is piled up, at rest, so that the edge of the pile on either side touches the edge of the belt. If a unit length (L = 1) of belt is considered, it has a cross-section similar to that sketched in Figure 7. The static capacity, C_{ST}, will be defined by the area of this cross-section, computed as

$$C_{ST} = \frac{h_1}{2} (w_1 + 2w'_2) + w'_2 (w'_2 + w_1) \tan \beta \qquad (1)$$

with $w'_2 = \frac{1}{2} w_2 \cos \beta$ where β is the idler angle and h_1 is measured.

Note that C_{ST} has the dimension of an area (L^2), and $C_{ST} \times L$ is the volume of material resting on a length L of belt.

Dynamic Capacity

If in the experiment outlined above we set the belt in motion, the material resting on the belt will tend to crumble along the sides of the (two-dimensional) pile, and the cross-sectional area occupied by the material will decrease below the value at rest, C_{ST}.

The belt volumetric carrying capacity will not be that which would be realized if the cross-sectional area C_{ST} could be maintained without spillage under dynamic conditions (belt at speed V_B); namely

$$Q = C_{ST}\, V_B \quad (L^3T^{-1}). \tag{2}$$

To quantify this reduction, it is proposed that a prescribed degree of spillage (per unit time and unit length of belt) be specified in advance, (for example, $\dot{s}$). Under such conditions, a measured (or computed) area of capacity C_{DYN} is obtained experimentally. The reduction in capacity resulting from the motion is then assessed by a reduction coefficient:

$$k_{RED} = \frac{C_{DYN}}{C_{ST}} \tag{3}$$

which itself is a function of the dynamic parameters, as described below, and of the prescribed degree of spillage. It is obvious that the dynamic capacity would, all other factors being equal, be expressed by a larger number if the allowed rate of spillage is larger.

One way to look at relationship (3) is to consider k_{RED} as a measure of the efficiency with which the volume above the belt is occupied under dynamic conditions, compared to the maximum volume achievable at rest, for a prescribed degree of spillage.

Fundamental Test Variables

It is now possible to state what the independent and dependent variables should be in the basic test proposed.

The geometry, size of the system and the conveyed material are given. Among other properties, its bulk density, in the conical mode, has been determined. It is assumed that the variations of this density with the speed and loading of the belt are small and neglected (a fact qualitatively confirmed by observation).

The fundamental variables:

- mass flow rate, $\dot{m}$
- area of cross-section of the belt occupied by the material, or dynamic capacity, C_{DYN}
- V, belt speed

are related to each other and the measured bulk density, ρ_b, by

$$\dot{m} = \rho_b \, C_{DYN} \, V \, . \qquad (4)$$

We are at liberty to select V, the belt speed, as an independent variable. Increasing the belt speed might increase the conveyor carrying capacity, but this is not uniformly true since excessive speeds would increase spillage beyond tolerable limits due to blow-back and vibrations.

Similarly, we could select C_{DYN}, the cross-sectional area of the material on the belt, as an independent variable, and attempt to increase it (for fixed V) to increase the carrying capacity. Again, this might only be possible to a point, due to excessive mass spillage from the crumbling sides of the moving load.

Finally, the throughput $\dot{m}$ and belt speed V could be varied, but the dynamic capacity, calculated from equation (4), would still need to be related to the observed spillage rate.

Thus, in actuality, equation (4) should be used to compute C_{DYN}, given a spillage rate $\dot{s}$ related to the throughput and belt speed by

$$\dot{m} = F\ (\dot{s},\ V) \qquad (5)$$

or solving for $\dot{s}$:

$$\dot{s} = F\ (\dot{m},\ V). \qquad (6)$$

In this preferred form, the choice of independent and dependent test variables is apparent:

- for a series of experiments, the mass flow rate $\dot{m}$ will be set at a fixed value, $\dot{m} = \dot{m}_1$ (independent variable: $\dot{m}$)
- in that series of experiments, the velocity of the belt, V, will be varied over an operating range, i.e., $V = V_1$ such that $V_{min} \leq V_1 \leq V_{max}$ (independent variable: V)

For every pair $(\dot{m}_1, V_1)$, the spillage rate $\dot{s}$ will be measured as the dependent variable. As explained before, if $\dot{s} = s_*$ (some chosen value) for some pair $(\dot{m}_*, V^*)$ obtained from experimental or graphed results, C_{DYN}, the dynamic capacity for spillage rate

s_*, is computed as

$$C^*_{DYN} = \frac{\dot{m}_*}{\rho_b V^*} . \qquad (7)$$

Dividing this expression by C_{ST}, previously defined, the dynamic coefficient of reduction in capacity, k^*_{RED} (corresponding to spillage rate $\dot{s}_*$) is

$$k^*_{RED} = \frac{C^*_{DYN}}{C_{ST}} = \frac{\dot{m}_*}{\rho_b C_{ST} V^*} . \qquad (8)$$

In summary, it appears logical to select the throughput $\dot{m}$ and belt velocity V as independent variables, and to measure the spillage rate $\dot{s}$ as a dependent variable. Other subsidiary quantities, such as the dynamic capacity or coefficient of reduction in dynamic capacity or coefficient of reduction in static capacity, can then be computed from the previous ones.

Functional Dependence of Spillage and Mass Flow Rate on Velocity

On physical grounds, the expected dependence of the spillage rate on belt speed and mass flow rate can be obtained.

(a) Fixed Spillage Rate: Consider for given spillage rate, $\dot{s} = \dot{s}_*$, the dynamic reduction coefficient, k^*_{RED}. At very low speeds, this quantity is expected to be smaller than, but on the order of, 1. At very large speeds, on the other hand, the whole mass being conveyed will be spilled, due to aerodynamic effects, vibrations and shocks on the idlers. Ideally, $k^*_{RED} \to 0$ when $V^* \to V^*_1$, as shown in Figure 8. Thus, k^*_{RED} is conjectured to have the shape of a monotonously decreasing function, over the range of interest for V^*. But, since the mass flow rate $\dot{m}_*$ corresponding

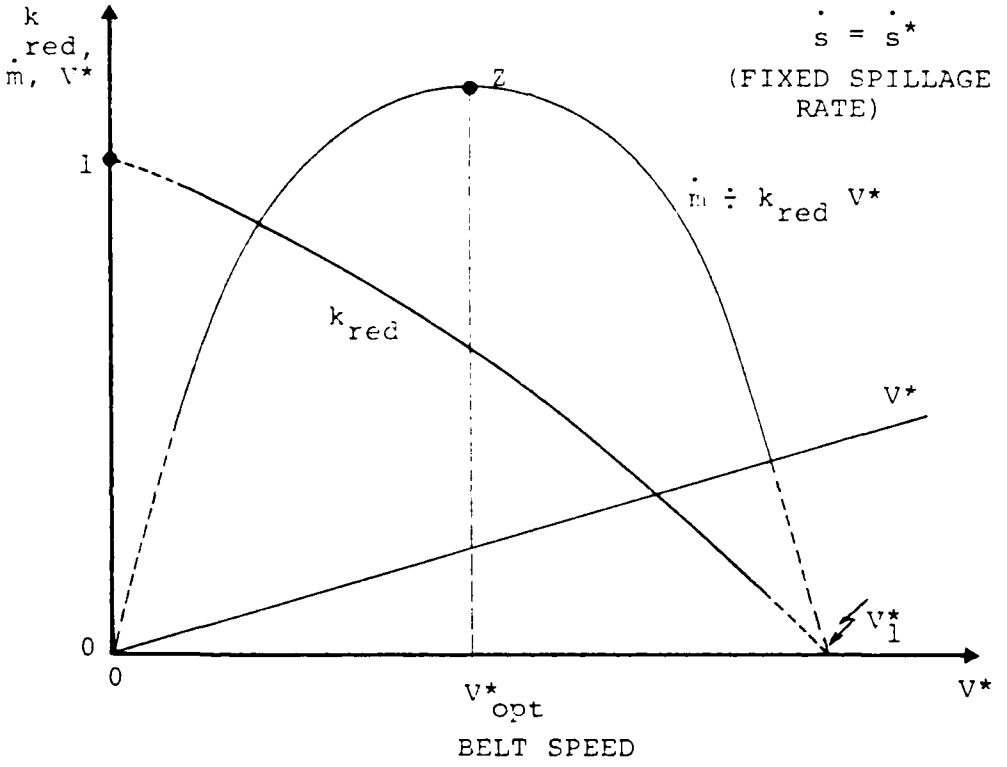

Figure 8. Shape of Curves of Dynamic Reduction Coefficient vs. Speed, and Mass Flow Rate vs. Speed (Fixed Spillage)

to velocity V* and spillage rate $\dot{s}_*$ is $\dot{m}^* = \rho_b C_{ST} k^*_{RED} V^{*2}$, it follows that $\dot{m}^*$ should have a maximum, shown as point Z in Figure 8. Thus: At given spillage rate, there should exist an optimal velocity for which throughput is maximized.

(b) Fixed Mass Flow Rate. Using Figure 8, in a plane of coordinates mass flow rate, velocity of $(\dot{m}, V)$, it is thus possible to locate two points, of abscissa V_C, V_D, respectively and ordinate $\dot{m}$, which are on a locus $\dot{m} = (\dot{s}_*, V)$, i.e., a curve of constant spillage rate, $\dot{s}_*$ (Figure 9).

If a number of plots such as Figure 8 were drawn, a family of curves having the shape sketched in Figure 9 and corresponding to various mass flow rates could be obtained. From these, in turn, curves giving the spillage rate vs. V, for given mass flow rate $\dot{m}$ are derived and given by equation $\dot{s} = (\dot{m}, V)$. For convenience, these curves will be labeled the "$\mathcal{S}$" curves (Figure 10).

(c) Use of the $\mathcal{S}$ Curves in System Design. In Figure 9, possible uses of the network of $\mathcal{S}$ curves are illustrated, such as:

- checking that a selected operating point, say P of coordinates $(V_P, \dot{m}_P)$ on Figure 10 corresponding to a combination of belt speed and throughput, has a spillage rate $\dot{s}_P$ which is considered acceptable.
- determining the maximum throughput, $\dot{m}_Q$, and corresponding velocity, V_Q, achievable at the prescribed maximum spillage $\dot{s}_{max}$ (Figure 10).
- choosing a preferred operating point between the two points (P and R on Figure 10) corresponding

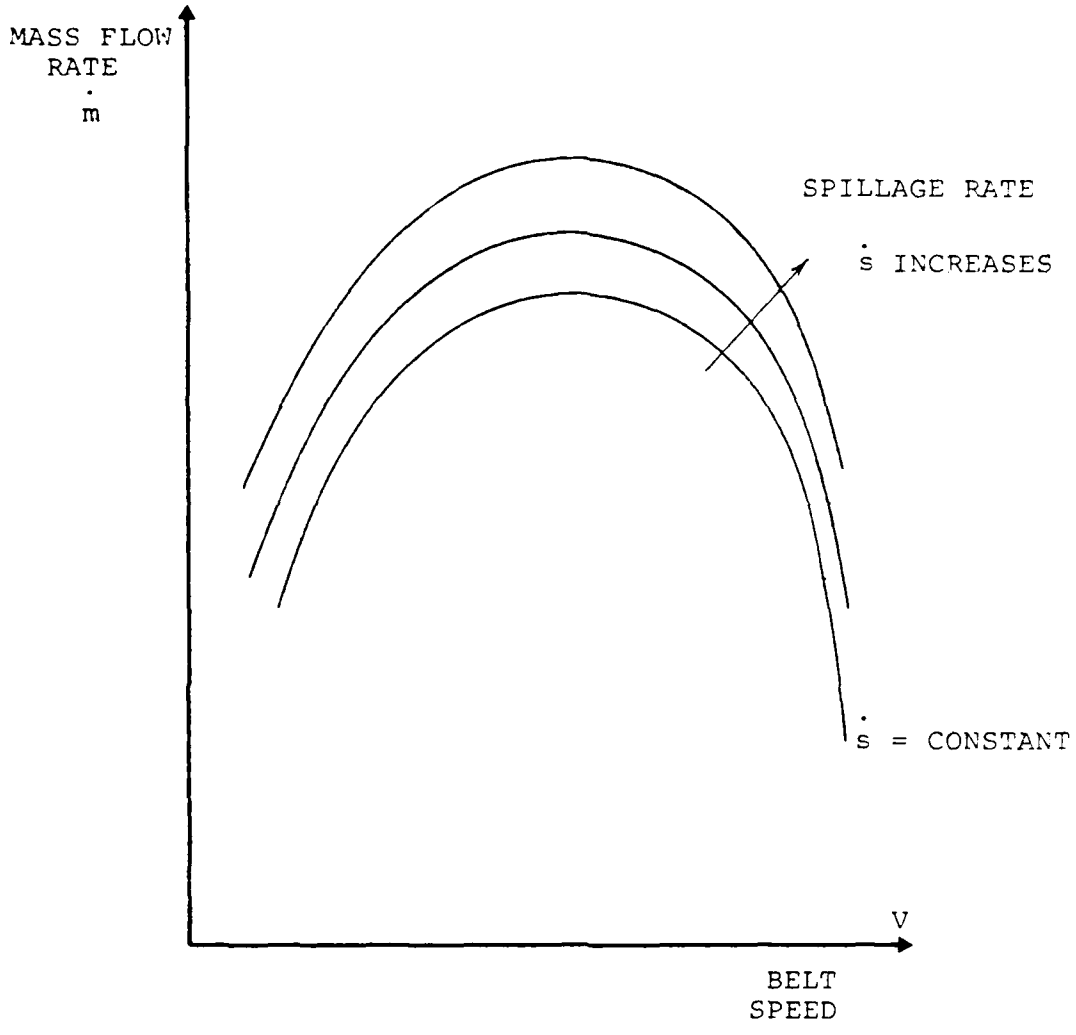

Figure 9. Curve of Mass Flow Rates vs. Belt Speed for Various Spillage Rates

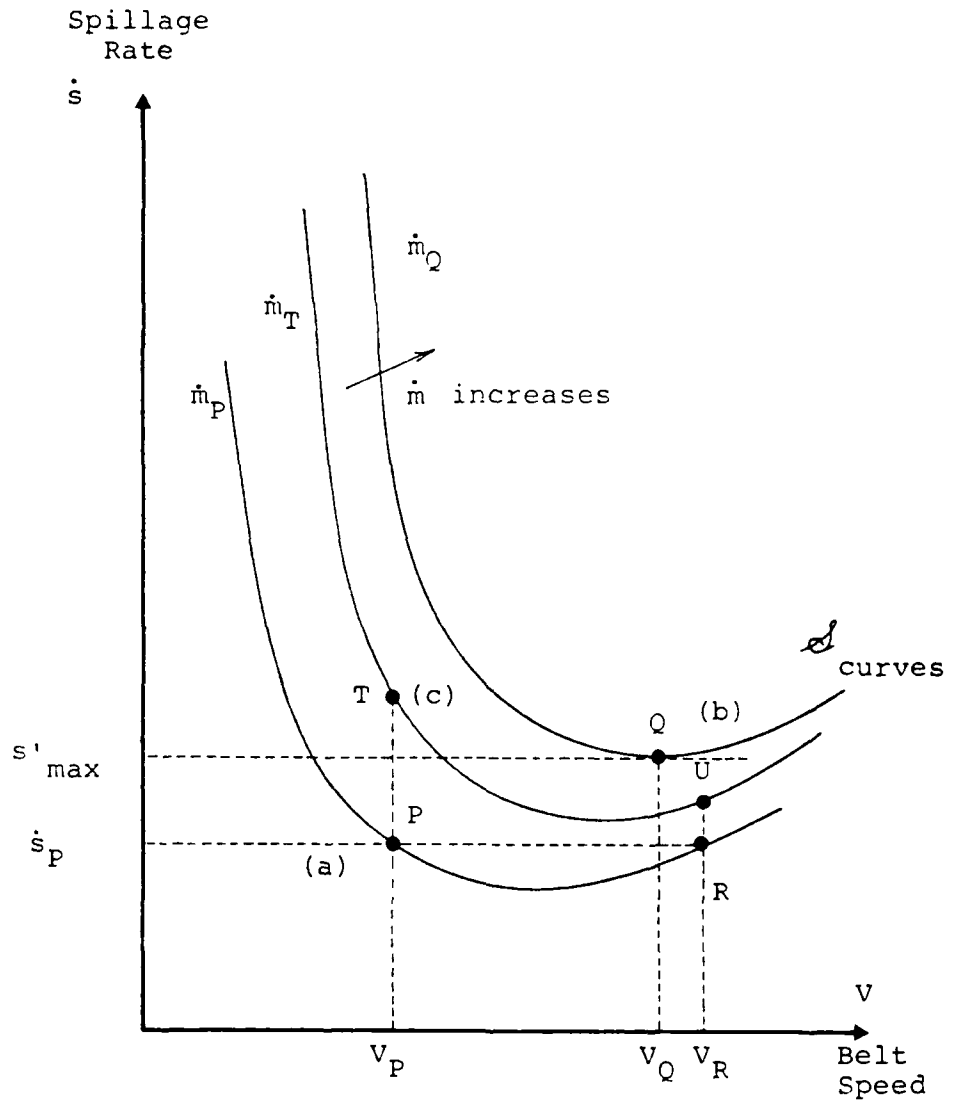

Figure 10. Examples of Use of $\mathscr{L}$ Curves

to a rate of spillage $\dot{s}_P < \dot{s}_{max}$. If, for example, the range ($\dot{m}_P$, $\dot{m}_T$) has to be covered in operation, then R would be preferable to P, since the rate of spillage corresponding to (V_P, $\dot{m}_T$) exceeds the maximum admissible $\dot{s}_{max}$. Such is not the case for point R, for which $\dot{s}_U$, corresponding to the higher speed V_R and a mass flow rate $\dot{m}_T$, is lower than the maximum admissible.

Inclined Belt: Analysis of Test Procedure and Variables

Preliminary Comments

The geometry of the inclined conveyor belt is sketched in Figure 11. In the present case, the inclination, α, is not zero.

If α is progressively increased until it reaches a threshold, α_{TH}, or angle of maximum inclination, the material will roll back on the belt. The forward motion of the material on the supporting inclined belt becomes impossible.

From the results in Table 3, Section II, it is observed that threshold α_{TH} is significantly lower than the angle of slide on the conveyor belting material. At angles equal to or larger than α_{TH}, backsliding becomes so pronounced that adequate, steady feeding cannot be maintained at the transfer point between the apron-feed/chute and the tail pulley of the belt. Accordingly, the experiments were limited to an upper limit for the inclination angle, α, relatively close to but lower than α_{TH}. For example, as described in detail in the test results below, for MSW:

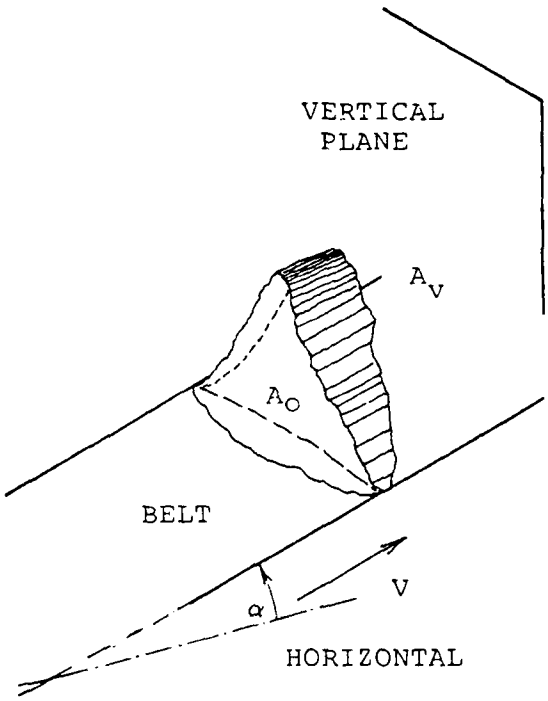

A_O: normal to belt through and belt speed

A_V: vertical - $A_V = \frac{A_O}{\cos \alpha} > A_O$

Figure 11. Increase in Vertical Cross Section with Inclination

Angle of maximum inclination of the belt: $\alpha_{TH} = 19°$

Angles selected for inclined tests: 18° (max.), 14°.

Choice of Variables

As explained above in the case of the horizontal belt, it appears logical to select as independent variables, for a given inclination angle α of the belt on the horizontal (refer to Figure 10):

- the belt speed V
- the mass flow rate, or carrying capacity, $\dot{m}$.

The dependent variable will again be: $\dot{s}$: spillage rate per unit mass of throughput and unit length of belt (as previously defined).

In a gross, qualitative sense, the arguments given in the preceding pages to justify the dependence of the spillage rate on the belt speed, at given mass flow rate $\dot{m}$, and of the spillage rate on the mass flow rate, at given belt speed, are expected to remain valid for the inclined belt, provided the angle of inclination is not too close to that leading to generalized slip and roll-back.

Hence the curves mass flow rate vs. belt speed, given V (belt speed), should have the general shape shown in Figure 9. Those giving the spillage rate vs. V (belt speed), given the capacity $\dot{m}$, would then look like the "$\mathcal{J}$" curves of Figure 10. The steepness of the sides, value of the optimum speed leading to minimum spillage and generally the position of the curve in the plane of

representation are expected to depart from those corresponding to the horizontal case.

Increasing the Inclination at Given Mass Flow Rate and Belt Speed

Qualitatively speaking, an argument could be put forth that increasing the inclination from zero leads to cross-section A_V (instead of A_0, for $\alpha = 0$) having larger and with steeper slopes (Figure 11). In the horizontal case, at relatively low V, the increase in carrying cross-section (or dynamic section) necessary to carry the same mass flow rate $\dot{m}$ at lower speed is accompanied by an increase in spillage rate. A similar effect can be presumed to exist if the belt is inclined: moderate for moderate inclinations, but extremely pronounced as α approaches the belt maximum inclination α_{TH}. As a function of V, the effect should be less important at high speeds than at low speeds, since less of the belt width is utilized and the height of burden can be kept smaller for the same capacity (Figure 11).

An increase in mass flow rate, when conveying a given material on a belt of given inclination α running at a given speed V, entails an increase in area of the cross-section on the belt occupied by material. This should cause an increase in spillage rate, as schematized in Figure 12.

Assuming the "$\mathcal{J}$" curves giving: $\dot{s} = \alpha(\dot{m}, V)$ for inclination α have the shape shown in Figure 13, there exists a minimum spillage $\dot{s} = \dot{s}_*$, at given mass flow rate $\dot{m} = \dot{m}_*$, corresponding to an optimum operating belt speed equal to V_*.

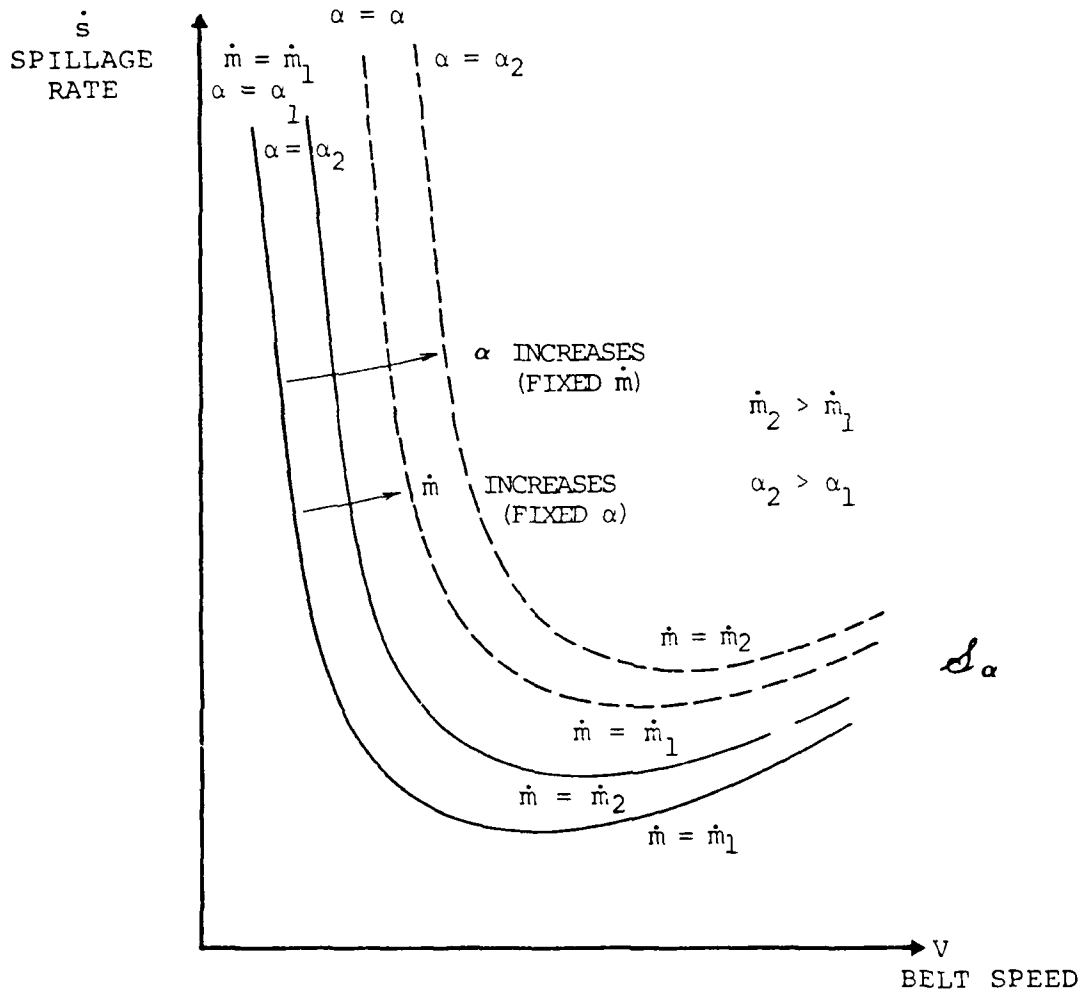

Figure 12. Family of Curves "$\mathscr{S}_\alpha$"

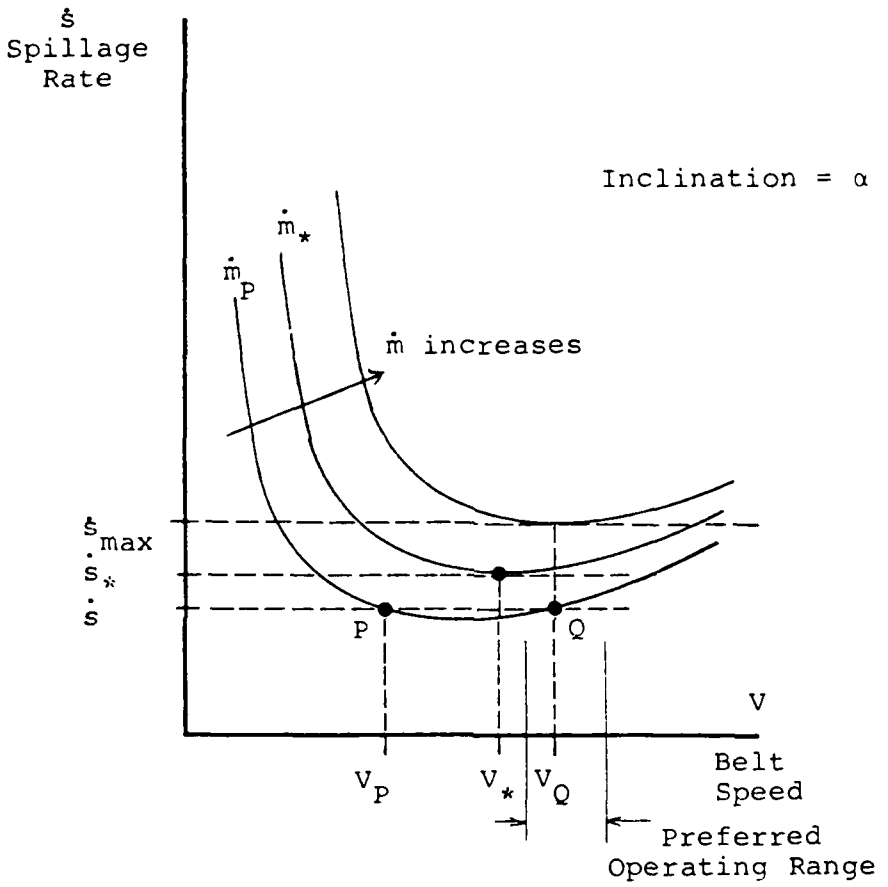

Figure 13. Optimum Speed V_* and Preferred Operating Range, at Inclination α

Operating Point

At inclination α and mass flow rate $\dot{m}_p$, two operating points (P and Q) might exist corresponding to a spillage rate $\dot{s}$ not exceeding the admissible one, $\dot{s}_{max}$ is reached.

Operating Range

The experimental results described below show that, in most instances, the sensitivity of the spillage rate to an increase in flow rate and/or inclination is, for the same level of spillage, much smaller in the upper range of belt speeds (i.e., to the right of the point). In such cases, it would be recommended to operate in this range (lower spillages under deliberate or accidental variations of belt speed and mass flow rates about the nominal design conditions). Figuratively speaking, at any practical inclination the belt should be operated "fast and lean" rather than "slow and loaded."

Other Comments

At high speed, the increase in spillage rate is due to aerdynamic "blow-back" and vibrations and shocks on the rollers and idlers. Physically, aerodynamic detachment and vibrations should not depend to any degree on inclination, at small angles to the horizontal. Thus, the level of spillages, all other factors being equal, should not vary much with the inclination α if the material is flat and self-compacting, as is the case with RDF. However, waste or fractions thereof containing a fair percentage of spherical or cylindrical pieces likely to roll down the inclined belt, should

show a rapid increase of spillage with speed in the upper range of speeds.

BELT CONVEYORS

Test Belt Conveyor and Test Procedures

The 7.63 m (25 ft) long and 0.457 m (18 in.) wide test belt conveyor was mounted in the closed loop rig shown in Figure 1. A variable speed drive provided a belt speed range of 0.20 m/s (40 fpm) to 2.55 m/s (480 fpm). Three-roller idlers of 20° and 35° and spaced at 0.91 m (3 ft) were used for the tests. A feed chute and 1:1 m (3.5 ft) of skirting were installed (following CEMA installation criteria) at the tail (feed) end of the conveyor in order to guide the material onto and across the conveyor belt. No other skirting was used during the tests.

By fixing the test conveyor speed (with all other belt speeds fixed) and placing a certain fixed mass of material on the test rig, a quasi-constant mass flow rate was provided. The material was recirculated for a period of 30 minutes and then all spillage from the test belt (including its frame), pulleys and floor was accumulated and weighed. The sides of the test conveyor were isolated plastic sheets to avoid including spillage from the return and feed conveyors (Figure 5).

Horizontal Mode Test Results

Results showing the dependency of spillage on speed and mass flow rate the dRDF and dRDF/coal blends are given in Figures 14 and 15 for several mass flow rates and 35° idlers. Figure 16, with

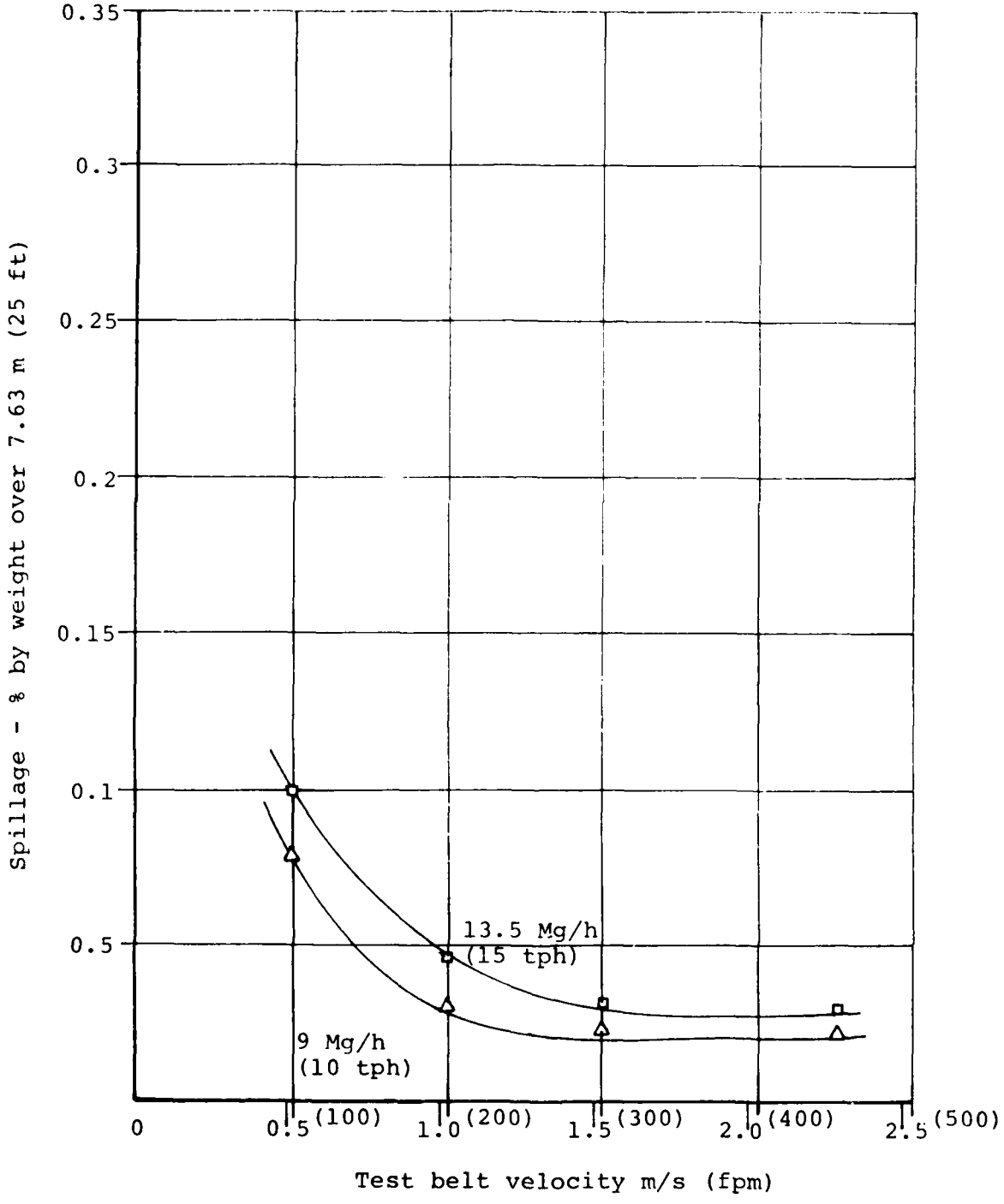

Figure 14. dRDF Sample Spillage vs. Belt Velocity and Mass Flow Rate with Horizontal Belt and 35° Idlers

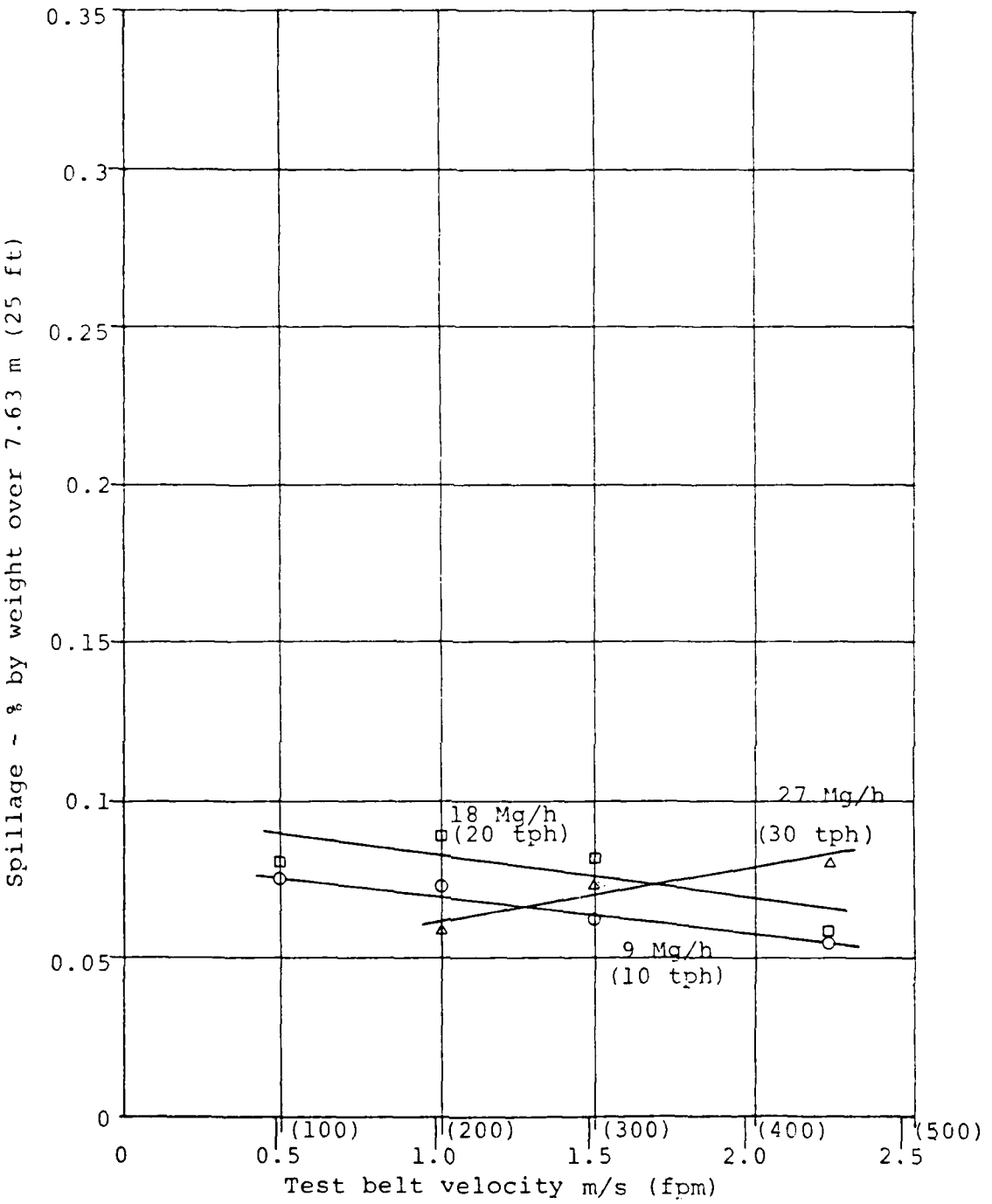

Figure 15. Coal/dRDF Blend Sample Spillage vs. Belt Velocity and Mass Flow Rate with Horizontal Belt and 35° Idlers

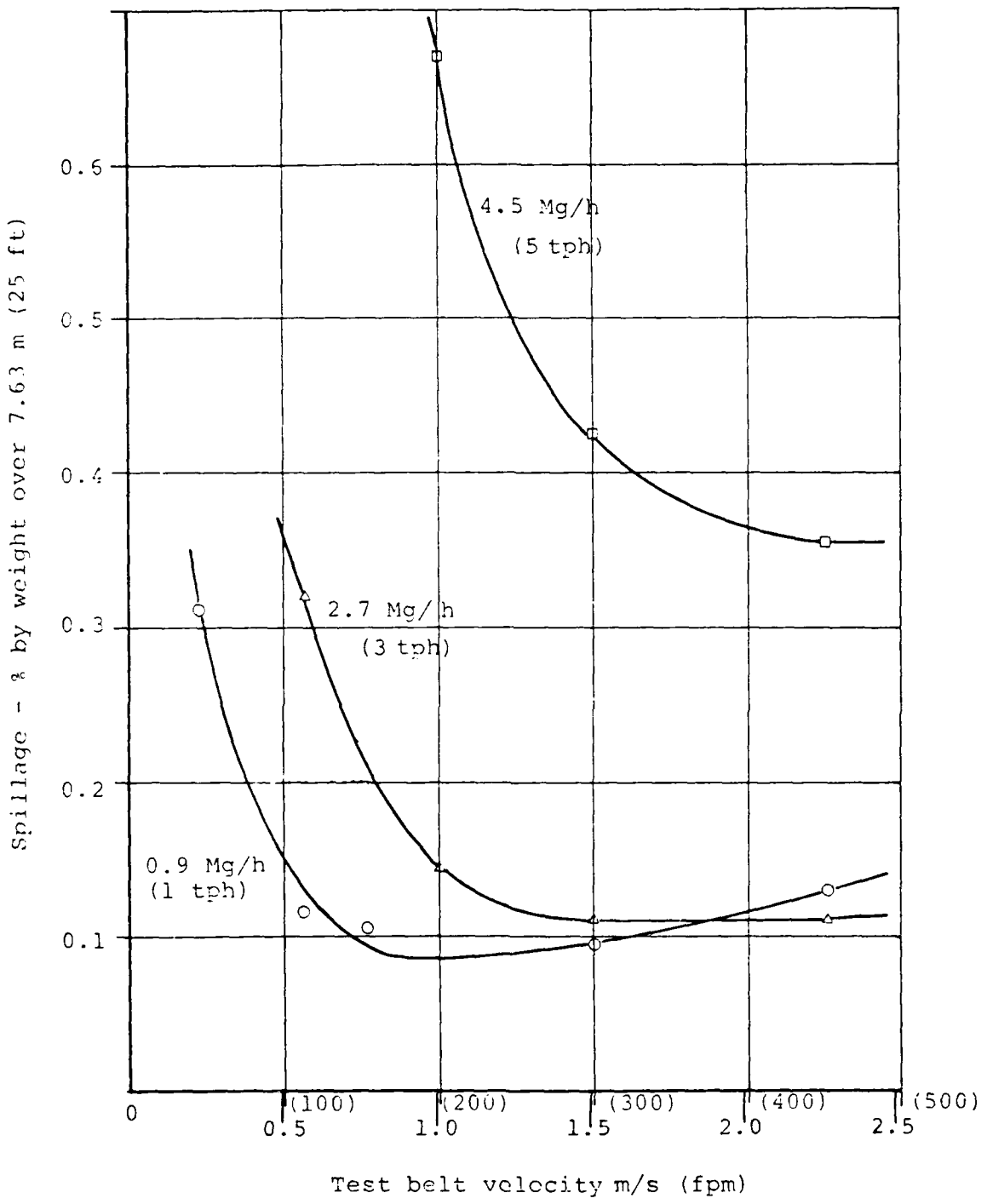

Figure 16. MSW Sample Spillage vs. Belt Velocity and Mass Flow Rate with Horizontal Belt and 35° Idlers

results for the MSW sample, is included for reference. The magnitude of spillage and shape of the curves in Figure 16 are most representative of that observed for the other processed waste fractions. These results are provided in full in the final EPA report (Reference 2). Note that the spillage is presented as a spillage rate reported as a percent of mass flow rate over the 7.63 m (25 ft) length test belt. Also, note the different scale in Figure 16.

Overall, the experimental results confirm the analysis outlined in the previous section.

High spillage rates are observed at lower belt speeds; as belt speed increases, the rate of spillage (for a constant mass flow rate) is reduced to a minimum. For all the materials except the dRDF and blend, spillage rates gradually increase again with increased velocity. Higher mass flow rates, for a given test material and belt speed, lead to higher spillages and the location of the minimum spillage points move toward the higher belt speeds. A discussion of the distribution and causes of spillage are discussed in the next section.

The results for the dRDF and dRDF/coal mixture indicate a much lower spillage rate than for any of the other materials evaluated. A number of factors would seem to be involved including the smaller, more uniform size, relatively homogeneous composition and increased bulk and particle densities.

The results for the dRDF sample in Figure 14 indicate a

---

[2] Z. Khan, Considerations in Selecting Conveyors for Solid Waste Applications.

leveling in spillage at about 1.0 m/s (200 fpm) and do not exhibit the increase at the higher speeds characteristic of the other fractions. This is probably due to the higher density and absence of easily windswept, flake-like material which accounts for much of the higher-speed spillage. It is likely that an increase in spillage would be observed were the belt velocities increased above the maximum 2.3 m/s (450 fpm) velocity evaluated (and achievable) with this test rig.

The scatter in the results for the dRDF/coal mixture (Figure 15) is greater than for any of the other materials evaluated. During the tests it was noted that the majority of the spillage measured for the dRDF/coal blend was in the form of fine coal dust generated in the transfer points in the test rig. It was not possible to isolate this coal dust or distinguish between the rapidly settling dust from particles of coal spilled off the conveyor. The magnitude (related to varying material contents) and settling patterns (related to air currents) of this coal dust may not have been constant for all the tests and the impact on the measured spillage was thereby inconsistant.

It is interesting to note from the data that operation of a conveyor belt to transport solid waste fractions, unless for very low throughputs, always generates spillage. Also, comparison of the results on several fractions in tests utilizing 20^{o} idlers clearly indicates that utilization of 35^{o} idlers helps in obtaining increased carrying capacity for the same velocity and amount of material spilled over a given time.

Spillage Distribution Along the Test Belt Conveyor

The test data reported in Figures 14-16 indicate the total weight of material spilled from the full length of conveyor length during the test period. On selected tests, data were also collected to establish the proportion of spillage from each of four conveyor sections. The results provide some insight to specific problem areas and suggest the zones where conveyor modifications (skirting, hoods, etc.) could most effectively reduce spillage.

For this test, the belt conveyor (Figure 17) was divided into four sections (labeled 1 to 4, measured from the tail to the head pulley) of length 1.1 m (3.5 ft), 1.7 m (5.5 ft), 3.7 m (12 ft) and 1.2 m (4 ft), respectively (Figure 17). Spillage was separately collected and weighed for each of these sections.

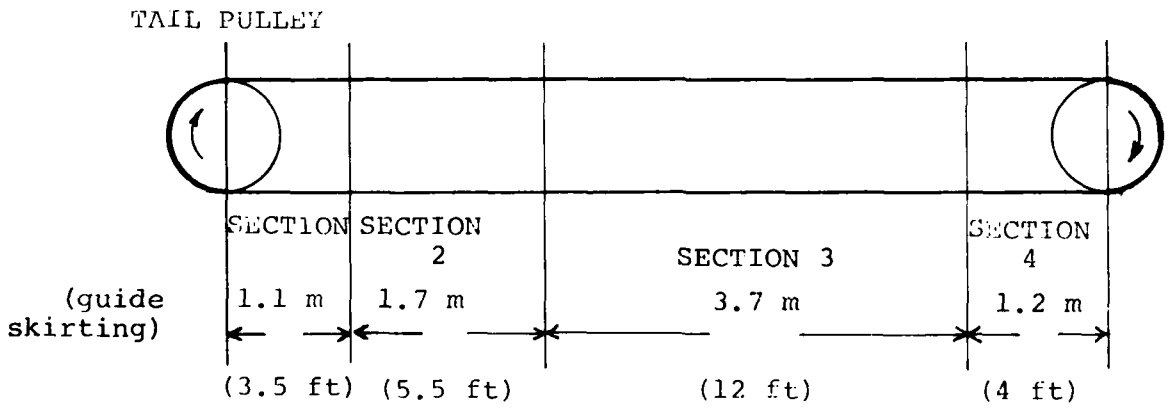

Figure 17. Subdivision of the Test Belt Conveyor for Sectional Spillage Measurements

Care was taken in isolating the spillage from one area and preventing carryover of material from one section to another. (Successful except in controlling the spread of coal dust as mentioned above.) Sheeting was used to prevent material falling on the return idler frame or on the return side of the belt and being carried back towards the tail pulley.

Table 12 presents the results of sectional spillage measurements on all six fractions at a single mass flow rate and three velocities. General observations on the nature and mechanisms of spillage from each belt section may be instructive. The spillage in Section 1 resulted from fines wedged between the belt and its skirting, and squeezed and blown out by material falling on the belt. The spillage in Section II is mainly the result of crumbling and sluffing of the material, particularly from surges, over the sides of the conveyor. The spillage in Sections III and IV may be the result of several factors. Air currents (blow-back) created at higher speeds are observed to sweep paper and lighter materials off the belt. The reaction of the belt as it passes over the idlers is also amplified at higher speeds and results in a rhythmic bounce which will increase spillage of more dense components of RDF (glass, wood) or higher density heterogeneous fractions (heavy fraction or ferrous metals). Higher speeds also result in more turbulence and associated dusting and spillage at the discharge.

The results for the dRDF fraction show a trend toward

TABLE 12. SECTION CONVEYOR SPILLAGE AS A PERCENT OF TOTAL SPILLAGE

Product	Belt Section	Percent of Total Spillage Test Conveyor Velocity, m/s (FPM) 46 (150)	92 (300)	137 (450)
RDF at 2.7 Mg/h (3.0 tph)	1	37.5%	23.5%	24.2%
	2	43.0%	9.5%	13.1%
	3	13.2%	14.6%	13.6%
	4	6.3%	52.4%	49.1%
MSW at 2.7 Mg/h (3.0 tph)	1	41.7%	30.2%	29.7%
	2	39.7%	16.4%	14.9%
	3	11.6%	10.9%	13.9%
	4	7.0%	42.6%	42.5%
Heavy Fraction at 9.1 Mg/h (10.0 tph)	1	38.5%	33.3%	50.0%
	2	46.2%	44.4%	25.0%
	3	6.4%	5.6%	8.3%
	4	9.0%	16.7%	16.7%
Ferrous Fraction at 9.1 Mg/h (10.0 tph)	1	25.0%	15.0%	6.7%
	2	50.5%	18.1%	56.3%
	3	17.9%	59.1%	31.9%
	4	6.7%	7.6%	5.1%

TABLE 12. SECTION CONVEYOR SPILLAGE AS A PERCENT OF TOTAL SPILLAGE (CONCLUDED)

Product	Belt Section	Percent of Total Spillage Test Conveyor Velocity, m/s (FPM) 46 (150)	92 (300)	137 (450)
d-RDF/coal blend at 9.1 Mg/h (10.0 tph)	1	89.1%	72.8%	67.0%
	2	2.9%	2.5%	4.8%
	3	3.0%	6.8%	11.7%
	4	4.9%	17.8%	16.4%
d-RDF at 13.6 Mg/h (15.0 tph)	1	15.0%	20.0%	66.7%
	2	2.5%	10.0%	11.1%
	3	47.5%	10.0%	11.1%
	4	35.0%	60.0%	11.1%

increased spillage on the feed end (Sections I and II) as velocity increases, contrasting with an opposite trend with the dRDF/coal mixture toward increased spillage in the running and discharge sections (Sections III and IV) with high velocity

It should be noted that the total spillage rates for the dRDF and blend are relatively small overall (Figures 14, 15) and the variation may only reflect the random spillage characteristics for the material or the effect of variations in dust generation and settling discussed earlier.

Belt Conveyor Discharge Trajectories

The trajectories or discharge paths of material over the end pulley of a conveyor are important to the proper design and function of discharge chutes, wear plates or splitters. A method for calculating discharge trajectories is available from CEMA (Reference 1) and was applied to the MSW, RDF, heavy and ferrous fractions, using the properties of these materials and conveyor dimensions and operational parameters from the test program. Corresponding experimental measurements were made of the discharge trajectories for the four fractions at a fixed mass flow and for varying belt velocities (similar calculations and measurements were not in the scope of the dRDF and blend testing). An example of the results of the theoretical and experimental discharge trajectories for RDF are plotted in Figure 18. It can be seen the values correspond reasonably well. The calculations would no doubt be as accurate in use to predict trajectories of even more homogeneous fractions and uniform materials such as dRDF and dRDF/coal blends.

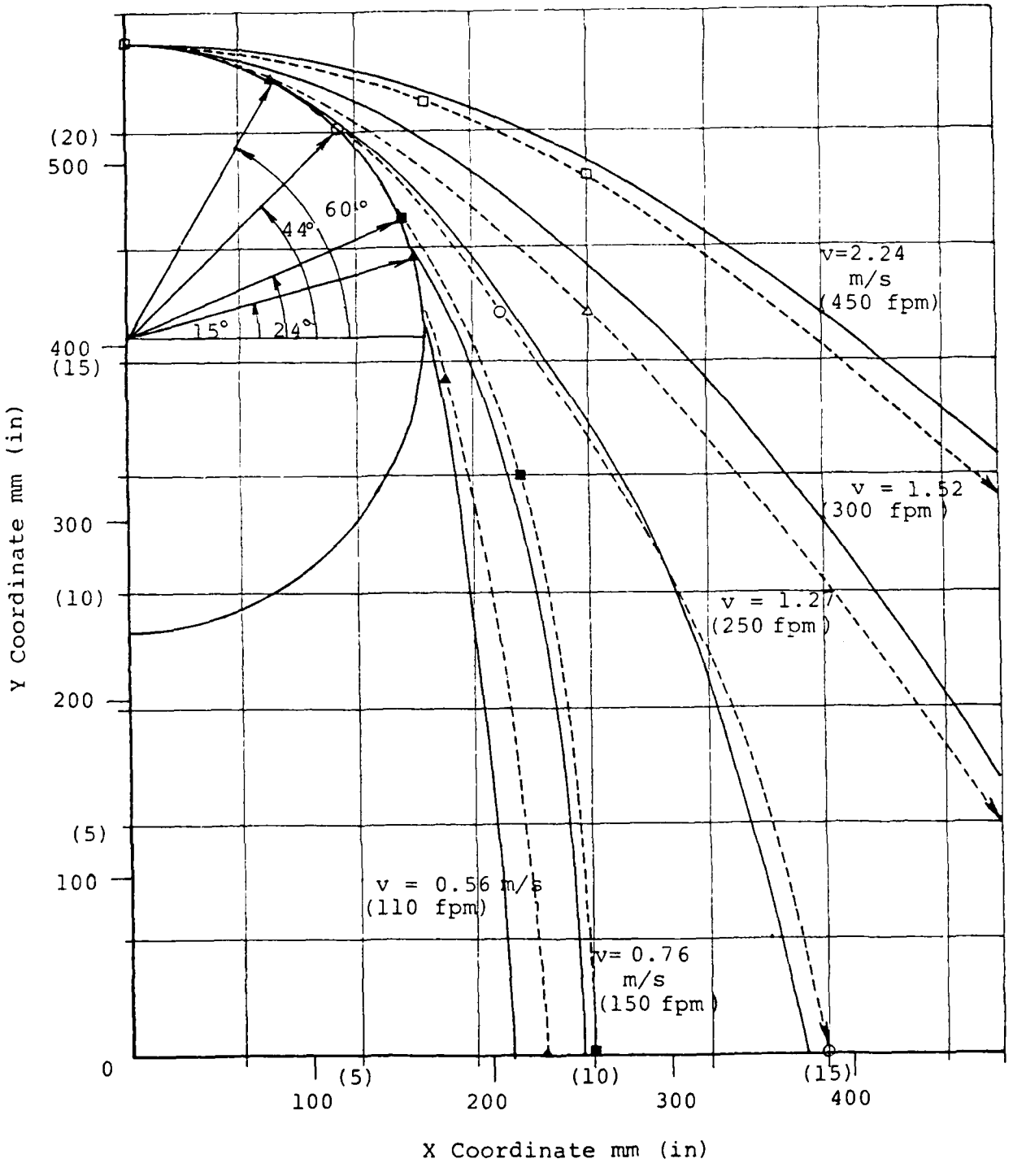

Figure 18. Trajectories for RDF Fraction at 0.9 Mg/h (1 tph) and 20° Idlers

Conveyor Power Consumption

The test belt conveyor drive includes a motor connected by variable pitch pulleys to a shaft-mounted reducer. Initial tests were conducted to establish relationships between mass flow rate and velocity and the power consumption, using an ammeter to measure motor current as an indicator of power consumption.

Contrary to what was expected, results showed negligible measurable change in the motor current for a wide range of velocities or flow rates. This negligible change in power consumption (despite extreme variations in conveying conditions such as speed, incline and load) is probably attributable to use of a motor larger than that required for these applications. Specific information and procedures for detailed calculation of conveyor power requirements is available in Reference 1.

Incline Mode Test Results

Tests were conducted to study the measured spillage vs. mass flow rate and speed for a given quantity of material and test belt inclination. For the dRDF and blend, an inclination of 14° was tested. The results are reported in Figures 19 and 20. When compared with the horizontal test results (Figures 14, 15), the results overall corroborate the analysis tht higher spillages are encountered on increasing the conveyor inclination and that, as before, a preferred speed or range of speeds exists for a given mass flow rate and inclination. For the dRDF test, the increase in spillage is not as great as for the dRDF/coal mixture where

---

[1]Conveyor Equipment Manufacturers Association, Belt Conveyors for Bulk Materials.

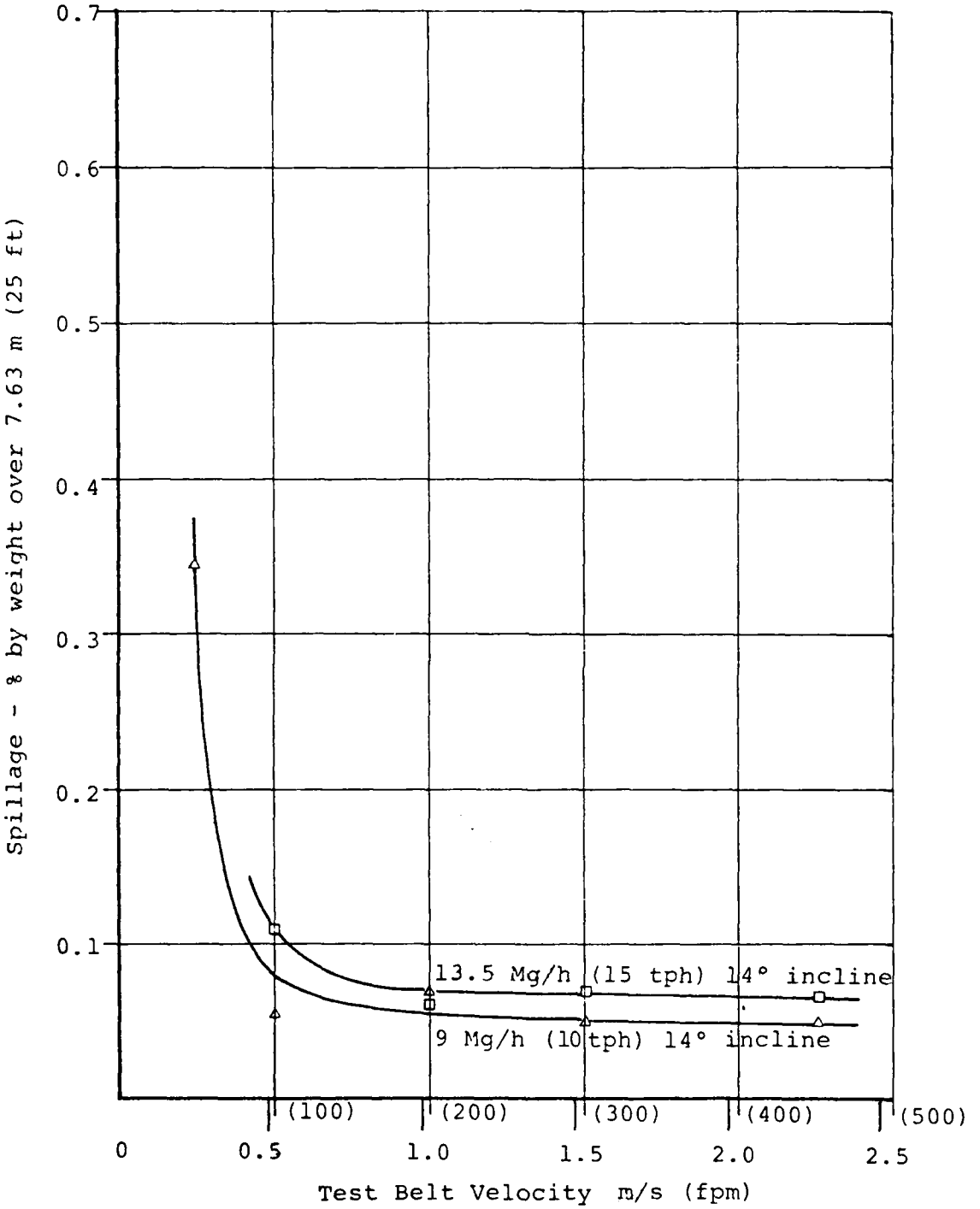

Figure 19. dRDF Sample Spillage vs Belt Velocity with Inclined Belt and 35° Idlers

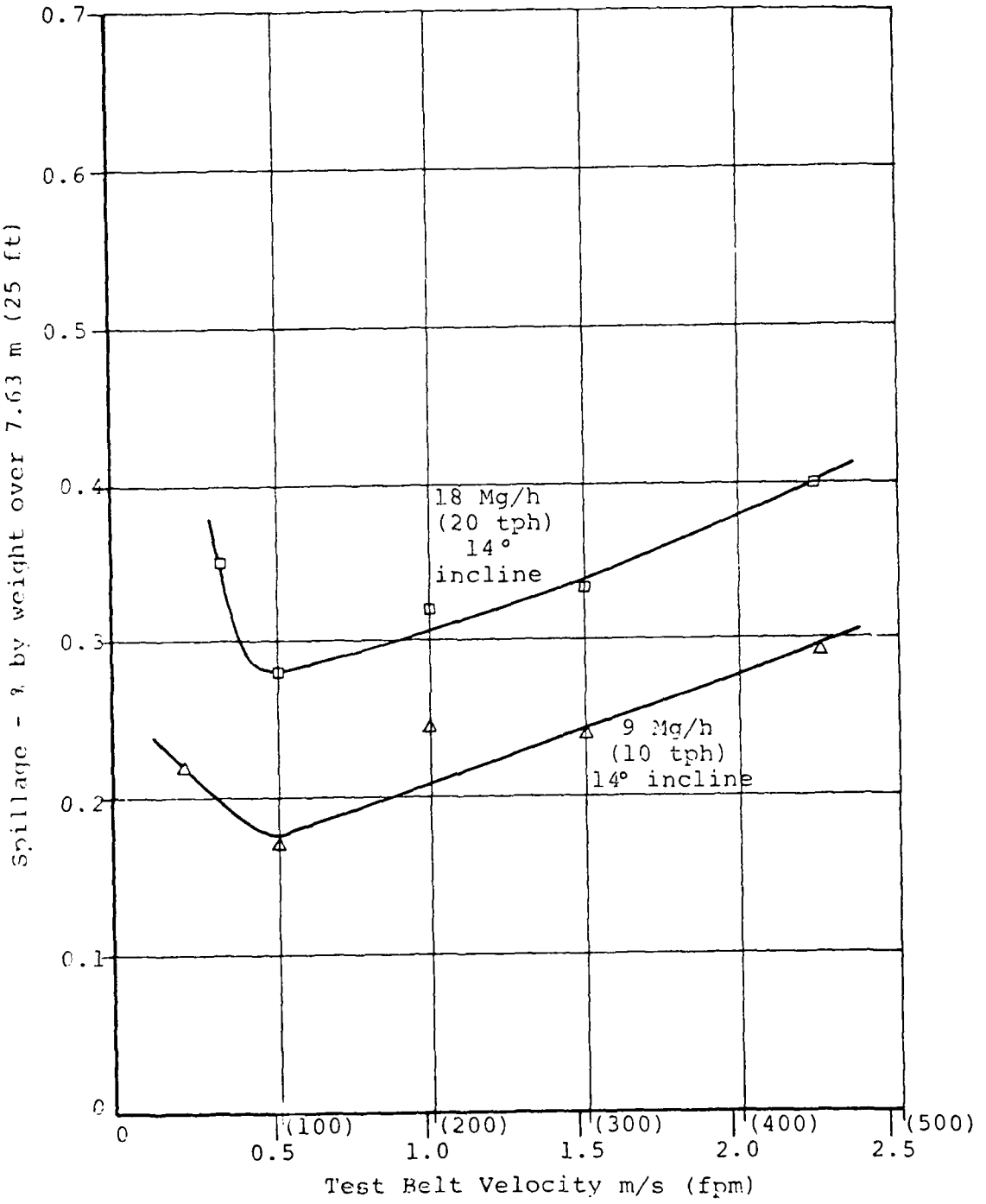

Figure 20. Coal/dRDF Blend Sample Spillage vs Belt Velocity with Inclined Belt and 35° Idlers

the increase is by a factor of 3 or 4. Also, note hyperbolic shape of the curves in Figure 20 which indicate a velocity range for lower spillages that were not observed in the horizontal test results.

Observations of the six materials evaluated indicated spillage on the inclined belt was often precipitated by slippage or roll back of material on the belt. For relatively homogeneous material such as dRDF and dRDF/coal blends, this was not as evident and the increase in spillage on increasing the conveyor inclination was not as severe compared to results for the lighter more heterogeneous material (Reference 2). Apparently, the higher density and relative uniformity makes such materials less prone to slipping or rolling back on the inclined conveyor.

Dust Generation

High volume air samplers (Sierra Model 305-205OH) were used to determine the magnitude of dust generated during transport of the solid waste fractions on the inclined test belt conveyor. The objective was to determine if any relationship between the extent of dust generated for parameters, such as the feed type, mass flow rate or the test belt velocity or angel of inclination. One dust sampler was placed approximately 1.6 m (5 ft) from the tail end to measure the quantity of dust generated around the infeed end of the belt conveyor. A second dust sampler was located approximately 6.1 m (20 ft) perpendicularly off the center of the conveyor system. The results of the second sampler were found to be inconsistent and unreliable. This may be due to

---

[2] Z. Khan, et al., Considerations in Selecting Conveyors for Solid Waste Application.

reflection of dust from the walls or air currents in the testing area. Therefore, only the dust loadings measured by the sampler located at the conveyor feed end are reported.

The test results provide the total suspended dust. Particle size distribution or any further characterization of the dust was not attempted. The test method and calculations are given in Appendix A.9. For complete details on dust sampling methods and procedures, also refer to ASTM Standards D 2009 and D 1356.

While there are inconsistencies in several cases and no trends common to all tests, the overall results indicate that for higher mass flow rates and belt conveyor inclinations, there is a tendency towards greater dust generation.

The test results for the dRDF and dRDF/coal mixture are reported in Figures 21 and 22. Dust loading for RDF and dRDF were comparable. The MSW and heavy fraction test results indicated relatively constant loadings at or below 5 mg/scm while the dRDF/coal mixture results are by far the highest. OSHA requires that employee exposure to total dust in any 8-hour work shift of a 40-hour week shall not exceed the time weighted average of 15 mg/scm (Reference 9). Although the sampling technique, location and test facility are not considered typical, the data does suggest that for RDF, dRDF or blends, dust control systems particularly at transition points may be necessary.

---

[9]U.S. Department of Labor, Occupational Safety and Health Administration, OSHA Safety and Health Standards, No. 2206, Part 1910, Paragraph 1000, Table 2-3, pp. 504-510.

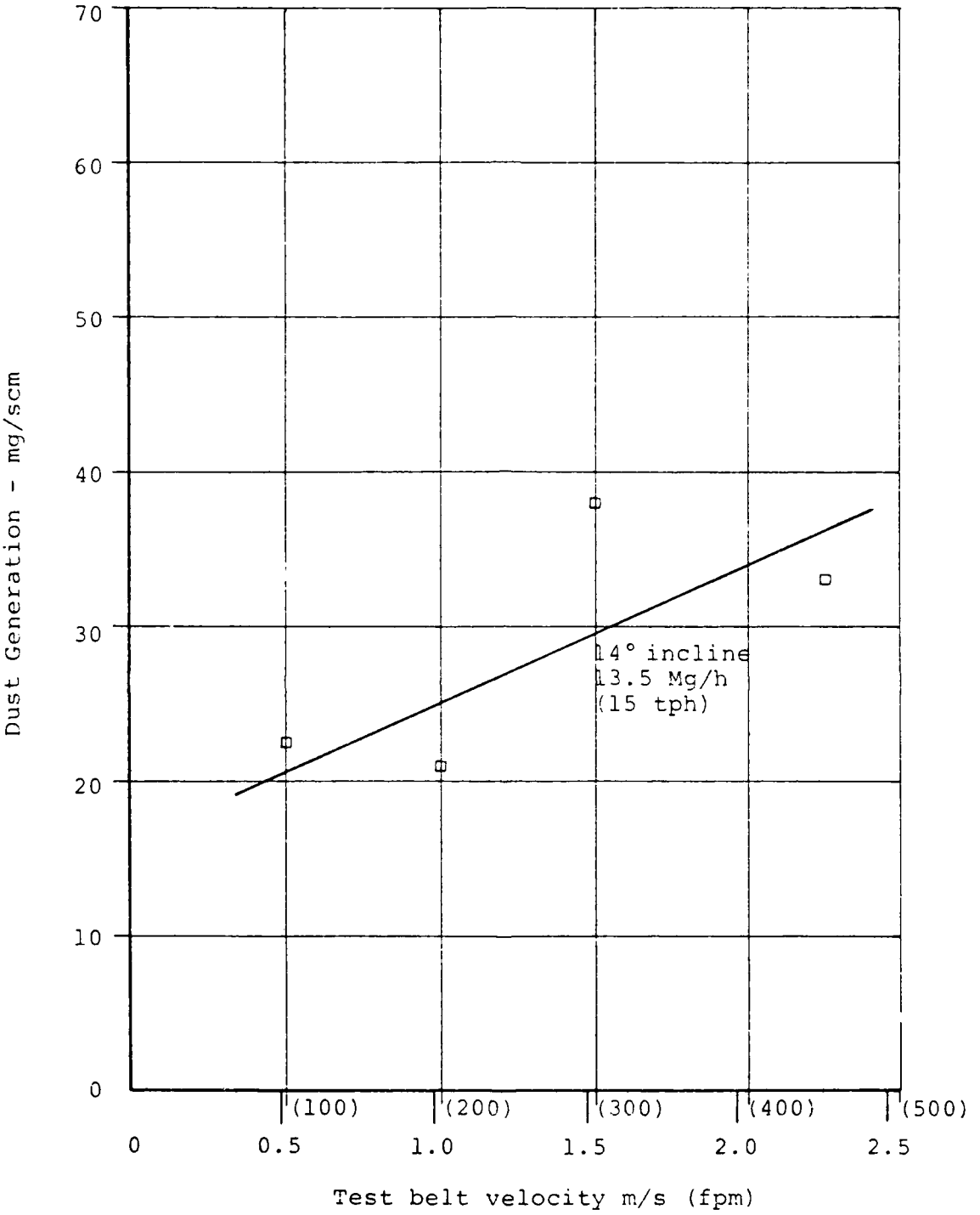

Figure 21. Magnitude of Dust Generated Conveying dRDF on Test Belt Inclined at 14°

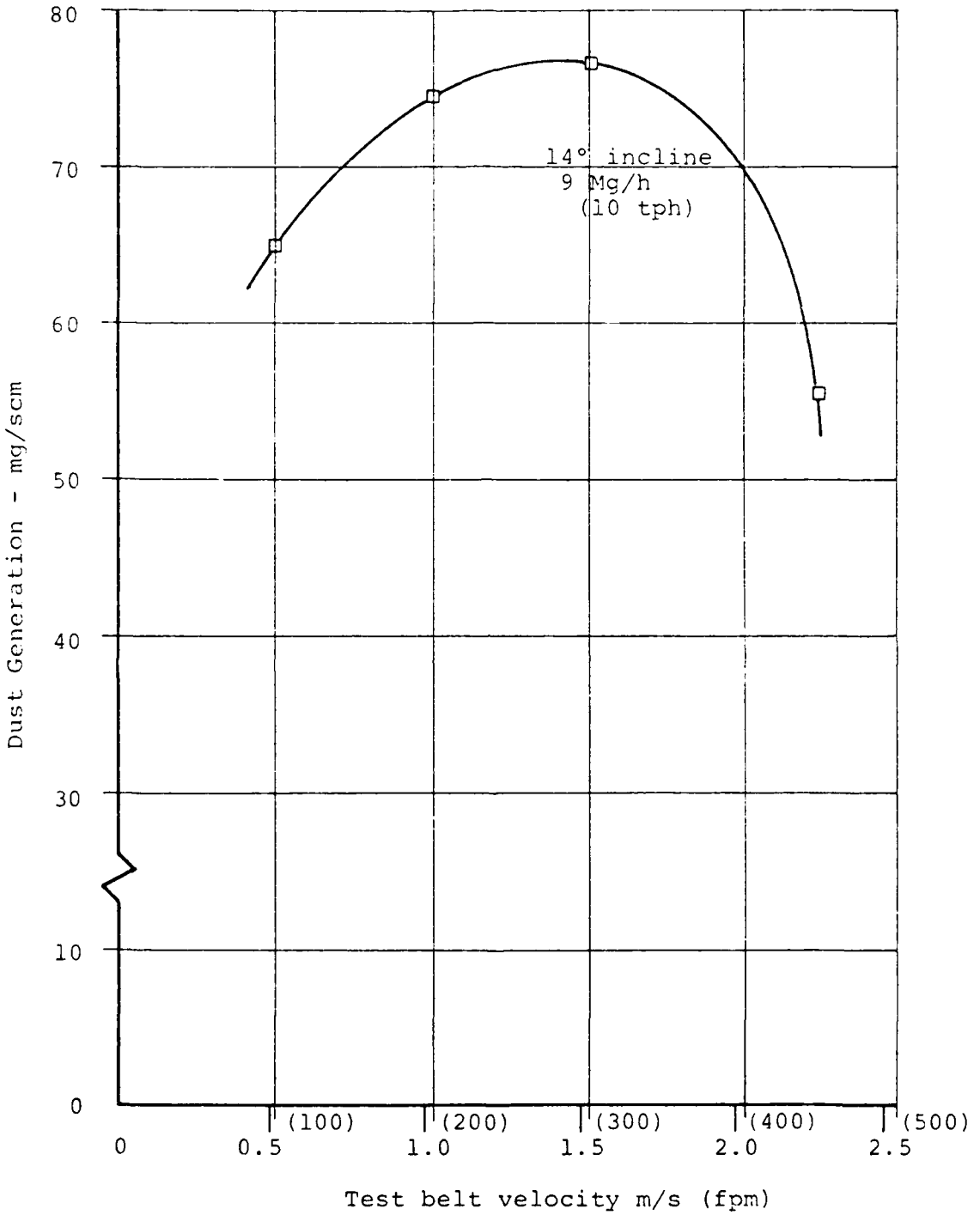

Figure 22. Magnitude of Dust Generated Conveying dRDF/coal Blend on Test Belt Inclined at 14°

SECTION IV

VIBRATING CONVEYORS

INTRODUCTION

Vibrating conveyors have been utilized to transport bulk materials in the mining and other industries for many years. This type of conveyor has relatively few moving parts and is designed to operate with minimum maintenance. Typical applications of vibrating conveyors in a resource recovery plant have been in the feed or discharge from unit processing equipment such as shredders and air classifiers. In comparison to a belt conveyor, vibrating conveyors can level and distribute the feed and will not be damaged by impact of hot or abrasive material discharging from a shredder.

The principle of operation of vibrating conveyors is illustrated in Figure 23. The drive provides an acceleration to the pan with both vertical and horizontal components. A particle resting on the pan is lifted up and forward and is throuwn in an arc that returns it to the pan during the next vibration period (one-cycle jump). Referring to the figure, the particle "a" leaves the pan at the time "t_s" (when the acceleration of the pan equals that due to gravity), strikes it again at "t_a" and leaves it at "$t_a + 1/f$", where f is the frequency of vibration (cycles/sec). In this example, the take-off and landing times are within one pan vibration period, referred to as a one-cycle jump. It is also possible to accelerate the material (by a higher stroke) to a two or more cycle jump, but that mode would require a much higher energy input.

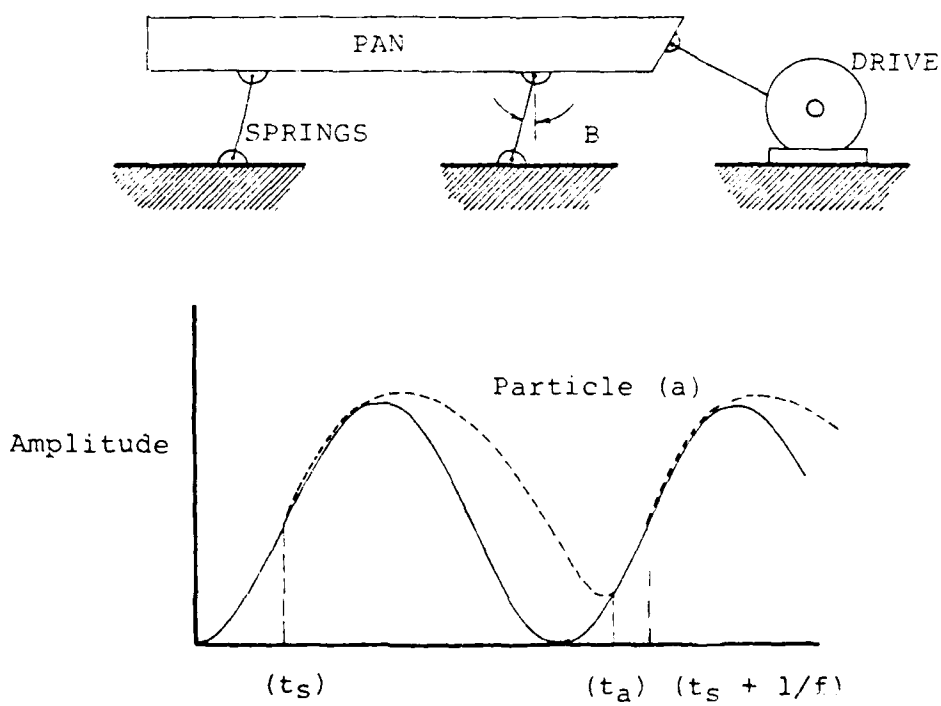

Figure 23. Vibrating Conveyor Principle of Operation

TEST VIBRATING CONVEYOR AND TEST PLAN

The test vibrating conveyor was 4.6 m (15 ft) long by 0.6 m (2 ft) wide with a pan height of 205 mm (8 in.). Manufactured by Carman Industries, the conveyor was driven by an eccentric rotating cam linked mechanically to the pan at 30°. Major components of the conveyor are depicted in Figure 24 and pictured in the test rig installation in Figure 25.

Utilizing a variable speed drive and two interchangeable eccentric cams, the frequency could be varied between 400 and 570 cycles/min and the stroke set at either 12.7 m (0.5 in.) or 22.2 mm (0.875 in.).

To maintain a fixed stroke and frequency, it was necessary to dynamically balance the conveyor through removal or addition of leaf springs or counter weights. These efforts were not completely successful as can be seen in Table 13. This table shows the variation of the length of stroke in the conveyor subcomponents with respect to frequency.

The conveyor is designed so that the pan and counter weight should operate at similar and offsetting stroke lengths and the base would thus remain steady. The results in Table 13 indicate that such was not the case and there remained an imbalance in the system, as well as limit on the range of operating frequencies. Unfortunately, the scope of this program did not allow resolution of this particular problem or, more generally, the investigation design of a variable stroke and frequency conveyor system.

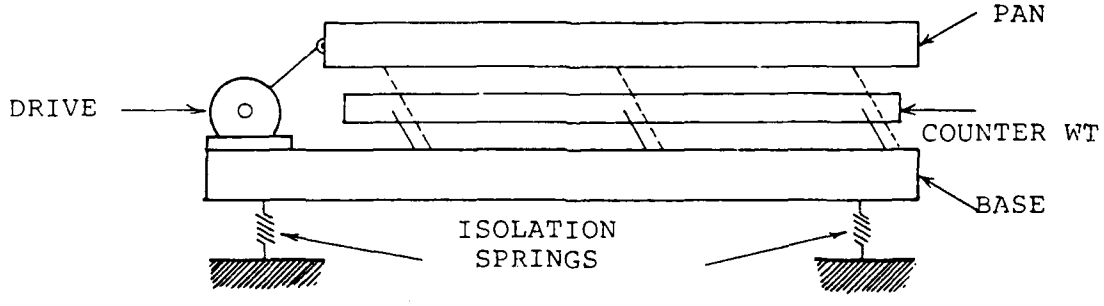

Figure 24. Schematic of Vibrating Conveyor

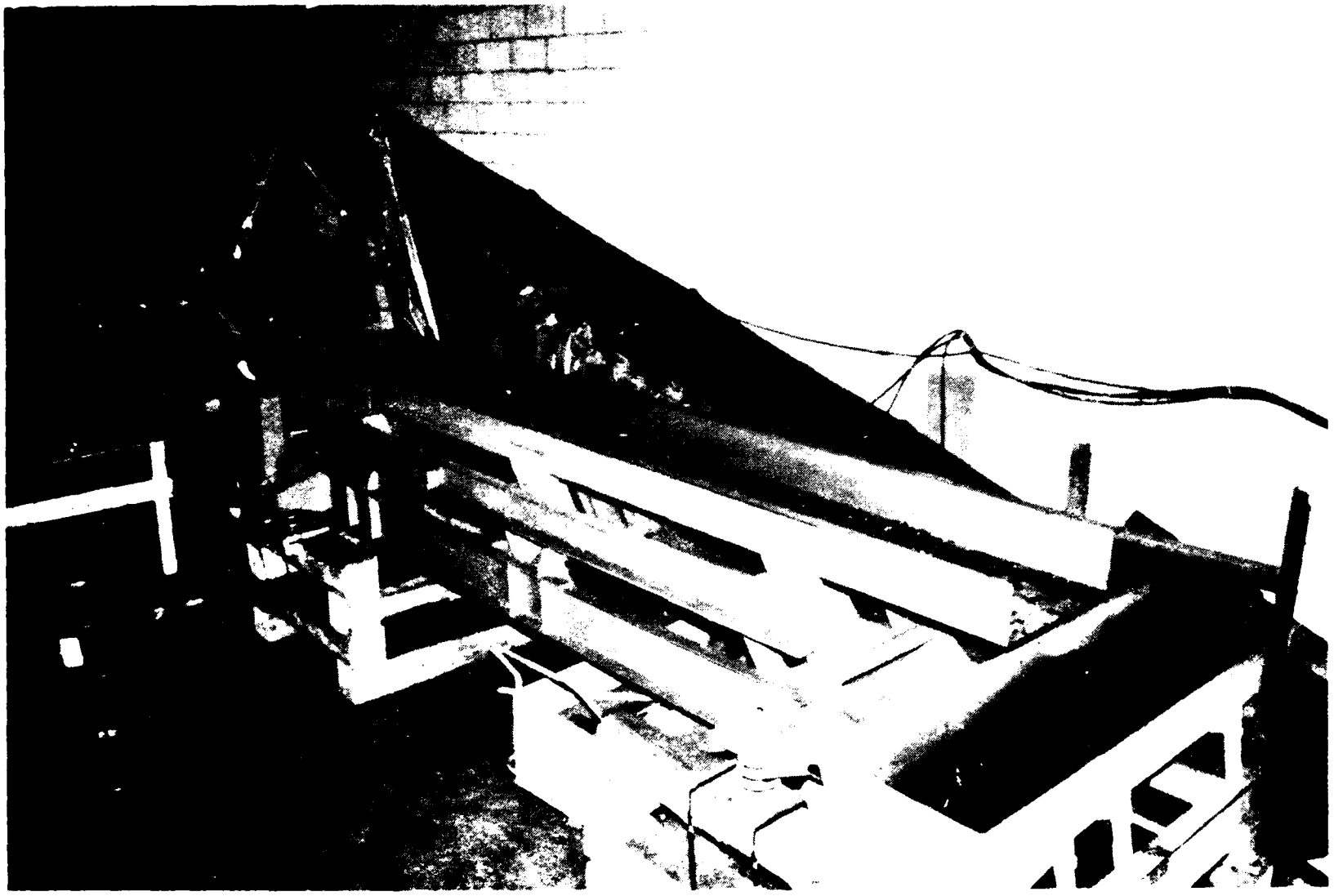

[illegible] Conveyor Installation

TABLE 13. TEST VIBRATING CONVEYORS OPERATING RANGE

Frequency (rpm)	7/8-in. Cam Stroke Counter Wt Pan	Base	1/2-in. Cam Stroke Counter Wt Pan	Base
390	5/8"	3/8"	3/16"	3/8"	3/16"	1/16"
410	5/8"	3/8"	1/8"	3/8"	3/16"	1/16"
430	11/16"	3/8"	1/8"	3/8"	1/4"	1/16"
450	11/16"	3/8"	1/8"	3/8"	1/4"	1/16"
470	3/4"	1/2"	1/16"	3/8"	1/4"	0
490	3/4"	1/2"	1/16"	7/16"	1/4"	0
510	13/16"	5/8"	0	1/2"	7/16"	0
530	7/8"	3/4"	0	9/16"	7/16"	0
550	1 1/16"	1 1/8"	3/16"	13/16"	9/16"	1/16"
570	Excessive vibration				1 1/16"	1/4"

Springs on Pan assembly 11

Springs on Counter weight assembly 14

The operating range thus had to be selected on an empirical basis with an imposed criteria that the vibration of the base not exceed 3.2 mm (1/8 in.). The variations in actual pan stroke have been accounted for in the presentation of the data in the following manner: all points corresponding to a pan vibration of 12.7 $\pm$ 3.2 mm (1/2 $\pm$ 1/8 in.) were considered "12.7 mm" stroke tests, and all points for which the amplitude was 22.2 $\pm$ 3.2 mm (7/8 $\pm$ 1/8 in.) were considered "22.2 mm" (7/8 in.) stroke tests. These conditions limited the range of operating frequency to 430 to 545 cpm at 22.2 mm stroke and 390 to 550 cpm for 12.7 mm stroke.

The objectives of the test were to determine, for the two values of stroke specified, the following:

- Vibration frequency and stroke vs. maximum carrying capacity.
- Vibration frequency and stroke vs. conveying speed for a given mass flow rate.
- Energy consumption vs. material burden depth for a given frequency.
- Compaction of material along length of pan.
- Dust generation.

TEST RESULTS

Vibration Frequency and Stroke vs Maximum Carrying Capacity

Maximum carrying capacity here is defined as the maximum mass flow rate the vibrating conveyor will transport with

negligible spillage. After fixing the conveyor frequency, the pan was loaded to the top of the sides with the solid waste fraction. The conveyor was started and the discharge timed and weighed to give the maximum carrying capacity.

From Figures 26 and 27, it is evident that the relative capacity is proportional to the material density and the maximum carrying capacity increases with both stroke and frequency. By increasing the amplitude from 12.7 m (1/2 in.) to 22.2 m (7/8 in.), the increase in carrying capacity (at 540 rpm) for the six materials varies between a 170% increase for heavy fraction to a 262% increase for the MSW.

Vibration Stroke and Frequency vs Conveying Speed for a Given Mass Flow Rate

At a given mass flow rate, the conveying speed was measured for variations in frequency and stroke.

From Figure 28, it is seen that in all cases the conveying speed increased with higher frequencies. Increased speed may be desirable in reducing potential for build-up, jammming and spillages. A similar effect, as observed with frequency, is seen with changes in stroke. At 12.7 mm (1/2 in) stroke and 540 cycles/min, velocities between 0.20 to 0.25 m/s (40 to 50 ft/min) were observed, while at 22.2 mm (7/8 in) stroke and 540 cycles/min, the material conveying speed increased to between 0.46 and 0.51 m/s (90 and 100 ft/min).

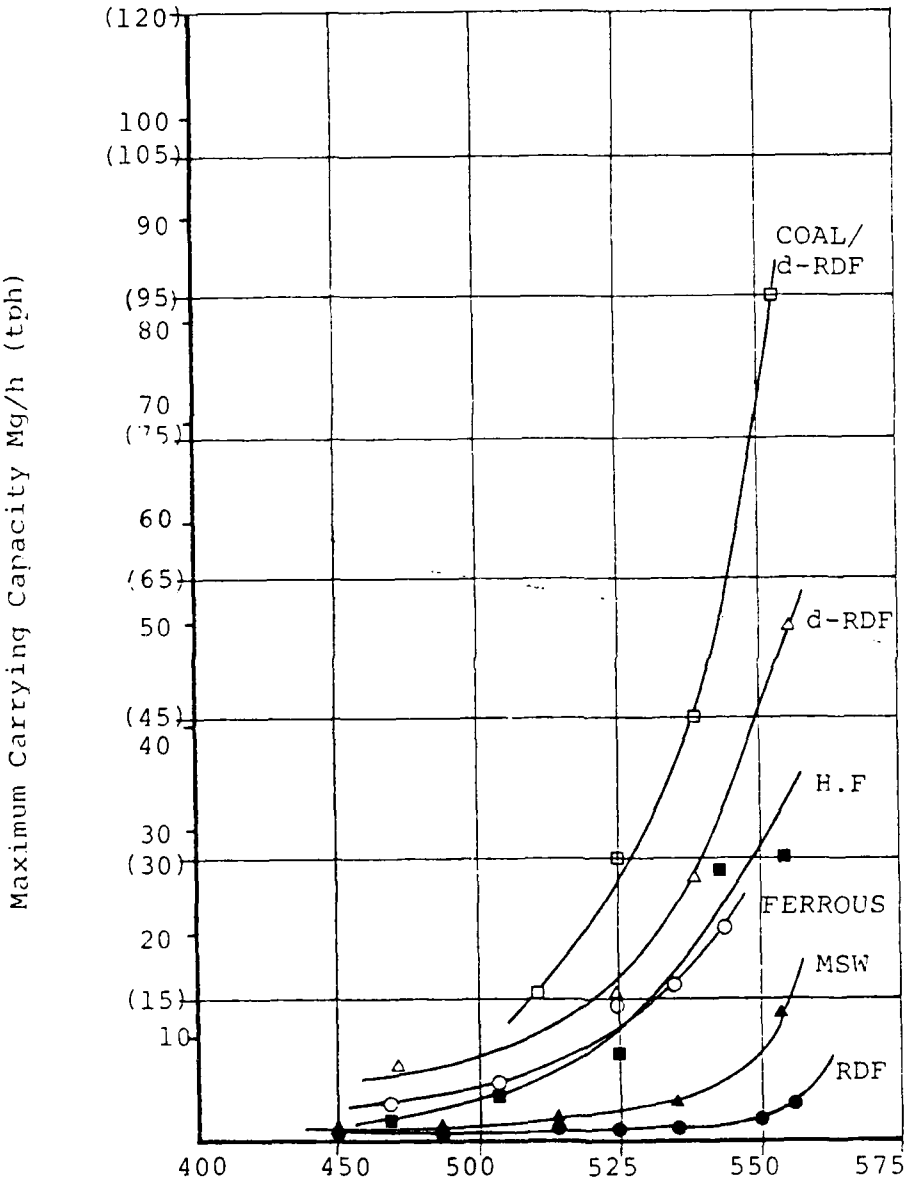

Figure 26. Maximum Carrying Capacity of Test Vibrating Conveyor vs Vibration Frequency for 12.7 mm (1/2 in) Stroke

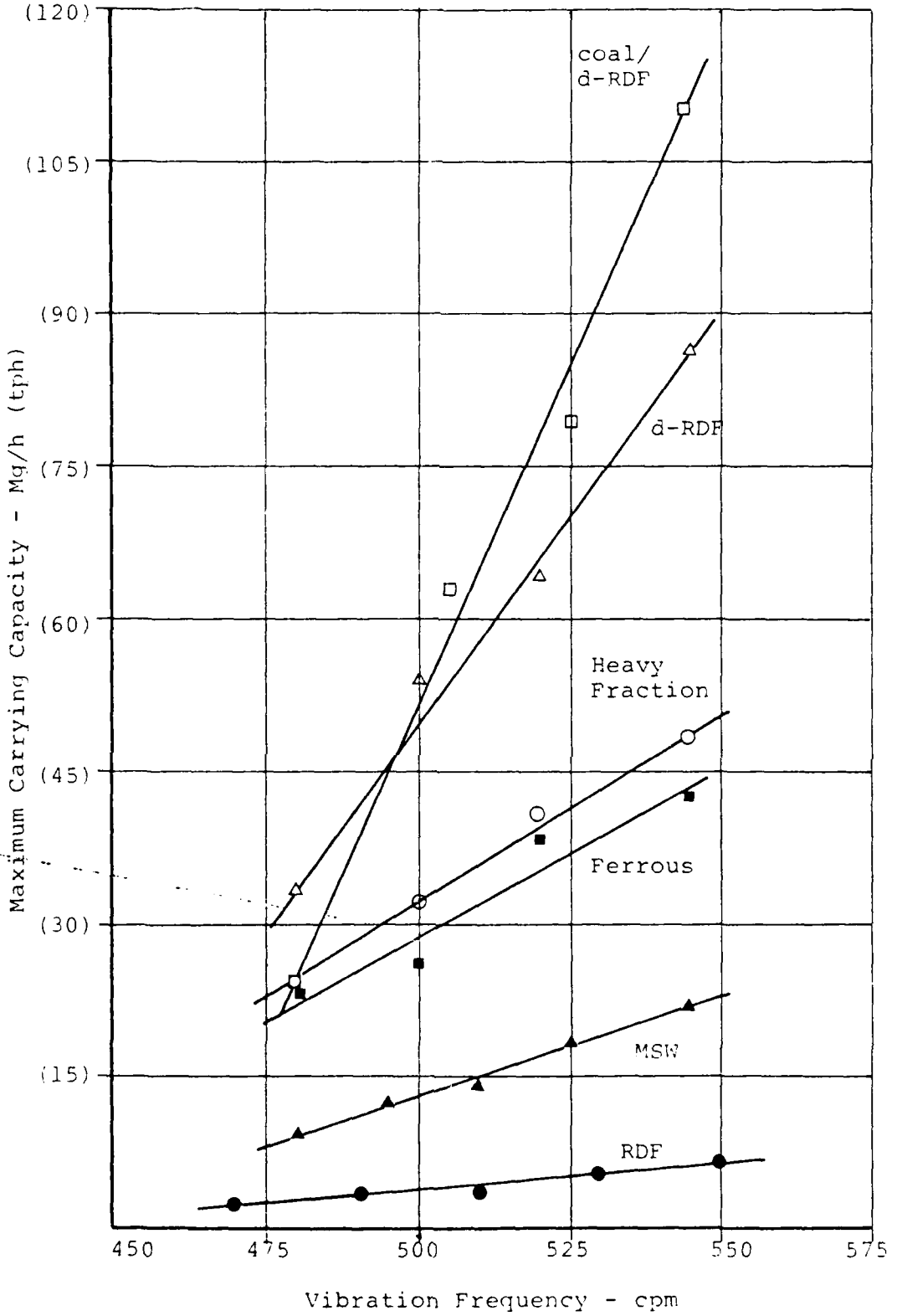

Figure 27. Maximum Carrying Capacity of Test Vibrating Conveyor vs Vibration Frequency for 22.2 mm (7/8 in) Stroke.

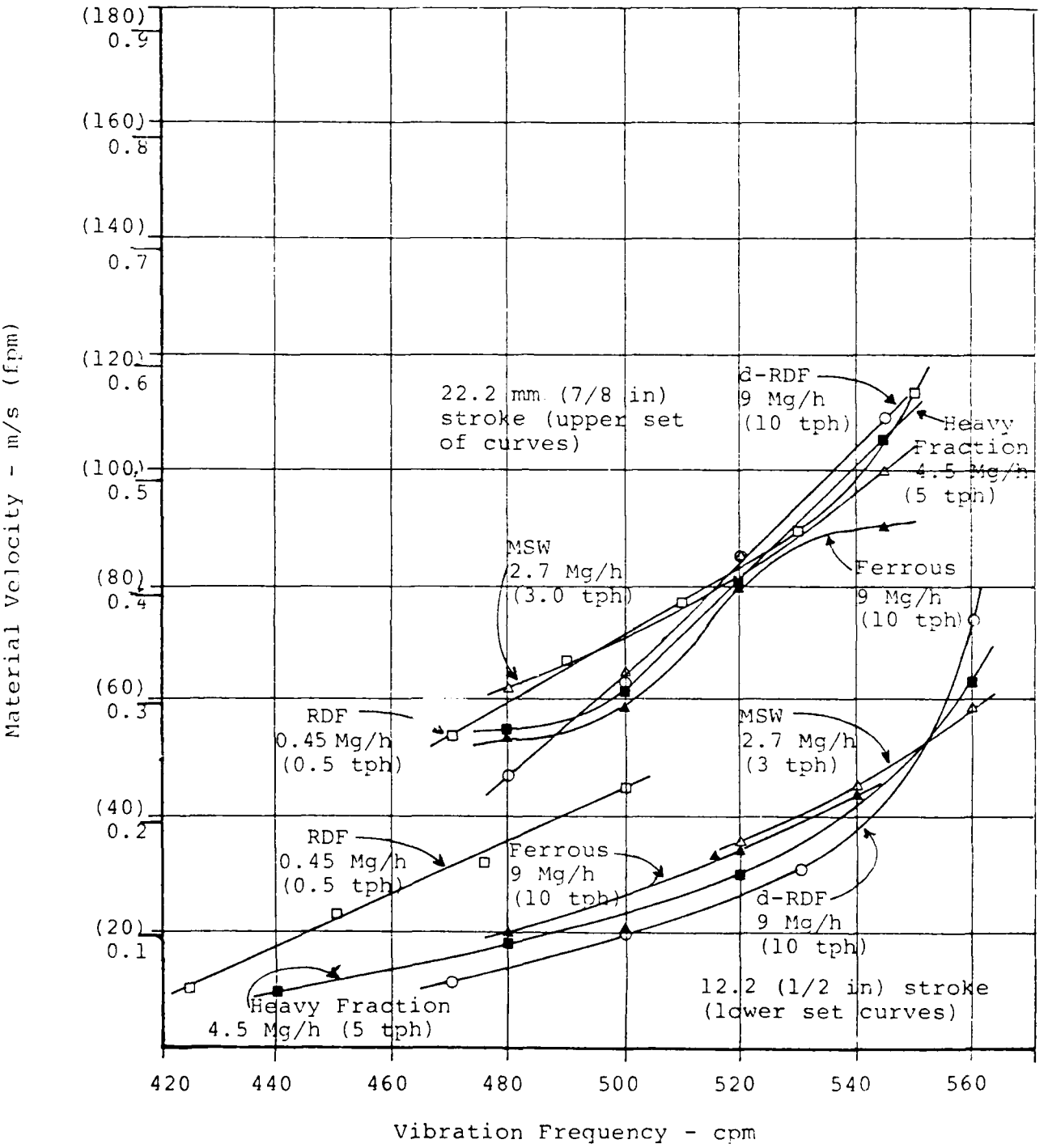

Figure 28. Material Velocity vs Vibration Frequency on the Test Vibrating Conveyor.

Energy Consumption vs Vibrating Frequency for a Given Mass Flow Rate

During the testing, the vibrating conveyor motor current was measured with a hand-held ammeter. The measurements indicated no significant difference in energy consumption with frequency or stroke length in the ranges studied. Nor was there any increase in consumption at a given frequency or stroke for transporting denser bulk solids (dRDF/coal vs. RDF, for example). The reason that changes in energy consumption were not detectable is probably attributable to use of a larger-sized drive motor than required for the application.

Conveying Speed vs Material Burden Depth for a Given Frequency

At a fixed frequency of 510 rpm, and at two stroke lengths, the vibrating conveyor was uniformly loaded with the solid waste fraction at three different vurden depths between 25 and 152 mm (1 and 6 in.). The conveying speed of the material was measured for each burden depth.

The results are given in Figure 29. For both the 12.7 and 22.2 mm strokes, a gradual decrease in conveying speed is observed for all material with increases in the material burden depth. Greater decreases in velocity were observed for the lighter materials (RDF and MSW) than more dense fractions (ferrous, heavy fraction). This suggests that lighter, lower density materials absorbed the energy imparted by the vibrating pan more than the denser materials.

AD-A119 065 NATIONAL CENTER FOR RESOURCE RECOVERY INC WASHINGTON DC F/G 13/3
INVESTIGATION OF ENGINEERING AND DESIGN CONSIDERATIONS IN SELEC--ETC(U)
AUG 81 Z KAHN, M L RENARD, J CAMPBELL MIPR-N-80-33

UNCLASSIFIED AFESC/ESL-TR-81-58 NL

2 of 2
AD A
119065

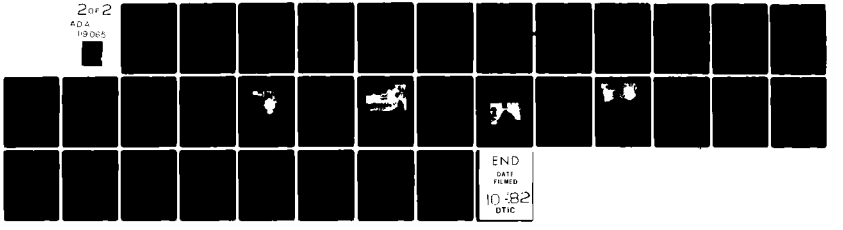

END
DATE FILMED
10-82
DTIC

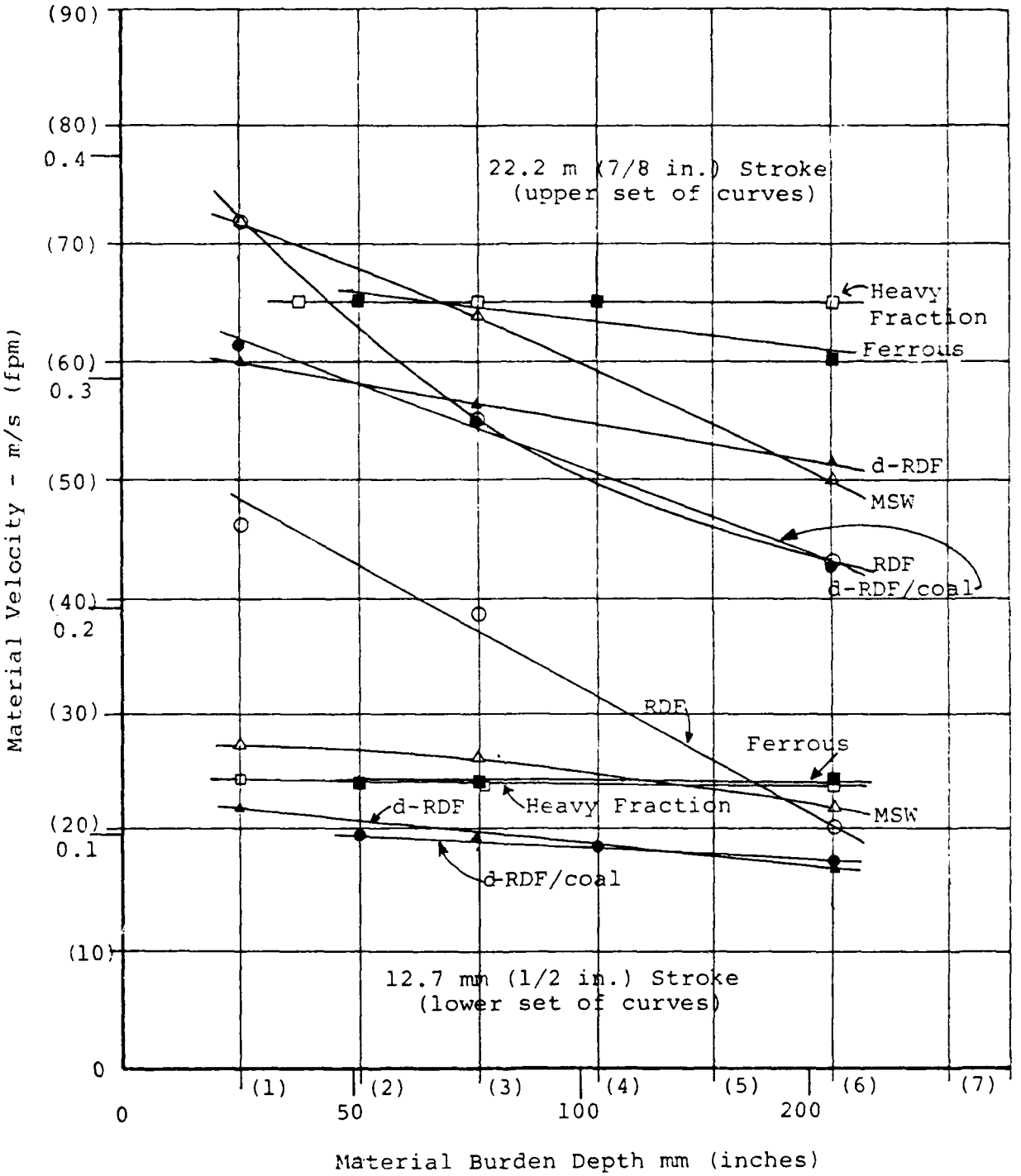

Figure 29. Material Velocity vs Material Burden Depth On the Test Vibrating Conveyor

Compaction of Material Along the Length of Pan

As the material vibrates on the conveyor, it has a tendency to gradually compact along the direction of travel. This test was conducted to determine the change in burden height and expected slope of material as it is being conveyed on the test vibrating conveyor at a fixed capacity. Test results are presented in Table 14.

TABLE 14. COMPARISON OF TENDENCY FOR COMPACTION.

Solid Waste Fraction	Stroke (in.)	Frequency (rpm)	Slope	Percent lowering of burden height over 4.6 mm (15 ft) of conveyor length
RDF	7/8	520	-0.0049	39.1
d-RDF	7/8	520	-0.0028	31.0
MSW	7/8	520	-0.0052	44.1
HF	7/8	520	-0.0014	18.3

Table 14 indicates that there is a consistent tendency among the solid waste fractions to compact due to the vibration of the pan. The MSW and RDF fractions, relatively the most compressible, showed the highest degree of compaction.

Dust Generation

As with the belt conveyor, high volume air samplers were used to measure the magnitude of dust generated for various equipment conditions and waste fractions. The test methods and calculations are given in Appendix A.

Fixing the frequency (at 510 cpm) and the material mass

flow rate on the conveyor system, measurements were made of dust generation for different fractions and two stroke lengths. The dust sampler was placed approximately 1.6 m (5 ft) from the mid-point of the vibrating conveyor.

Table 15 provides the results and shows that the magnitude of dust generated at 22.2 m (7/8 in) stroke is higher for the RDF, MSW and coal/dRDF blend than for the 13.7 mm (1/2 in) stroke and virtually unchanged for the heavy fraction and dRDF. The dRDF/coal blend at 22.2 mm (7/8 in) stroke exhibited exceptionally high dust levels relative to the results for the 12.7 mm stroke and to the other test materials. While it is possible for one or both of the dust loadings reported for the dRDF/coal blend to be inaccurate, it is important to be aware of this trend in equipment design or selection.

TABLE 15. RELATIONSHIP BETWEEN DUST GENERATION AND STROKE LENGTH

Solid Waste Fraction	Stroke Length mm (in)	Mass Flow Rate Mg/h (tph)	Dust Generated (mg/scm of air)
RDF	12.7 (1/2)	0.9 (1.0)	8.4
RDF	22.2 (7/8)	0.9 (1.0)	14.7
MSW	12.7 (1/2)	0.9 (1.0)	1.9
MSW	22.2 (7/8)	0.9 (1.0)	5.4
HF	12.7 (1/2)	4.5 (5.0)	0.9
HF	22.2 (7/8)	4.5 (5.0)	0.9
d-RDF	12.7 (1/2)	4.5 (5.0)	31.2
d-RDF	22.2 (7/8)	4.5 (5.0)	29.4
d-RDF/coal blend (1:1)*	12.7 (1/2)	8.2 (9.2)	18.1
d-RDF/coal blend (1:1)*	22.2 (7/8)	8.2 (9.2)	235.0

* Volumetric Basis

SECTION V

APRON CONVEYORS

INTRODUCTION

Apron conveyors in resource recovery plants are most commonly used as receiving conveyors for unprocessed waste or at the discharge of size reduction equipment where loading or ballistic impact of material on the conveyor is of concern. An apron conveyor is made up of a series of hinged steel pans on a chain and roller assembly which ride on tracks underneath or outboard of the pans.

Because of limitations in equipment size, testing of a small pan conveyor in this program was conducted only on a batch basis and only on feedstocks of dRDF and a dRDF/coal blend.

The apron conveyor utilized for the tests was a 0.76 m (30 in) wide by 2.06 m (6.75 ft) long apron conveyor with 152 mm (6 in) wide pans, 102 mm (4 in) sides and 51 mm (2 in) cleats spaced every 406 mm (16 in). The conveyor was equipped with an adjustable speed drive with a range of 0.05 - 0.23 m/s (10 - 45 fpm). The conveyor was configured to allow inclinations of 0° to 39°.

The apron conveyor evaluation involved measurement of the maximum angle of surcharge and tests to establish the maximum angle of inclination, maximum conveying capacity for various conveying speeds and inclinations.

TESTS RESULTS

Maximum Angle of Surcharge

The maximum angle of surcharge (static) was obtained utilizing the same procedure used for the belt conveyors and outlined in Appendix A. The angle of surcharge is shown schematically in Figure 3. For the dRDF, the angle of surcharge was determined to be 40.5^{o} and, for the dRDF/coal blend, the angle was 38.5^{o}.

As with the measurements on the belt conveyor, the angle of surcharge for the dRDF is higher than for the dRDF/coal blend, although in magnitude both materials have a lower angle than on the belt (Table 6).

Maximum Carrying Capacity vs Conveyor Speed and Inclination

Maximum carrying capacity is the maximum mass flow rate that was obtained on the apron conveyor for a given speed and inclination. For the test, a 1 to 1.5 m (3 to 5 ft) section of the conveyor was hand loaded to maximum static capacity. The conveyor was started and the discharge collected and weighed over a measured time period. Care was taken to avoid uneven material flows during starting and stopping. Multiple tests at single conditions showed good repeatability.

The results are presented in two formats for each material. Figures 30 and 32 show the results for the dRDF and Figures 31 and 33 show the results for the dRDF/coal blend.

When carrying capacity is plotted vs. conveyor speed as in Figures 30 and 31, maximum carrying capacity is found to

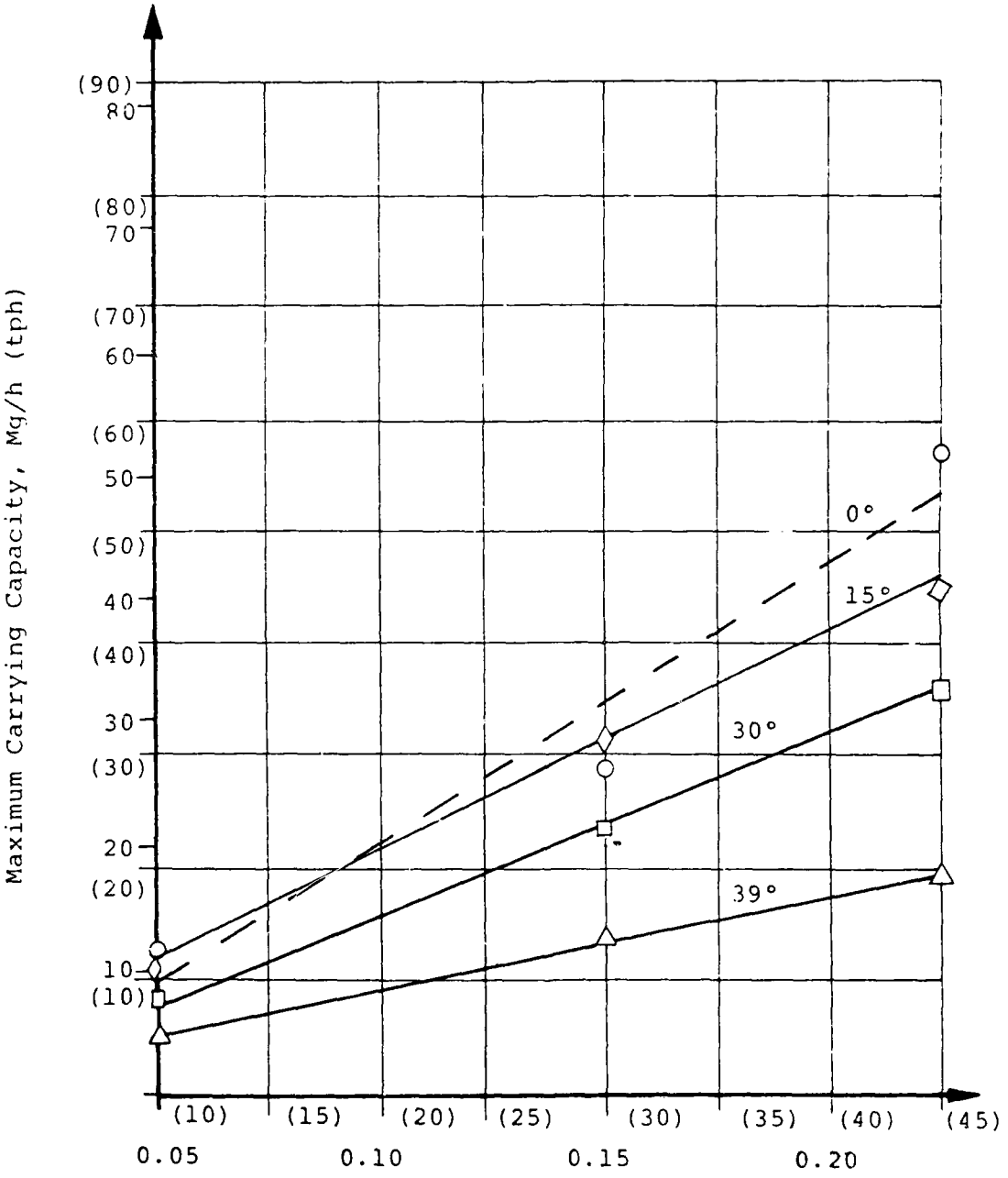

Figure 30. dRDF Maximum Capacity vs Apron Conveyor Velocity

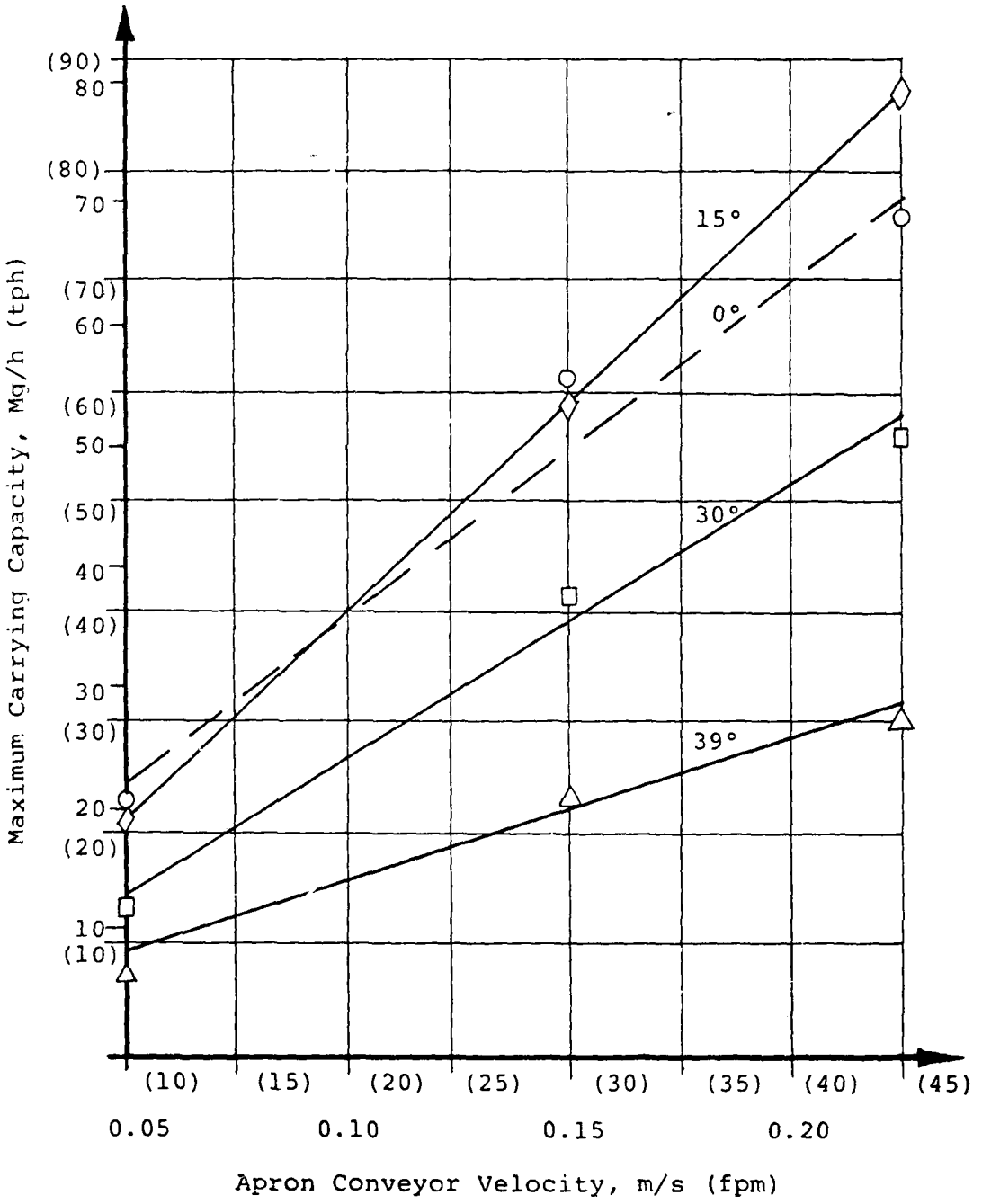

Figure 31. Coal/dRDF Maximum Capacity vs Conveyor Velocity

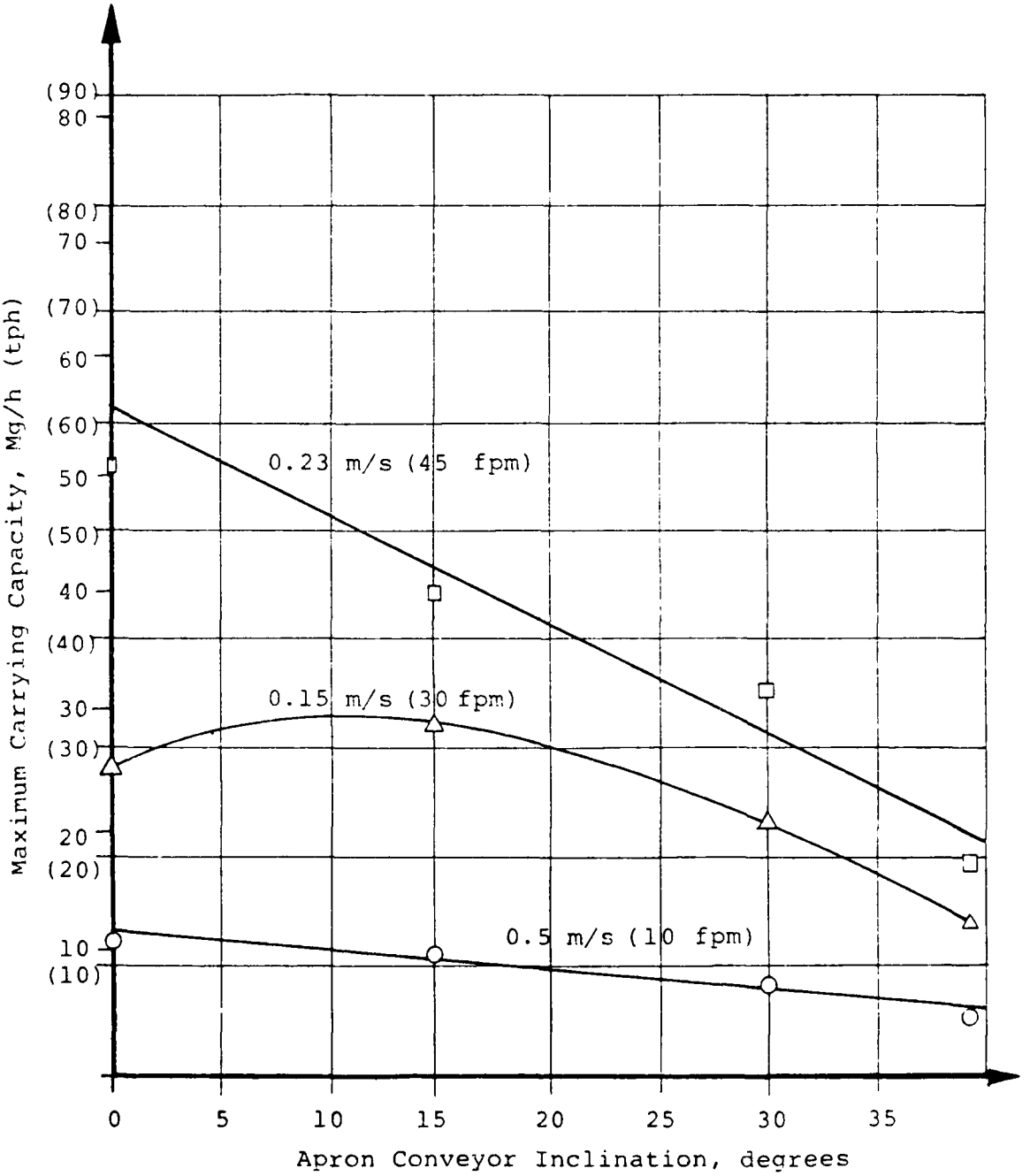

Figure 32. dRDF Maximum Capacity vs Apron Conveyor Inclination

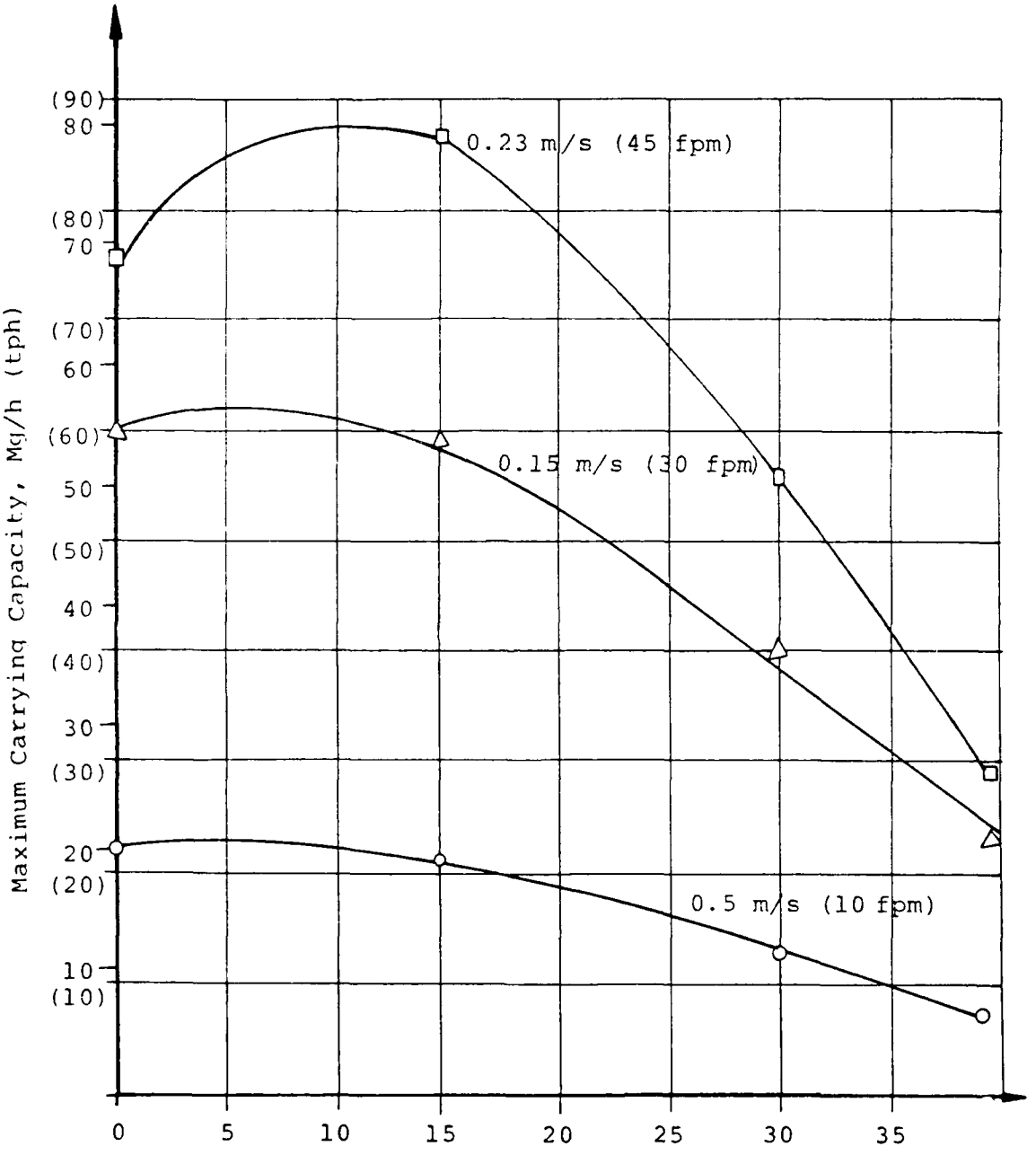

Figure 33. Coal/dRDF Maximum Capacity vs Apron Conveyor Inclination

increase linearly with increasing velocity. This is to be expected, since in the speed range evaluated (typical for apron conveyors carrying solid waste) the velocity is below the point at which the material would slip and bounce or be windblown off the belt. Also, since the conveying surface is rigid, there is no bouncing effect as was seen with the conveyor belt passing over idlers.

During the test it was observed that there was very little spillage off the sides. Most of the spillage that was observed occurred above 30° because of material falling back and off t tail (low) end of the conveyor.

When carrying capacity is plotted vs. inclination (Figu 32, 33), it can be seen that between 0° and 15° inclination h little effect. (The reason for the anomaly at 0° for the top curve in Figure 33 and the middle curve in Figure 32 is not known.) However, from 15° to 39°, carrying capacity drops sharply with increased inclination.

Maximum Angle of Inclination

The maximum angle of inclination for an apron conveyor was defined in this test as the maximum slope up which material can be conveyed for a given feed rate with the velocity fixed at 10 ft per minute. For this test, the apron conveyor was supplied by a vibrating feeder. Feed rates were 4 Mg/h (4.5 pth) for dRDF and 5.9 Mg/h (6.5 tph) for the dRDF/coal blend.

Although the cleats were removed, the hinge pin between each pan provided some resistance to back sliding. The criteria

for assessing the maximum angle of inclination is the same as discussed in Appendix A, i.e., the inclination at which a pronounced (and intolerable) increase in the fallback and splippage of material occurs. For the dRDF, the angle was 35^{o} compared to 30^{o} observed on the belt conveyor (see Table 3) and, for the dRDF/coal blend, the angle was 30^{o} compared to 27^{o} on the belt conveyor.

REFERENCES

1. Conveyor Equipment Manufacturers Association (CEMA), Engineering Conference. Belt Conveyors for Bulk Materials, 2nd Edition. Boston, Massachusetts: CBI Publishing Company, 1979.

2. Khan, Z.; Renard, M; and Campbell, J. Considerations in Selecting Conveyors for Solid Waste Applications, Draft Final Report, EPA Grant No. R806709. Washington, D.C.: National Center for Resource Recovery, Inc., 1981.

3. Conveyor Equipment Manufacturers Association (CEMA), Bulk Materials Classification and Definitions Committee. Classification and Definitions of Bulk Materials No. 550. Washington, D.C., 1970.

4. Johanson, J.R. Know Your Material - How to Predict and Use the Properties of Bulk Solids, Chemical Engineering, Deskbook Issue. 30 October 1978.

5. Jenike and Johanson, Inc. Bin and Feeder Design for Refuse-Derived Fuel, Report to U.S. Army, CERL, Project 78206.

6. Campbell, J.A., and Renard, M.L. Densification of Refuse-Derived Fuels: Preparation, Properties and Systems for Small Communities, Final Report EPA Grant 804150. Washington, D.C.: National Center for Resource Recovery, Inc., December, 1980.

7. Khan, Z., and Renard, M.L. The Use of Waste Oils to Improve Densified Refuse-Derived Fuels, Contract DOE-ES-76-C-01, 3851, Task 5. Washington, D.C., October, 1979.

8. Renard, M.L., and Khan, Z. Design Considerations for Municipal Solid Waste Conveyors, in Municipal Solid Waste: Resource Recovery, Proceedings of the Seventh Annual Research Symposium. Philadelphia, Pennsylvania: Environmental Protection Agency, March, 1981. pp. 30-66.

9. U.S. Department of Labor, Occupational Safety and Health Administration. OSHA Safety and Health Standards, No. 2206, Rev. January 1976, Part 1910, Paragraph 1000, Table 2-3, pp. 504-510.

APPENDIX A

METHODS FOR TESTING WASTE SAMPLES

Method A.1 Angle of Maximum Inclination

Definition - Angle of Maximum Inclination - maximum angle a conveyor belt may be inclined and successfully convey material at a specified feedrate and a belt speed of 0.51 m/s (100 fpm). (The feedrate should be set at a level near but below the maximum capacity established for horizontal operation typically between 70 and 90 percent of this maximum.)

1.0 Apparatus

1.1 Recirculating set of conveyors - controlled throughput.

1.2 Test conveyor - variable speed and incline.

1.3 Angle finder or protractor.

1.4 Tachometer.

1.5 Weighing scale - platform-type with precision of ± 50 g (0.1 lb).

2.0 Sample Collection

2.1 Obtain a gross sample of waste in an amount necessary to maintain the desired feedrate on the test conveyor.

3.0 Test Procedure

3.1 Incline the test belt to an angle at which the material is known to be transported without difficulty.

3.2 Load the pre-weighed material onto the conveyor system and establish desired and constant feedrate.

3.3 Run the conveyor system for approximately 5 minutes.

3.4 Observe and note how material is transported. If the conveyor operates without significant material

fallback, slippage and resulting spillage, increase the angle of inclination by 1 degree.

3.5 Continue the procedure of increasing (or decreasing) the inclination by 1 degree running the system for 5-minute intervals until the angle (or often a range of 2-3 degrees) is reached where there is a pronounced (and intolerable) increase in fallback, slippage and spillage. This angle (or mean of range of angles) is considered the maximum angle of inclination.

4.0 Factors Affecting Results

4.1 Minimum belt sag tension.

4.2 Length of skirt boards.

4.3 Centrally loaded and uniform feed.

Method A.2 Angle of Repose

Definition - The angle of repose is the angle between horizontal and the sloping line from the top of pile to the base.

1.0 Apparatus

1.1 Angle finder or protractor.

1.2 Measuring tape, straight edge.

2.0 Sample Collection

2.1 Obtain a gross sample of approximately 23 kg (50 lbs) from the incoming solid waste fraction.

3.0 Test Procedure (See Figure A-1)

3.1 Cone and quarter the 23 kg (50 lbs) of material.

3.2 Form a pile of material on a horizontal surface by carefully discharging the representative sample from a hand-held container. The container is held closely to the horizontal surface to start with and is gradually raised as the height of the pile is increased with about 50 mm (2 in) clearance. Final height of the pile to represent load height on belt conveyors at maximum capacity and static conditions. (Determined to be 203 mm (8 in) for tests reported here).

3.3 Measure and record the angle of repose at four equally spaced intervals.

3.4 Repeat steps 3.2 and 3.3 for a total of three piles.

4.0 Calculations

4.1 Calculate and report the average angle of repose for each pile.

$$\alpha = \frac{\alpha_1 + \alpha_2 + \alpha_3 + \alpha_4}{4}$$

Figure A-1. Angle of Repose Measurement (Method A.2)

Method A.3 Angle of Slide

Definition - Angle of Slide - The angle at which materials on at rest on air inclined surface will begin to slide.

1.0 Apparatus

1.1 Mild steel plate 10 mm (.037 in.) thick having dimensions 1.2 m x 0.9 m (4 ft x 3 ft).

1.2 Rubber sheet (conveyor skirting) mounted on 13 mm (1/2 in.) plywood sheet having dimensions 0.9 m x 0.6 m (3 ft x 2 ft).

1.3 Angle finder or protractor.

2.0 Sample Collection

2.1 Obtain a sample of approximately 0.014 m^3 (0.5 ft^3) from the test material.

3.0 Test Procedure (See Figure A-2)

3.1 Rest one end of the steel plate on the floor with the other end slightly raised and supported on a wooden block. This arrangement facilitates easier lifting of the plate.

3.2 Place the sample on the plate to form a pile approximately 75 mm (3 in.) high.

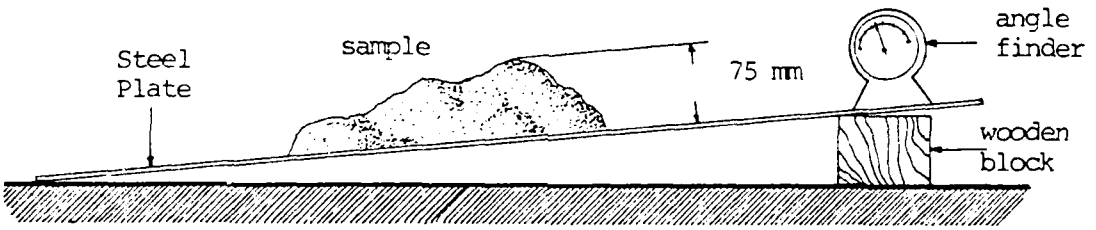

3.3 Slowly raise the plate and record the angle when the material just begins to slide.

3.4 Test three times and report mean angle of slide in degrees.

Figure A-2. Angle of Slide Measurement (Method A.3)

Method A.4 Test Procedures for Maximum Angle of Surcharge

Definition - Maximum Angle of Surcharge - The angle made between the slope of material on a fully loaded belt and the horizontal.

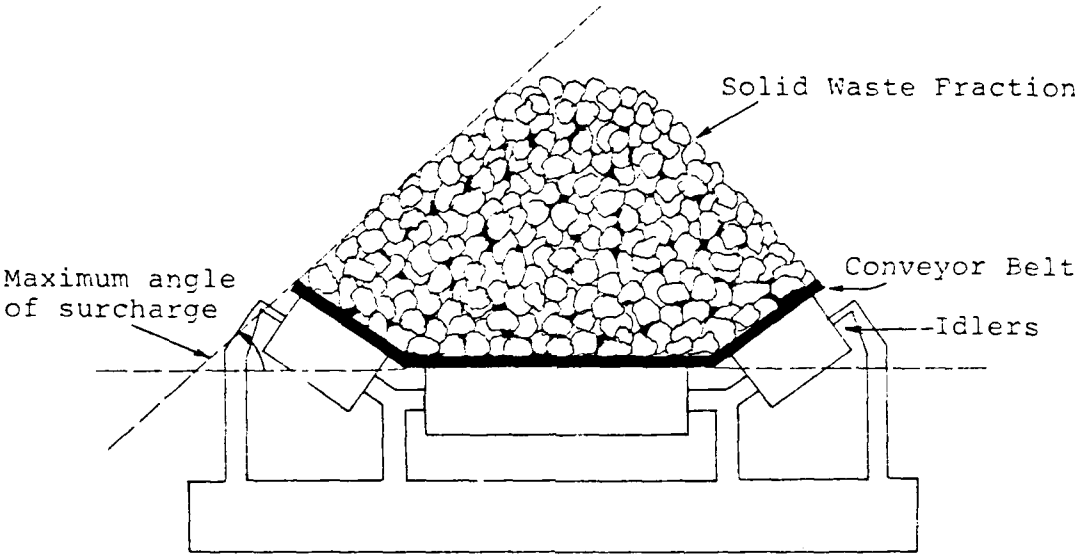

1.0 Apparatus

1.1 Conveyor belt.

1.2 Angle finder or protractor.

1.3 Straight edge.

2.0 Sample Collection

2.1 Obtain a representative sample of waste in an amount required to fully load a 1.5 m length of conveyor belt.

3.0 Test Procedure (see Figure A-3)

3.1 Using a shovel, load a 1.5 m (5 ft) length of the belt with material. The material should be dropped from a height of approximately 150 mm (6 in.) above the top of the pile. The belt is considered fully loaded when the material starts to slip or roll off the belt.

3.2 Place a straight edge against the slope of the pile. Measure and record the angle with an angle finder or protractor.

3.3 Repeat step 3.2 three times (two along each side of the belt) for a total of four readings.

4.0 Calculations

4.1 Maximum angle of surcharge =

$$\frac{\text{Reading 1} + \text{Reading 2} + \text{Reading 3} + \text{Reading 4}}{4}$$

Figure A-3. Maximum Angle at Surcharge Measurement (Method A-4).

Method A.5 Bulk Density ("Loose") by the Cone Method

Definition - The bulk density determination by the Cone Method provides data representative of "as conveyed" bulk density of materials transported on belt conveyors.

1.0 Apparatus

1.1 Weighing scale - platform-type with precision of 50 g (0.1 lb).

1.2 Angle finder or protractor.

1.3 Measuring tape, straight edge.

2.0 Sample Collection

2.1 Obtain a gross sample of approximately 23 kg (50 lbs) from the incoming solid waste fraction.

3.0 Test Procedure (See Figure A-4)

3.1 Cone and quarter the 23 kg (50 lbs) of incoming material. Retain one quarter for measurement of bulk density.

3.2 Form a pile of material on a horizontal surface by carefully discharging the representative sample from a hand-held container. The container is held closely to the horizontal surface to start with and is gradually raised as the height of the pile is increased with about 50 mm (2 in.) clearance. Final height of the pile to represent load height on belt conveyors at maximum capacity and static conditions. (Determined to be 203 mm (8 in.) for tests reported here).

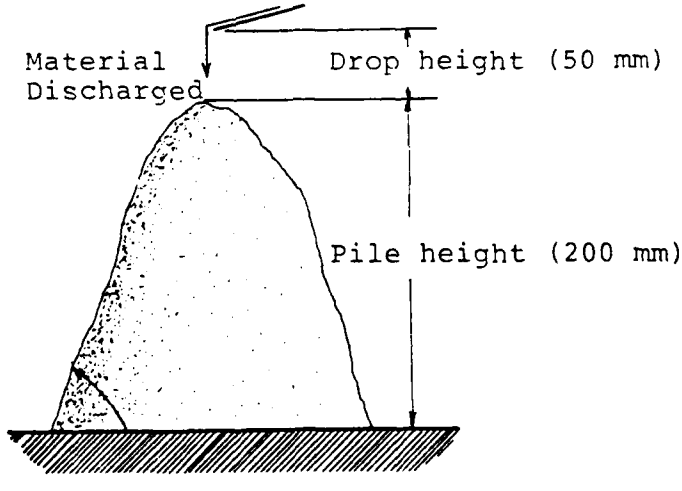

Figure A-4. Loose Bulk Density Measurement
(Method A.5)

3.3 Measure and record diameter of the base of the pile twice.

3.4 Measure and record height of the pile.

3.5 Weigh and record the weight of material in the pile.

3.6 Repeat steps 3.2-3.5 for a total of three piles.

4.0 Calculations

4.1 Calculate the average diameter of each pile ($\bar{D}$).

4.2 Calculate the volume (V) of each pile.

$$V(ft^3) = \left(\frac{1}{3}\right)\frac{\pi(\bar{D})^2}{4}H$$

where: $\bar{D}$ = average pile diameter

H = height of pile

4.3 Calculate the "as conveyed" bulk density of each pile.

$$B.D. = \frac{W}{V}$$

where: W = weight of pile

V = volume of pile

B.D. = bulk density

4.5 Report average of the three bulk densities.

Method A.6 Bulk Density ("Vibrated") by the Container Method

Definition - The bulk density determination by the Container Method provides density representative of materials constrained and piled upon itself such as in a storage bin.

1.0 Apparatus

1.1 Bulk density sample box - wooden, 30.5 cm x 30.5 cm x 30.5 cm interior. Box is tared.

1.2 Scale - platform-type; precision, 50 g (0.1 lb).

2.0 Sample Collection

2.1 Obtain a sample of approximately 0.06 m^3 (2 ft^3) from the test material.

3.0 Test Procedure

3.1 Fill the container in three increments. After each increment, vibrate the box by lifting and dropping each of the four edges one time.

3.2 Carefully level the top, removing overflow. Weigh and record weight of box and contents. Empty material.

3.3 Repeat steps 3.1 and 3.2 three times, using the remainder of sample for a total of three determinations.

4.0 Calculations

4.1 Bulk density kg/m^3 (lb/ft^3) =

$$\frac{(W_1 - T) + (W_2 - T) + (W_3 - T)}{V}$$

where

W_{1-3} = Weight of sample and box in kg (lb)

T = Tare weight of box in kg (lb)

V = Volume of box in m^3 (ft^3)

Method A.7 Moisture Content Determination

Definition - Moisture content is determined on an as-received and dry weight basis.

1.0 Apparatus

1.1 Drying pans 38 cm x 28 cm x 5 cm (15 in x 11 in x 2 in.) having approximatley 0.5 cu ft capacity.

1.2 Drying oven - Freas Model 845 - 0-200°C range, internal volume 0.13 m^3 (4.5 ft^3).

1.3 Balance - precision, 0.1 g.

2.0 Laboratory Sample Collection

2.1 Subdivide gross sample to laboratory samples of 0.014 m^3 (0.5 ft^3); place in sealed polyethylene bag.

2.2 Label sample as to sample number, date, time, contents, and collection point.

3.0 Test Procedure

3.1 Empty content of bag onto clean, tared drying pan, spreading evenly across pan. If required, split sample between two or more pans.

3.2 Weigh and record weight of pan and samples.

3.3 Dry in oven at approximately 105°C ± 1°C. Remove after 24 hours. Record weight of dry sample.

4.0 Calculations

4.1 Percent moisture, dry weight basis = $\frac{A - B}{B} \times 100$

4.2 Percent moisture, as-received basis = $\frac{A - B}{B} \times 100$

where:

A = weight of as-received sample

B = weight of dry sample

Method A.8 Particle Size Distribution and Largest Lump Size Determination

Definition - This method provides the particle size distribution and largest lump size. (Ref.).

1.0 Apparatus

1.1 Gilson screen (Model TS-2) including the necessary screens and bottom tray (available: 102 mm (4 in.), 76 mm (3 in.), 51 mm (2 in.), 25 mm (1/2 in.) and 6 mm (1/4 in.)).

1.2 Drying oven with capability of maintaining 104°C ±1°.

1.3 Weighing scale with precision of ±1.0 gram.

1.4 Weighing pans.

1.5 Ruler or tape measure.

2.0 Sample Collection

2.1 Subdivide the gross sample to obtain laboratory samples of approximately 0.014 m^3 (0.5 $ft.^3$).

3.0 Sample Preparation

3.1 Place trays containing sample from 2.1 in a drying oven. Dry for 24 hours at 104 ± 1°C. (Ref. Test Method A.7).

4.0 Test Procedure

4.1 Place and clamp appropriate screens onto the Gilson screener. Choice of screen sizes to be used will vary depending on the solid waste fraction.

4.2 Spread dried sample on top screen being careful not to push material through the screen openings. Do not overload the machine. Maximum starting load is approximately 0.014 m^3 (0.5 ft^3). If larger sample is obtained, then batch sieving would be required.

4.3 Screen the material for exactly 10 minutes.

4.4 Observe all but the top screen for blinding or plugging after 1 minute. Blinding is indicated if more than 25 percent of the sample is on any one screen. In case of blinding of a screen, either

reject test and re-run the sample with smaller starting load (eg., 0.07 m^3) (0.25 ft^3); or, if available, insert a screen of the next larger size above the blinded screen.

4.5 At end of 10 minutes, remove material from each screen, place their individual contents in tared pans and weigh.

4.6 Weigh and record sample weight of each pan.

4.7 From the fraction retained on the largest screen remove the particle(s) with the largest cumulative dimensions. Measure and record the maximum dimension(s) (largest lump size) and weight (largest lump weight). If necessary, repeat test with the remaining dried sample from 4.2 and/or 4.4.

5.0 Calculations

5.1 Calculate the total weight of material retained on each screen (including the bottom tray).

5.2 Calculate the weight percentage of material retained on each screen.

5.3 Calculate the cumulative weight and percentages of material retained on each screen.

6.0 Result

6.1 The particle size distribution is reported on a moisture-free basis.

6.2 The largest lump size and weight.

Method A.9 Dust Concentration Determination

Definition - This test provides measurement of the mass concentration of total suspended particulates per cubic meter of air.

1.0 Apparatus

1.1 Air Sampler - Sierra Instruments Model 305-2000H recording high volume air sampler.

1.2 Filter Media - 203 mm x 252 mm (8 in. x 10 in.) glass fiber.

1.3 Recorder Charts - 102 mm (4 in.) dia.; 4.7 - 31 l/s (10 to 65 CFM) range; 24-hour time scale.

1.4 Balance - precision $\pm$ 0.001 g.

1.5 Barometer.

1.6 Thermometer.

1.7 Orifice calibrator and water manometer.

2.0 Test Procedure

2.1 Air Sampler Calibration - Calibrate the air sampler using a special orifice calibrator and a water manometer. For detailed calibration instructions, refer to Sierra Instruments instruction manual series 305.

2.2 Sampler Location - Place the air sampler on a stable platform and away from moving equipment to avoid formation of wind eddies around the sampler.

2.3 Weigh the 203 mm x 252 mm (8 in. x 10 in.) filter. Place and align the filter (rough side up) on the air sampler screen and tighten the hold-down frame clamps, to form an air-tight seal on the outer edges of the filter.

2.4 Set-up Pressure Transducer Flow Recorder - Slip recorder chart under the pan arm and push it flat against dial plate.

2.5 Activate the motor/blower and the flow recorder.

2.6 Record the initial and the final times of the sampling period.

2.7 After the sampling period, remove the filter from the frame, and weigh it.

2.8 Remove the flow recorder chart.

2.9 Record the ambient temperature and the atmospheric pressure.

3.0 Calculations

3.1 Calculate the weight of total suspended particulates (TSP) collected on the filter.

$W_P = W_F - W_I$

W_P = total weight of TSP, (mg)

W_F = final weight of filter and TSP, (mg)

W_I = initial weight of filter, (mg)

3.2 Obtain the sampling flow rate from the recorder chart, Q_R (cfm). If the recorder chart does not show a constant flow rate over the sampling period graphical intigration may be necessary to obtain accurate sampling flow rate.

3.3 Using the Calibration curve (see 2.1) read off the actual sampling flow rate, Q indicated (cfm).

3.4 Calculate sampling flow rate at standard conditions (25°C, 1 atm.):

$Q_S = (Pa/Ps) \times (Ts/Ta) \times Q$ ind.

$Q_S = (Pa/Ta) \times 3.156 \times Q$ ind.

where:

Q_S = flow rate in SCFM

$Q_{ind.}$ = flow rate obtained from calibration curve

Pa = Barometric pressure, (in. Mg).

Ps = Standard barometric pressure, (29.92 in. Mg)

Ta = Ambient temperature, degrees Kelvin (°K)

T_s = Standard temperature, 25°C = 298°K

°K = Degrees Centrigrade (°C) + 273

3.5 Calculate the mass concentration of TSP:

$C = (W_p/Q_s) \times (1/T_i) \times (SCFM/0.0283\ SCMM)$

where: T_i = Sampling time interval, (min)

C = Mass concentration of TST, (mg/SCM)

3.6 Example of a sample calculation:

Test Conditions:
(1) Sample: Heavy Fraction
(2) Belt Velocity = 200 fpm
(3) Mass flow rate = 15.0 tph
(4) Belt inclination = 14°
(5) Sampler location - 5' perpendicular off mid-print of test belt

W_F = 3602.3 mg

W_I = 3540.0 mg

W_P = 62.3 mg

Q_R = 66.0 cfm

Q_{ind} = 68.0 cfm

$Q_S = (29.88/287) \times 3.156 \times 68$

Q_S = 69.25 SCFM

$C = (62.3\ mg/69.26\ SCFM) \times (1/15\ min) \times (SCFM/0.0283\ SCMM)$

C = 2.1 mg/SCM

APPENDIX B

EFFECT ON SPILLAGE ON PROPOSED MEASUREMENT

This short appendix examines the effect of the mass spilled during a test on the conveyor circulating loop on the measured spillage rate itself.

A. Spillage Rate over One Cycle.

Figure B-1 schematizes the physical situation studied.

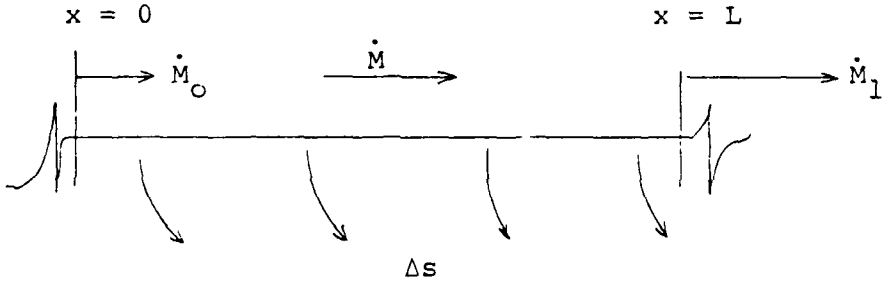

Figure B-1. Spillage, Inlet and Exit Mass Flow Rates

On a horizontal or inclined section of belt, of length, L, a "theoretically constant" mass flow rate $\dot{M}_o$ is maintained at the inlet section, x = 0. In actuality, as explained in the body of the text, a given mass M is distributed on the loop. If the time for a cycle around the loop is T_c, $M \simeq M/T_c$.

Let the incoming mass flow rate be $\dot{M}_o$. The measured spillage rate, per unit length of belt, is

$$\dot{s} = \lim_{\Delta t \to 0} \frac{\Delta s}{\Delta t}$$

in which Δs is the amount of material spilled, over a unit length of belt and time Δt.

By definition, $\dot{s}_o = k_s \dot{M}_o$, where $k_s << 1$ and is taken to be of order 2 of smallness (10^{-2}, say).

Now, $\dot{M}_1 = \dot{M}_o - \dot{s} \simeq \dot{M}$ to 0 (k_s); $\dot{s}_o = \dot{s}_1 = \dot{s}$ to 0 (k_s). Thus if $k_s = 10^{-2}$, the spillage rate can be measured anywhere along $0 \leq x \leq L$ with an accuracy on the order of 10^{-4}.

B. Measurements Over Several Cycles, No Mass Replacement

Let T_c be the time interval (period) between two successive passages of a particle at x = 0. If the spillage is limited to the section of length L,

$$(\dot{M}_1)_{\substack{j = 1 \\ \text{cycle index}}} = (\dot{M}_o)_{j = 2} = (1 - k_s)\,\dot{M}_o$$

$$(\dot{M}_1)_{j} = (\dot{M}_o)_{j+1} = (1 - k_s)^j \dot{M}_o = [1 - j\,k_s + \frac{j(j-1)}{2!} k_s^2 \ldots]\,\dot{M}_o.$$

The experiment duration is defined by $T_e \equiv j_{max}\, T_c$. It is required that

$$j_{max}\, k_s^2 << k_s$$

$$j_{max} << \frac{1}{k_s}, \text{ or } 10^{-1}\, k_s^{-1} \text{ (say)}$$

Thus if $k_s = 0.01$, $j_{max} = 10$ or $T_e = 10\, T_c$. In the Upper Marlboro test system (see Figure 2), the times spent on the remaining elements of the circuit are: $T_{VIBR.\ CONV.} = 7.7$ sec, $T_{INCL.\ CONV.} = 9.5$ sec, $T_{OTHERS} = 15$ sec for a fixed total of 32.2 sec. If V_B is the belt speed, in m/s,

$$T_c = 32.2 + \frac{7.63}{V_B} \text{ (seconds)}$$

The maximum duration of the test, T_e, or $j_{max}\, T_c$ is represented in Fig. B-2 vs. the belt speed V_B, for $k_s = 0.005$ ($j_{max} = 0.01$ ($j_{max} = 10$). It is seen that at the "target level" of approximately 0.2%, the test duration can be in the range 15 to 30 min without appreciable error due to the material spilled and not replaced on the belt.

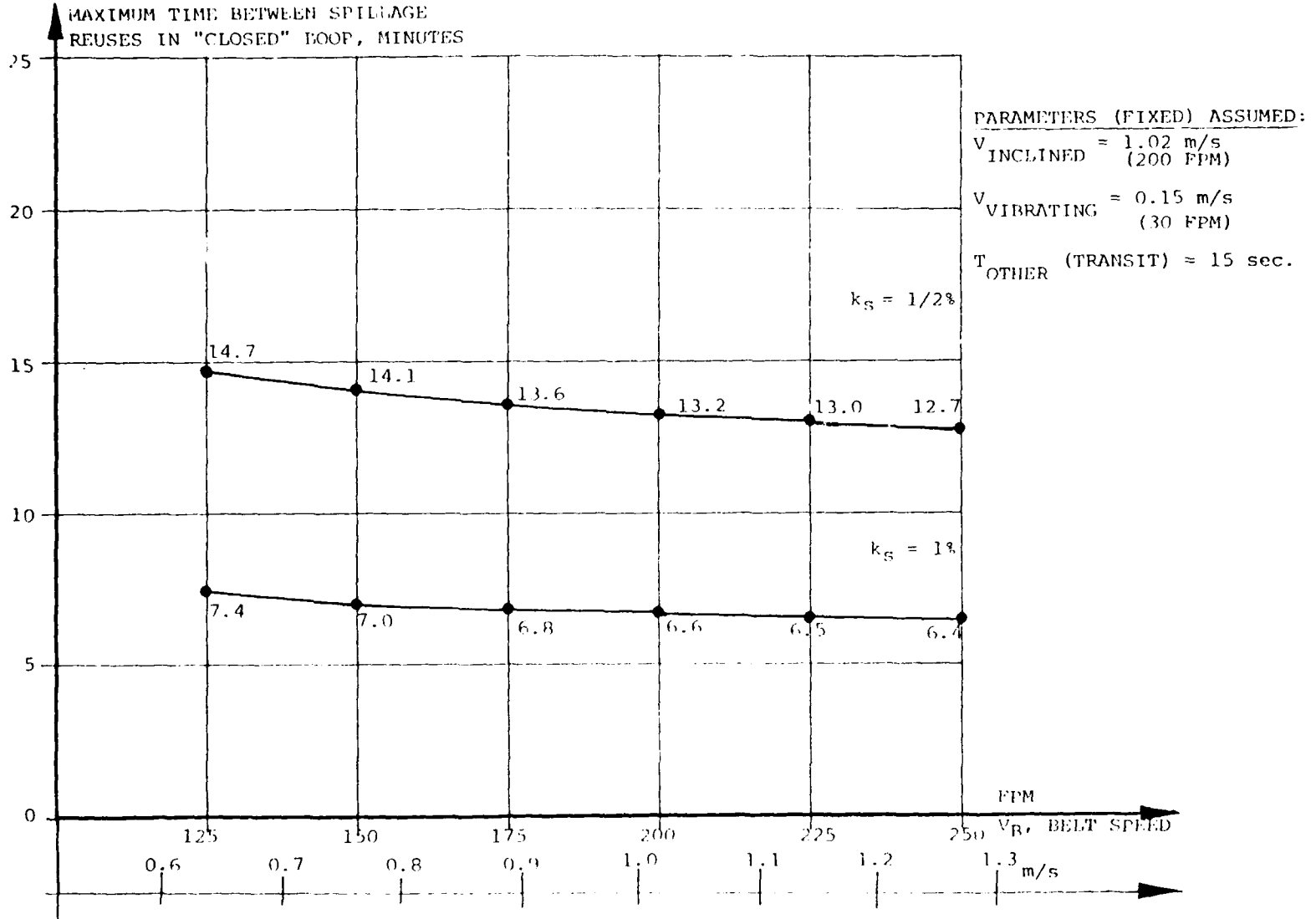

Figure B-2. Maximum Time Between Spillage Reuses vs. k_S and Speed of Belt

(The reverse of this page is blank.)

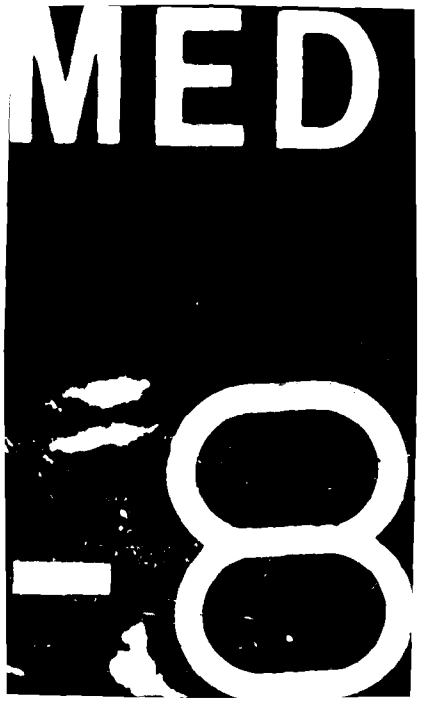
MED
8